POLITECNICO DI MILANO
ELECTRICAL ENGINEERING DEPARTMENT
DOCTORAL PROGRAM IN ELECTRICAL ENGINEERING

SENSITIVITY ANALYSIS OF POWER SYSTEM STATE ESTIMATION REGARDING TO NETWORK PARAMETER UNCERTAINTIES

Doctoral Dissertation of:
Mehdi Davoudi
(ID: 738962)

Supervisor:
Prof. Gabriele D'Antona

The Chair of the Doctoral Program:
Prof. Alberto Berizzi

2009-2012 (XXIV Cycle)

Abstract

In this thesis the effects of both network parameters uncertainty and measurement uncertainty on Weighted Least Squares (WLS) State Estimates has been analyzed. An algorithm for simulation of the uncertainty effects on the state estimator is proposed and simulated on IEEE 14-Bus, 30-Bus, 57-Bus and 118-Bus power network test cases.

The implementation of this algorithm on the test cases enables us to analyze how much the state estimator's output is affected according to the network parameters uncertainty by means of state errors distribution (in terms of error bars representing the distribution mean and 1σ standard deviation) versus the network parameters uncertainty.

Generally a serious defect in an estimator is the lack of unbiasedness. In literature the analysis of network parameters effects on WLS State Estimator's bias performance is missing, hence it motivated us to perform a new prominent analysis to find how network parameters uncertainty can affect the state estimator bias (for a given measurement uncertainly). It is done using distribution of the ratio of the absolute value of the state errors mean by the related standard deviations versus the network parameters uncertainty and comparing it with a predefined threshold.

In order to decrease the sensitivity of state estimates on network parameters uncertainty, a clue can be using Phasor Measurement Unit (PMU) because according to the simulations, it is proven that when PMU measurement data are included in the traditional measurement set, the State Estimator's sensitivity to the network parameters uncertainty will be notably smaller.

WLS State Estimation provides a mathematical expression for calculating the variance covariance matrix of State Estimates. It is confirmed numerically that the standard deviation of State Estimator's output is underestimated significantly when there is network parameter uncertainty. Thus the State Estimator's uncertainty has been analyzed versus the parameters uncertainty and compared with the theoretical WLS value.

Lastly an analysis is carried out to illustrate how much the State Estimator's results are correlated having network parameters uncertainty. Interestingly it is seen that when the network parameters uncertainty increases, it uncorrelates significantly the estimation errors.

Acknowledgement

First of all, I would like to express my deepest gratitude to my advisor, Prof. Gabriele D'Antona, for his admirable support and guidance throughout the research. I am truly indebted to my professors at department of Electrical Engineering at Politecnico di Milano for their guidance and support through my studies.

I would also like to extend my appreciation to my wife, Fahimeh Sadeghian for her love, patience, and encouragement. She allowed me to spend most of my time on this thesis.

Very thanks also go to all those who have somehow contributed to the thesis namely Mohsen Davoudi and I like to give my gratefulness to Prof. Marco Riva and Prof. Emanuele Ciapessoni for letting me to concentrate more on finalizing the writing of my thesis at last month.

Last but not least, I must acknowledge my kind parents whom without their support, I could never been capable of accomplishing my studies and academic work.

Mehdi Davoudi

Politecnico di Milano

February 2012

Dedication

This work is dedicated to Professor D'Antona

and my family.

Contents

CHAPTER 1

Introduction

1.1 Foreword

In large power networks, there are vast number of connected generators and loads so there will be large number of nodes and branches. Electric power systems are one of the biggest subjects that scientists have been putting too many efforts to understand and predict their complex behavior through mathematical models. The hugeness of the power transmission system forced early power engineers to be among the first to develop computational approaches to solving the equations that describe them.

The computational methods are essential for power system planners and operators to keep a consistent and secure operating environment [Crow 2007]. Between the computational tools, State Estimation (SE) has key role in order to analyze the contingencies of power system to determine any required corrective actions.

1.2 State Estimation

Estimation theory is a subdivision of statistics and signal processing that deals with estimating the values of parameters dependent upon measured data that has random components. The parameters describe an underlying physical setting in such a way that their values affect the distribution of the measured data. The estimator's task is to approximate the unknown parameters using the available measurements.

Power system state estimation is a tool to determine the voltage and phases on all nodes of power network that is firstly proposed by Fred Schweppe in [Schweppe 1970a, 1970b, 1970c].

Therefore all of the node voltages along with the angles across the network are of interest to be calculated using power network parameters and also a set of measurements in the power network including: voltage magnitudes and power fluxes and angles which provided by Phasor Measurement Units (PMU).

Implementation of synchronized phasor measurements presents an opportunity for improvements of power system state estimation and if PMU's were installed at all nodes, the State Estimation wouldn't be essential but from the economical point of view, having PMU's installed all over network is not applicable, therefore the task of State Estimation still is crucial.

As already stated, the data which are fed into a State Estimator are including the parameters of the power grid such as the transmission line's resistance, reactance and susceptance along with a set of measurements and the output of State Estimator is the states of the power network (i.e. voltages and related phases). The traditional measurements include a portion of the bus voltage magnitudes, active and reactive power injections at buses and active and reactive power flow through transmission lines. The nominal parameters of network and also the measurements across the network actually are not accurate and have various uncertainties.

Form the viewpoint of power system planners, to improve the network quality, reliability and security it is very important to know where to invest. To get better State Estimators, they can either increase the accuracy of measurements by purchasing new high precision measurement devices or perform accurate measurement of network parameters across

network and make a model of it in real-time. Rationally having both measurement and parameters accuracy improvement is the best way but could not be economical and they have to find an optimized solution. Having exact measurements but very uncertain network parameters (or vice versa) will not necessarily improve dramatically the SE but it is very interesting to know that how much it is effective. This paper focuses on the effects of parameters uncertainty and measurement noise on State Estimator and the results will be useful to determine tolerable uncertainty values of measurement and parameter.

In this thesis an algorithm is proposed in order to observe the effects of parameter and measurement uncertainties on the quality of power system state estimation. In the algorithm the core components include a load flow and a WLS State Estimation, so in the next two chapters the implementation of Load Flow and State Estimator are focused and then development of algorithm and Monte Carlo procedure are described in detail. Afterward the algorithm is tested on different standard power system test cases to analyze the sensitivity of power system state estimation regarding to the parameters and measurements noise.

1.3 Desirable properties of an estimator

In order to evaluate an estimator, it is needed to define clearly the mean of a "good" estimator. A deterministic parameter X, is derived from n points of a random data sequence $x(n)$ and the estimation of X gives $\hat{X}$ that is a random variable which basically is a function of $x(n)$, i.e.

$\hat{X} = F\big(x(n)\big)$.

$\hat{X}$ is pertaining to an *estimator* and each single value taken by the random variable $\hat{X}$ is an *estimate* [Clarkson 1993].

Generally there may not be a "natural estimator" of a parameter X, hence several possible estimators must be considered, with no clear insight of which one to be chosen. For this regard, we must decide on the criteria by which we judge the quality of an estimator, therefore a list of desirable properties of estimators is set out in the following subsections briefly [Priestly 1981] [Clarkson 1993].

1.3.1 Unbiasedness

The $\hat{X}$ is an unbiased estimator for X if the average value of $\hat{X}$ over all possible samples is equal to "true value" X whatever value X takes, that is $E(\hat{X}) = 0$ for all X.

The estimator is said to be "biased" if the above equation does not hold. The bias of $\hat{X}$ is defined as:

$bias(\hat{X}) = \bar{X} - X$

where $\bar{X} = E\{\hat{X}\}$.

Since the sampling distribution of $\hat{X}$ will depend on n, the number of observations in the sample $bias(\hat{X})$ will also depend on n.

If $bias(\hat{X}) \to 0$ as $n \to \infty$ then $\hat{X}$ is said to be *asymptotically unbiased*. Unbiasedness is clearly a desirable property but a biased estimator may still be quite useful provided if it is asymptotically unbiased. On the other hand, generally the lack of asymptotically unbiasedness would be considered a serious defect in an estimator.

In general, the basic structure of power system state estimation implies some assumptions which consequently introduce a bias meaning the inconsistency between the physical system and the mathematical model and have resulted in practical difficulties manifested by poor numerical reliability of the iterative state estimation algorithm [Meliopoulos 2001].

1.3.2 Efficiency of an Estimator and Minimum Variance

The efficiency of an estimator is determined by its variance. An estimator is more efficient if its variance is lower. The variance of the estimated states is an indicator of the **state estimator performance** [Bi 2008]. In this thesis, the average value of the variances of the estimated states is taken as the performance indicator of the proposed state estimator. The variance of an estimator $\hat{X}$ is:

$Var(\hat{X}) = E\left\{(\hat{X} - \bar{X})^2\right\}$

In the case that there are several different estimators e.g. X_1 and X_2 for the same parameter X, if the bias of the estimators are the same then the estimator would be

preferred that its sampling distribution has the smaller variance. Suppose two sampling variances are shown in Figure 1.1 that X_1 has the smaller variance. The values of $\hat{X}_1$ over different samples are more concentrated around the true value X than are the values of $\hat{X}_2$. Consequently the probability that $\hat{X}_1$ lies in a distinct interval is higher than the probability that $\hat{X}_2$ lies in the same interval. In this case the $\hat{X}_1$ is said to be a more efficient estimator than $\hat{X}_2$.

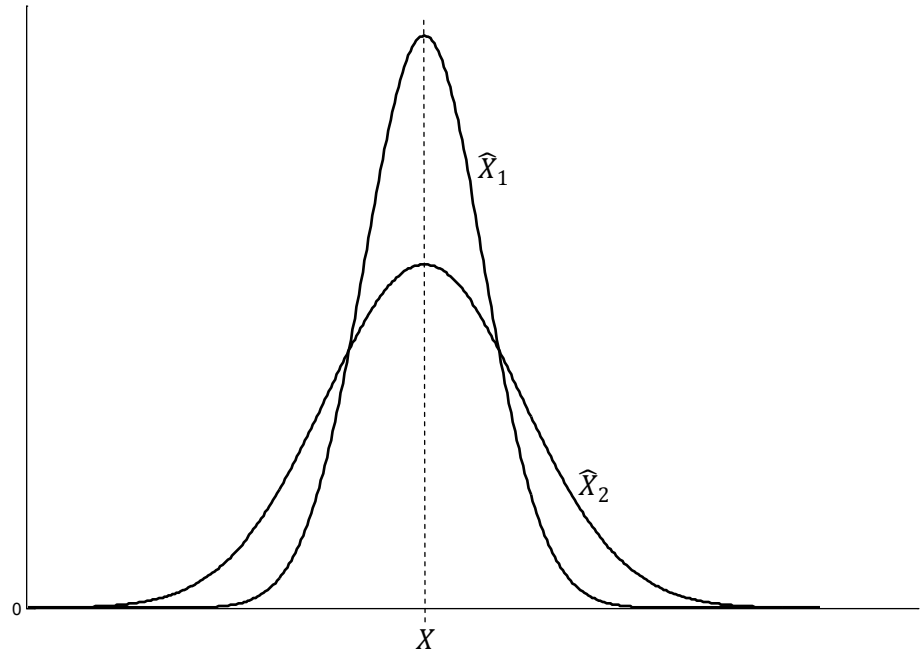

Figure 1.1: Sampling distributions of two different estimators.

Relative efficiency of two different estimators X_1 and X_2 for the same parameter X, is commonly evaluated as a percentage of the ratio between the related variances:

$$Relative\ Efficiency = \frac{Var(\hat{X}_1)}{Var(\hat{X}_2)} \times 100\%$$

1.3.3 Minimum Mean-Squared Error (MSE)

In general, when an estimation procedure is biased, the efficiency is not a good measure of quality of the estimator e.g. in the case of having two different estimators X_1 and X_2 for the same parameter, $\hat{X}_1$ may be unbiased but have a high variance, whereas $\hat{X}_2$ may be biased but have low variance.

Under this situation it is important to define the measure of *mean-squared error* which considers both bias and variance to determine which estimator is better. The mean-squared error for the estimator $\hat{X}$ is defined as:

$$MSE(\hat{X}) = E\left\{\left(\hat{X} - X\right)^2\right\}$$

Using the stated definitions of variance and bias, the mean-squared error could be expressed in other form as:

$$MSE(\hat{X}) = E\left\{\left(\hat{X} - E\{\hat{X}\} + bias(\hat{X})\right)^2\right\}$$

$$MSE(\hat{X}) = E\left\{\left(\hat{X} - E\{\hat{X}\}\right)^2 + bias^2(\hat{X}) + 2\, bias(\hat{X})\left(\hat{X} - E\{\hat{X}\}\right)\right\}$$

$$MSE(\hat{X}) = E\left\{\left(\hat{X} - E\{\hat{X}\}\right)^2\right\} + bias^2(\hat{X}) + 2\, bias(\hat{X})E\left\{\left(\hat{X} - E\{\hat{X}\}\right)\right\}$$

Considering that in the above equation the $E\left\{\left(\hat{X} - E\{\hat{X}\}\right)\right\} \equiv 0$, the first term is the variance and the second term is the bias squared, the mean-squared error will be finally:

$$MSE(\hat{X}) = Var(\hat{X}) + bias^2(\hat{X})\ .$$

The mean-squared error is more complete measure of the quality of an estimator than bias or variance itself. So, if there are several estimators which are biased, a sensible procedure would be to choose the estimator with smaller mean squared error.

This procedure is perfectly consistent with the measure of efficiency, when an estimator is unbiased. In the latter case, mean squared error will reduce only the variance. So, for an unbiased estimator, the MSE is the variance. Like the variance, MSE has the same units of measurement as the square of the quantity being estimated. Similar to standard deviation, taking the square root of MSE gives the root mean square error (RMSE), which has the same units as the quantity being estimated. For an unbiased estimator, the RMSE is the square root of the variance which obviously is the standard deviation.

1.3.4 Consistency

Another desirable feature for any estimator is that the more observations used, the closer the parameter estimate $\hat{X}$ should be to the parameter X. It is reasonable to expect that an estimator based on more observations should be more accurate than one based on less observations.

Formally, $\hat{X}$ is called a *consistent estimator* for X if $\hat{X}$ converges to X as the sample size goes to infinity. One of the sufficient conditions for consistency is that the mean squared error of $\hat{X}$ should converge to 0 as the sample size goes to infinity:

$$\lim_{n\to\infty}\left(MSE(\hat{X})\right) = 0$$

The mean squared error is the summation of variance with the bias squared, hence equivalently the sufficient conditions for consistency could be:

$$\lim_{n\to\infty}\left(Var(\hat{X})\right) = 0 \quad \text{and} \quad \lim_{n\to\infty}\left(bias^2(\hat{X})\right) = 0.$$

1.3.5 Sufficiency

The $\hat{X}$ is a *sufficient statistic* for X, if the distribution of the observed data conditioned on $\hat{X}$ is not depended on X, i.e. the observed data only give information about X if their probability density functions depend on X.

In a simpler words, sufficiency means that the estimator contains all of the information in the observations which is relevant to X. If the estimation process is such that all relevant information form observations are included in $\hat{X}$, then the density of the data conditioned on the estimate will not depend on X, hence the estimator will be sufficient.

1.4 Novelty of This Study and Literature Review

In the literature, the topics which are more investigated on power system State Estimation include the optimal placement of measurement devices (in particular considering PMU), bad data detection and data loss, network observability, wide-area state estimation and dynamic state estimation (DSE) techniques.

At present Least Squares (LS) method of state estimation is most widely used in power system and Weighted Least Squares (WLS) method is the one that used more often in algorithms [Li 2011].

This thesis investigates the effects of parameter and measurement uncertainties on the results of the power system Weighted Least Squares (WLS) State Estimation. The

performance of State Estimator is based mainly on the accuracy of its inputs hence this investigation is exactly related to the uncertainty of them.

The novelty of this thesis lies in the analysis of how the results of WLS State Estimation are affected when there exist both:

- The network parameters uncertainty.
- The measurements uncertainty.

This study contains useful approaches for power system planners to improve the State Estimation by determining whether to invest on increasing the measurement preciseness or perform an accurate measurement along power network to get accurate values of network parameters.

There are two interesting researches are done by Muscas et al. in [Muscas 2007a] and [Muscas 2007a] which both the uncertainty introduced by the measurement devices and the tolerance of the network parameters (line impedances) are taken into account and the aim is the optimal number and location of measurement devices. In contrast, the analyses used in this thesis are more focused on the changes of the results of State Estimator versus the network parameters uncertainty. Therefore the difference with this thesis work is that the goals are different while the approaches are similar.

Recently there is also a relevant investigation done by Rakpenthai et al. in [Rakpenthai 2012] that the network parameter uncertainty is also considered based on Parametric Interval Linear Systems. They proposed an analytical approach to find the bounds of state variables of the power system whose transmission line network parameters are within particular upper and lower bounds. The state estimation problem is formulated as a parametric interval linear system of equations and a novel method to find the outer solution or the bounds of state variables is suggested. On the contrary, in this thesis a statistical approach is utilized and we are dealing with uncertainties, not the intervals.

1.5 Notations and Operators

In this thesis the following notation for expressing matrices and the mathematical operations are used:

- **Rectangular matrices** expressed by uppercase and boldface letters, e.g. $\boldsymbol{A}$

- **Vectors** expressed by lowercase and boldface letters, e.g. $\boldsymbol{a}$
- **Scalars** expressed by lowercase and italic letters, e.g. a
- **Complex quantities** expressed by a hat over the letters, e.g. $\overline{\boldsymbol{A}}$
- **Magnitude of a complex matrix** expressed by bars around the matrix, e.g. $|\boldsymbol{A}|$

The following operators are also used for some matrix operations:

- $\mathbf{real}(.)$ and $\mathbf{imag}(.)$ operators denote the extractions of real and imaginary elements of a complex vector or matrix respectively**.**
- $\mathbf{diag}(.)$ operator returns the main diagonal elements of a matrix as a vector.
- $\mathbf{vect}(.)$ operator creates a vector from all the columns of a matrix.

CHAPTER 2

Implementation of Load Flow

In this chapter a load flow method is described. It is used to make the calculated measurement that is one of main components of the proposed algorithm.

Load flow analysis is the most important and fundamental tool including numerical analysis applied to a power system to investigate problems in power system operating and planning. It analyzes the power systems in normal steady-state operation and it usually uses simplified notation such as a one-line diagram and per-unit system. The power flow problem consists of a given transmission network where all lines are represented by a Pi-equivalent circuit and transformers by an ideal voltage transformer in series with an impedance. Once the loads, active and reactive power injections and network parameters are defined, load flow analysis solves the bus voltages and phases hence the branch power flow can be calculated. Generators and loads represent the boundary conditions of the solution. Mathematically, the power flow requires a solution of a system of simultaneous nonlinear equations. With the increase of power system scale continuously, the dimension of load flow equations now becomes very high and for the equations with such high dimensions, we cannot ensure that any mathematical method can converge to the right solution. Hence, choosing the reliable method is essential [Wang 2009], [Grainger 1994].

2.1 Literature Review on Load Flow Methods

Early on the development of first digital computers, the widely used method was Gauss-Seidel iterative method that was based on the nodal admittance matrix of the power system the impedance matrix that represents the topology and parameters of the power network [Stagg 1968]. The fundamental of this method is rather simple and its memory requirement is relatively small but its convergence is not satisfactory.

To solve this problem, the sequential substitution method based on the nodal impedance matrix is used which is also called the impedance method. The main difficulty of the impedance method is [Brown 1963]:

- High memory requirement.
- Computing burden.

The first solution for overcoming the disadvantages of the impedance method is a piecewise solution of the impedance matrix load flow. It presents a method which involves splitting a power system into pieces so that it permits use of the impedance matrix method on large systems. This method retains the same features and convergence characteristics of impedance method [Andreich 1968].

The other -and better- solution for overcoming the disadvantages of the impedance method is the Newton–Raphson method [Tinney 1967] which is more widely used and preferred even at this time. Its prominent features are:

- More accurate and reliable.
- Less number of iterations for convergence.
- Independency of the iteration number to number of buses in the system.
- Faster computations.

The Newton–Raphson power flow is the most robust power flow algorithm used in practice but however since 1970s the load flow methods continue to develop and among them the most successful is the fast decoupled method [Scott 1974].

Comparing the Newton method with the fast decoupled method, the latter method is faster and much simpler and more efficient algorithmically and needs less storage, but it may fail to converge when some of the basic assumptions do not hold. Convergence of

iterative methods depends on the dominance of the diagonal elements of the bus admittance matrix. A comparison of the convergence of the Gauss-Seidel, Newton-Raphson and the fast decoupled method power flow algorithms is shown in Figure 2.1 [Wood 1996].

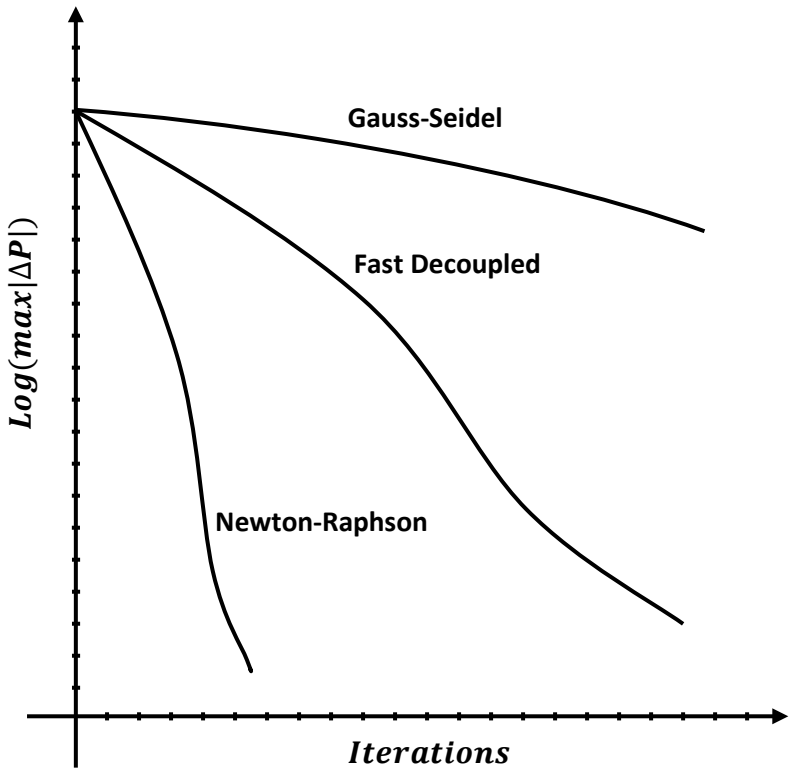

Figure 2.1: Comparison of Various Methods for Power Flow Solution [Wood 1996].

Since, Newton–Raphson method is a gradient method, the method is quite complicated and therefore, programming is also comparatively difficult and complicated. With this method the memory that is needed is rather large for large size systems but still the method is versatile, reliable and accurate and best matched for load flow calculation of large size systems [Murty 2011].

Until now the research on load flow analysis has been still very active. The artificial neural network algorithm [Nguyen 1995] [Chan 2000], the genetic algorithm [Wong 1999] and Fuzzy-logic method [Lo 1999], have also been applied to load flow analysis. However, up to now these new models and new algorithms still cannot replace the Newton-Raphson or fast decoupled methods.

According to the literature review, because of the applicability of the Newton-Raphson method on large size systems and its stability for convergence, in this thesis Newton-Raphson method is implemented for the calculation of actual state of power system based on the network parameters, power injections and loads regardless of its complicated programming.

2.2 Formation of Nodal Admittance Matrix

The formulation of an appropriate mathematical model is the first step in the analysis of an electrical network. The model must be able to describe the characteristics of individual network components and the relations that rule the interconnection of the components.

The network matrix equations provide a suitable mathematical model for digital processing. The elements of a network matrix depend on the selection of independent variables like currents or voltages (the elements of network matrix, hence, will be impedances or admittances) [Stagg 1968].

In the simulations of this thesis, the method of singular transformations is used for forming the bus admittance matrix. This method is chosen because in practice it performed faster simulations in Matlab simulation environment, compared to the methods that are described in [Zimmerman 2011] and [Wang 2009].

This section will explain the basic power network models and matrices and finally works ut the bus admittance matrix by singular transformations.

2.2.1 Bus incidence matrix *A*

The incidence of branches to buses in a connected power network is shown by the element-node incidence matrix $\boldsymbol{A}$. It does not provide any information about the electrical characteristics of the power network parameters.

This matrix is rectangular and the dimension of it is $N_{bus} \times N_{branch}$. The a_{ij} elements of $\boldsymbol{A}$ are 1 if the i^{th} branch is incident to and oriented *away from* the j^{th} bus and the a_{ij} elements will be -1 if the i^{th} branch is incident to and oriented *toward* the j^{th} bus. The other elements are zero.

If the rows of $\boldsymbol{A}$ are arranged according to a particular tree, the matrix can be partitioned into two sub-matrices. The first part is the incidence of the links going from buses to the zero reference bus that is equal to identity matrix $\boldsymbol{I}$ of the size N_{Bus} and the last sub-matrix is the incidence of network branches as shown in **Figure 2.2**.

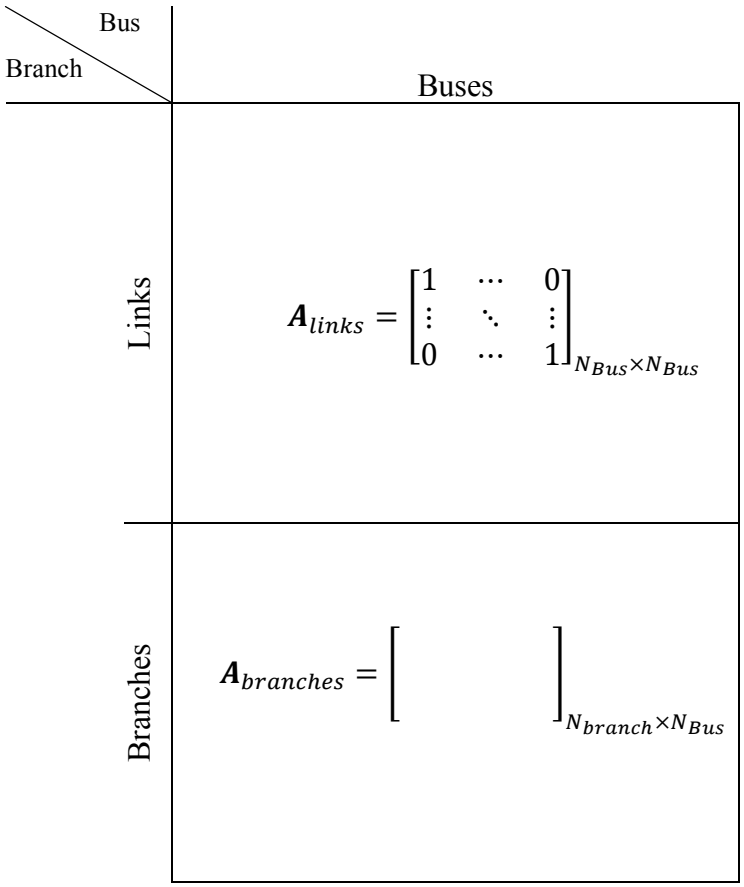

Figure 2.2 Illustration of the structure of Bus Incidence Matrix by the two sub-matrices.

2.2.2 Branch Model

A transmission line can be modeled by a two port pi-model as shown in **Figure 2.3**. Where for each line connecting bus h to k, a positive sequence series impedance of $R_{hk} + jX_{hk}$ and total line charging susceptance of jB_{hk} is considered.

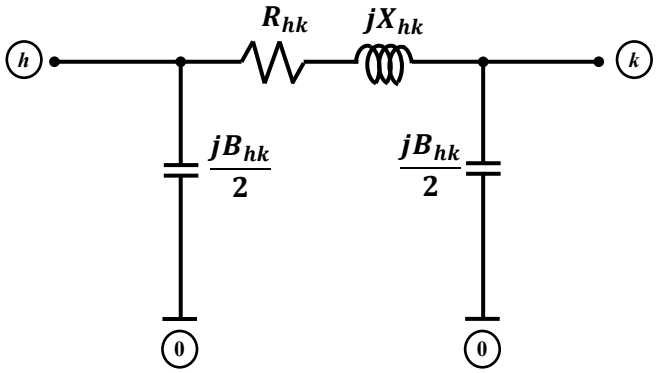

Figure 2.3 Equivalent pi-model for a transmission line.

2.2.3 Shunt Elements

Shunt capacitors or reactors for voltage and/or reactive power control, are represented by their per phase susceptance at the corresponding bus. The sign of the susceptance value will determine the type of the shunt element (positive sign shows a shunt capacitor and negative sign shows a reactor). The **Figure 2.4** Illustrates the shunt conductance and susceptance for an instance bus, *k*.

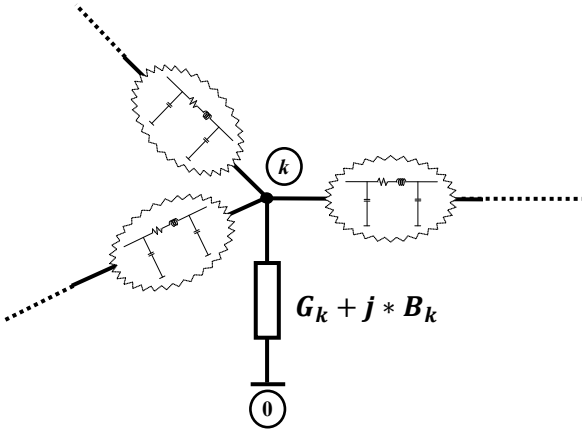

Figure 2.4 Illustration of Shunt conductance and Shunt Susceptance for an instance bus, *k*.

2.2.4 Transformers Model

Transmission lines with transformers can be modeled as series impedances, in series with ideal transformers as shown in **Figure 2.5**. The two transformer terminal buses *h* and *k* are named as the tap side bus and the impedance side bus respectively.

Figure 2.5 One-line diagram of a transmission line with transformer.

In **Figure 2.6** the two port pi-model of a transmission line is shown considering the effects of transformer tap value, a.

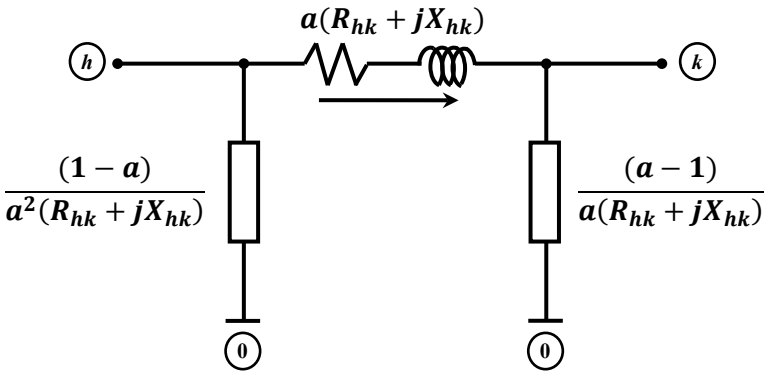

Figure 2.6 Equivalent pi-model for a transmission line with transformer tap parameter.

2.2.5 Primitive Network Matrix

The electrical characteristics of the individual network components can be presented easily in the form of a primitive network matrix $\overline{\boldsymbol{Y}}_{primitive}$. The primitive network matrix describes the characteristics of each component. It does not present anything about the network connections.

The diagonal elements of matrix $\overline{\boldsymbol{Y}}_{primitive}$ are the self-admittances and the off-diagonal elements are the mutual admittances. Assuming there is no mutual coupling between elements, the $\overline{\boldsymbol{Y}}_{primitive}$ matrix will be a diagonal matrix. The diagonal elements of

$\bar{\boldsymbol{Y}}_{primitive}$ are like a vector that consists of two parts, first the total bus admittances that are connected from buses to the Reference bus (Bus number 0) and next the branch admittances as clearly depicted in **Figure 2.7**.

$$\begin{bmatrix} \left.\begin{matrix} \bar{Y}_{1,0} \\ \vdots \\ \bar{Y}_{N_{bus},0} \end{matrix}\right\} Total\ Bus\ Admittances \\ \left.\begin{matrix} \bar{y}_1 \\ \vdots \\ \bar{y}_{N_{branch}} \end{matrix}\right\} Branch\ Admittances \end{bmatrix}_{(N_{bus}+N_{branch}) \times 1}$$

Figure 2.7 The vector of diagonal elements of $\bar{Y}_{primitive}$.

The Bus Admittance elements of this vector <u>for tap side buses</u> are defined as:

$$\bar{Y}_{i,0} = \sum_{n=1}^{\text{all the branches connected to bus i}} \left(\frac{jB_n}{2} + \frac{(1-a)}{a^2(R_n + jX_n)}\right) + Y_{shunt}$$

Where R_n and X_n are respectively the resistance and reactance of the branches that are connected to bus *i*. Y_{shunt} is the shunt admittance connected to bus *i*.

The Bus Admittance elements <u>for impedance side buses</u> are defined as:

$$\bar{Y}_{i,0} = \sum_{n=1}^{\text{all the branches connected to bus i}} \left(\frac{jB_n}{2} + \frac{(a-1)}{a(R_n + jX_n)}\right) + Y_{shunt}$$

The transformer tap value *a,* for a non-transformer branch is considered 1. The Branch Admittance elements are defined as:

$$\bar{y}_{1:N_{branch}} = \frac{1}{a(R_{hk} + jX_{hk})}$$

Where R_{hk} and X_{hk} are respectively the resistance and reactance of an instance branch that connects bus *h* to *k*.

2.2.6 Nodal Admittance Matrix

It is necessary to convert the primitive network matrix into a network matrix that describes the performance of the interconnected network. It is done by using singular transformations of the bus primitive network matrix with the bus incidence matrix. Therefore, the bus admittance matrix $\overline{\boldsymbol{Y}}_{bus}$ can be extracted by using the bus incidence matrix $\boldsymbol{A}$ to relate the primitive network's variables and parameters to the bus quantities of interconnected network [Stagg 1968].

$$\boldsymbol{Y}_{bus} = \boldsymbol{A}^T\, \overline{\boldsymbol{Y}}_{primitive}\, \boldsymbol{A}$$

The bus incidence matrix is singular, so the $[\boldsymbol{A}^T\, \overline{\boldsymbol{Y}}_{primitive}\, \boldsymbol{A}]$ is singular transformation of $\overline{\boldsymbol{Y}}_{primitive}$.

2.3 Nodal Power Equations Using the Nodal Admittances

Power system load flow is considered as the problem of finding the voltage and phase for each bus when all the active and reactive power injections are specified. If the complex power can be represented by equations of complex voltages, then a nonlinear equation solving method can be used to find a solution of the node voltage. In this section the nodal power equations are deduced using the nodal admittances. [Wang 2009, p.76]

The complex node power equations have two representation forms, polar and rectangular form:

$$\bar{S}_h = P_h + jQ_h = \bar{V}_h \sum_{k=1}^{n} \bar{Y}_{hk}^* \bar{V}_k^*$$

Which the index h is the bus number from 1 to N_{bus}. The node admittance matrix $\bar{Y}_{hk}$ is a sparse matrix and accordingly the terms in the summation are not many. The elements of node admittance matrix can be written as:

$$\bar{Y}_{hk} = G_{hk} + jB_{hk}$$

Consequently the complex node power can be expressed as:

$$P_h + jQ_h = \bar{V}_h \sum_{k=1}^{N_{bus}} (G_{hk} - jB_{hk}) \bar{V}_k^*$$

And if we consider the voltages in polar form: $\bar{V}_h = |V_h|e^{j\theta_h}$,

$$P_h + jQ_h = |V_h|e^{j\theta_h} \sum_{k=1}^{N_{bus}} (G_{hk} - jB_{hk})|V_k|e^{-j\theta_k}$$

$$P_h + jQ_h = |V_h| \sum_{k=1}^{N_{bus}} |V_k|(G_{hk} - jB_{hk})e^{j(\theta_{hk})}$$

That $\theta_{hk} = \theta_h - \theta_k$ is the voltage phase difference between node h and k. By using Euler rule: $e^{j\theta} = \cos\theta + j\sin\theta$ we can combine the exponential forms:

$$P_h + jQ_h = |V_h| \sum_{k=1}^{N_{bus}} |V_k|(G_{hk} - jB_{hk})\,(\cos\theta_{hk} + j\sin\theta_{hk})$$

$$P_h + jQ_h = |V_h| \sum_{k=1}^{N_{bus}} |V_k|(G_{hk}\cos\theta_{hk} + jG_{hk}\sin\theta_{hk} - jB_{hk}\cos\theta_{hk} + B_{hk}\sin\theta_{hk})$$

Dividing above equation into real and imaginary parts gives the **active and reactive power injection at bus h** in polar form:

$$P_h = |V_h| \sum_{k=1}^{N_{bus}} |V_k|(G_{hk}\cos\theta_{hk} + B_{hk}\sin\theta_{hk})$$

$$Q_h = |V_h| \sum_{k=1}^{N_{bus}} |V_k|(G_{hk}\sin\theta_{hk} - B_{hk}\cos\theta_{hk})$$

The last two equations are the polar form of the nodal active and reactive power equations which are the main equations in the Newton-Raphson calculation procedure.

2.4 Newton–Raphson Power Flow

Since the active and reactive powers are represented by equations of voltage magnitude and phases in previous section, a non-linear equation solving method can be applied to extract the voltage and phases for each bus.

The Newton–Raphson method is an efficient step-by-step procedure to solve nonlinear equations that it transforms the procedure of solving nonlinear equations into the

procedure of repeatedly solving linear equations. This chronological linearization process is the main part of the Newton–Raphson method [Wang 2009].

For building the mathematical models of the load flow problem, the simultaneous nonlinear equations of node voltage phasors, which are derived in the previous section, are expressed in the following forms to define the power mismatches in polar coordinates:

$$\Delta P_h = P_{sp,h} - |V_h| \sum_{k=1}^{N_{bus}} |V_k|(G_{hk}\cos\theta_{hk} + B_{hk}\sin\theta_{hk}) = 0$$

$$\Delta Q_h = Q_{sp,h} - |V_h| \sum_{k=1}^{N_{bus}} |V_k|(G_{hk}\sin\theta_{hk} - B_{hk}\cos\theta_{hk}) = 0$$

- ΔP_h and ΔQ_h are the magnitudes of active and reactive power errors respectively and the index h is the bus number (from 1 to N_{bus}).
- $P_{sp,h}$ and $Q_{sp,h}$ are the specified active and reactive powers at bus h.
- G_{hk} and B_{hk} come from the definition of bus admittance matrix in previous chapter which it was divided into real and imaginary parts as : $\bar{Y}_{hk} = G_{hk} + jB_{hk}$.

Reminding that for the load flow analysis, active and reactive powers at all the buses (except slack bus) in the power system network are specified explicitly.

Assuming that the slack bus is the first bus and the number of PV buses is N_{PV}. Hence there will be $(N_{bus} - 1)$ equations for active power:

$$\begin{cases} \Delta P_2 = P_{sp,2} - |V_2| \sum_{k=1}^{N_{bus}} |V_k|(G_{2k}\cos\theta_{2k} + B_{2k}\sin\theta_{2k}) = 0 \\ \quad \vdots \\ \Delta P_{N_{bus}} = P_{sp,N_{bus}} - |V_{N_{bus}}| \sum_{k=1}^{N_{bus}} |V_k|(G_{N_{bus}k}\cos\theta_{N_{bus}k} + B_{N_{bus}k}\sin\theta_{N_{bus}k}) = 0 \end{cases}$$

and $(N_{bus} - N_{PV} - 1)$ equations for reactive power:

$$\begin{cases} \Delta Q_2 = Q_{sp,2} - |V_2| \sum_{k=1}^{N_{bus}} |V_k|(G_{2k}\sin\theta_{2k} - B_{2k}\cos\theta_{2k}) = 0 \\ \vdots \\ \Delta Q_{N_{bus}} = Q_{sp,N_{bus}} - |V_{N_{bus}}| \sum_{k=1}^{N_{bus}} |V_k|(G_{N_{bus}k}\sin\theta_{N_{bus}k} - B_{N_{bus}k}\cos\theta_{N_{bus}k}) = 0 \end{cases}$$

Hence the total number of above equations will be $(2N_{bus} - N_{PV} - 2)$ that is equal to the number of unknowns which are $(N_{bus} - N_{PV} - 1)$ voltage magnitudes and $(N_{bus} - 1)$ angles.

The load flow analyzer considers the acceptable tolerance for ΔP_h and ΔQ_h and it solves the bus voltages (on all buses except slack and PV buses) along with the bus angles (on all buses except slack bus).

Considering the first order of Taylor Series expansion and neglecting the higher order terms of the non-linear equations for active and reactive power around the vector of unknowns that is composed of voltage magnitudes and angles of size $(2N_{bus} - N_{PV} - 2)$ gives:

$$\underbrace{\begin{bmatrix} \Delta P \\ \hline \Delta Q \end{bmatrix}}_{\textbf{Mismatches}} = \underbrace{\begin{bmatrix} \boldsymbol{A} = \frac{\partial P}{\partial \theta} & \boldsymbol{B} = \frac{\partial P}{\partial V} \\ \boldsymbol{C} = \frac{\partial Q}{\partial \theta} & \boldsymbol{D} = \frac{\partial Q}{\partial V} \end{bmatrix}}_{\textbf{Jacobians}} \underbrace{\begin{bmatrix} \Delta\theta \\ \hline \Delta V \end{bmatrix}}_{\textbf{Corrections}}$$

$\Delta\theta$ and ΔV are the voltage angle correction values and voltage magnitude correction values respectively. The last expression in extended from will be:

$$\begin{bmatrix} \Delta P_2 \\ \vdots \\ \Delta P_{N_{bus}} \\ \hline \Delta Q_2 \\ \vdots \\ \Delta Q_{N_{bus}} \end{bmatrix} = \begin{bmatrix} \begin{bmatrix} A_{22} & \cdots & A_{2,N_{bus}} \\ \vdots & \ddots & \vdots \\ A_{N_{bus},2} & \cdots & A_{N_{bus},N_{bus}} \end{bmatrix} & \begin{bmatrix} B_{22} & \cdots & B_{2,N_{bus}} \\ \vdots & \ddots & \vdots \\ B_{N_{bus},2} & \cdots & B_{N_{bus},N_{bus}} \end{bmatrix} \\ \begin{bmatrix} C_{22} & \cdots & C_{2,N_{bus}} \\ \vdots & \ddots & \vdots \\ C_{N_{bus},2} & \cdots & C_{N_{bus},N_{bus}} \end{bmatrix} & \begin{bmatrix} D_{22} & \cdots & D_{2,N_{bus}} \\ \vdots & \ddots & \vdots \\ D_{N_{bus},2} & \cdots & D_{N_{bus},N_{bus}} \end{bmatrix} \end{bmatrix} \begin{bmatrix} \Delta\theta_2 \\ \vdots \\ \Delta\theta_{N_{bus}} \\ \hline \Delta V_2 \\ \vdots \\ \Delta V_{N_{bus}} \end{bmatrix}$$

The matrices of $\boldsymbol{A}$, $\boldsymbol{B}$, $\boldsymbol{C}$ and $\boldsymbol{D}$ are the sub-blocks of the Jacobian matrix where their elements can be calculated by differentiating the equations of active and reactive power with respect to voltage angles and magnitudes. Hence the elements of the Jacobian matrix can be obtained using the following equations (for each sub-block, the first equation is related to the off-diagonal elements and the second one is for diagonal elements):

$$\begin{cases} A_{ij} = \dfrac{\partial P_i}{\partial \theta_j} = -V_i V_j \left(G_{ij} \sin\theta_{ij} - B_{ij} \cos\theta_{ij}\right) & for\ i \neq j \\ A_{ii} = \dfrac{\partial P_i}{\partial \theta_i} = V_i \sum\limits_{j \in N_{bus}}^{j \neq i} V_j \left(G_{ij} \sin\theta_{ij} - B_{ij} \cos\theta_{ij}\right) \end{cases}$$

$$\begin{cases} B_{ij} = \dfrac{\partial P_i}{\partial V_j} = -V_i \left(G_{ij} \cos\theta_{ij} + B_{ij} \sin\theta_{ij}\right) & for\ i \neq j \\ B_{ii} = \dfrac{\partial P_i}{\partial V_i} = \sum\limits_{j \in N_{bus}}^{j \neq i} -V_j \left(G_{ij} \cos\theta_{ij} + B_{ij} \sin\theta_{ij}\right) - 2V_i G_{ii} \end{cases}$$

$$\begin{cases} C_{ij} = \dfrac{\partial Q_i}{\partial \theta_j} = V_i V_j \left(G_{ij} \cos\theta_{ij} + B_{ij} \sin\theta_{ij}\right) & for\ i \neq j \\ C_{ii} = \dfrac{\partial Q_i}{\partial \theta_i} = -V_i \sum\limits_{j \in N_{bus}}^{j \neq i} V_j \left(G_{ij} \cos\theta_{ij} + B_{ij} \sin\theta_{ij}\right) \end{cases}$$

$$\begin{cases} D_{ij} = \dfrac{\partial Q_i}{\partial V_j} = -V_i \left(G_{ij} \sin\theta_{ij} - B_{ij} \cos\theta_{ij}\right) & for\ i \neq j \\ D_{ii} = \dfrac{\partial Q_i}{\partial V_i} = \sum\limits_{j \in N_{bus}}^{j \neq i} -V_j \left(G_{ij} \sin\theta_{ij} - B_{ij} \cos\theta_{ij}\right) + 2V_i B_{ii} \end{cases}$$

Jacobian matrix is a sparse matrix, and the place of zeros in this matrix is the same as place of zeros in bus admittance matrix because considering the equations of Jacobian matrix for off-diagonal elements, it can be seen that each of them is related to only one element of the bus admittance matrix. Therefore, if the element in the admittance matrix is zero, the corresponding element in the Jacobian matrix is also zero. The Jacobian matrix is not, however, symmetrical. The elements of Jacobian matrix are a function of node voltage phasors and so during the iterative process they vary with node voltages [Wang 2009].

For saving the computation time, the voltage magnitudes in the correction vector can be changed to $\frac{\Delta V}{V}$ because in this case the equations for calculating sub-matrices for A and D $A_{ij} = D_{ij}$ and $B_{ij} = -C_{ij}$. If we consider this situation, the number of elements to be calculated for Jacobian matrix are only $2(N_{bus} - 1) + [2(N_{bus} - 1)]^2/2$ instead of $[2(N_{bus} - 1)]^2$ [Murty 2011].

2.5 Newton–Raphson Solution Algorithm

The flowchart for implementation of Newton-Raphson Load Flow procedure in Polar Coordinates is depicted in Figure 2.8.

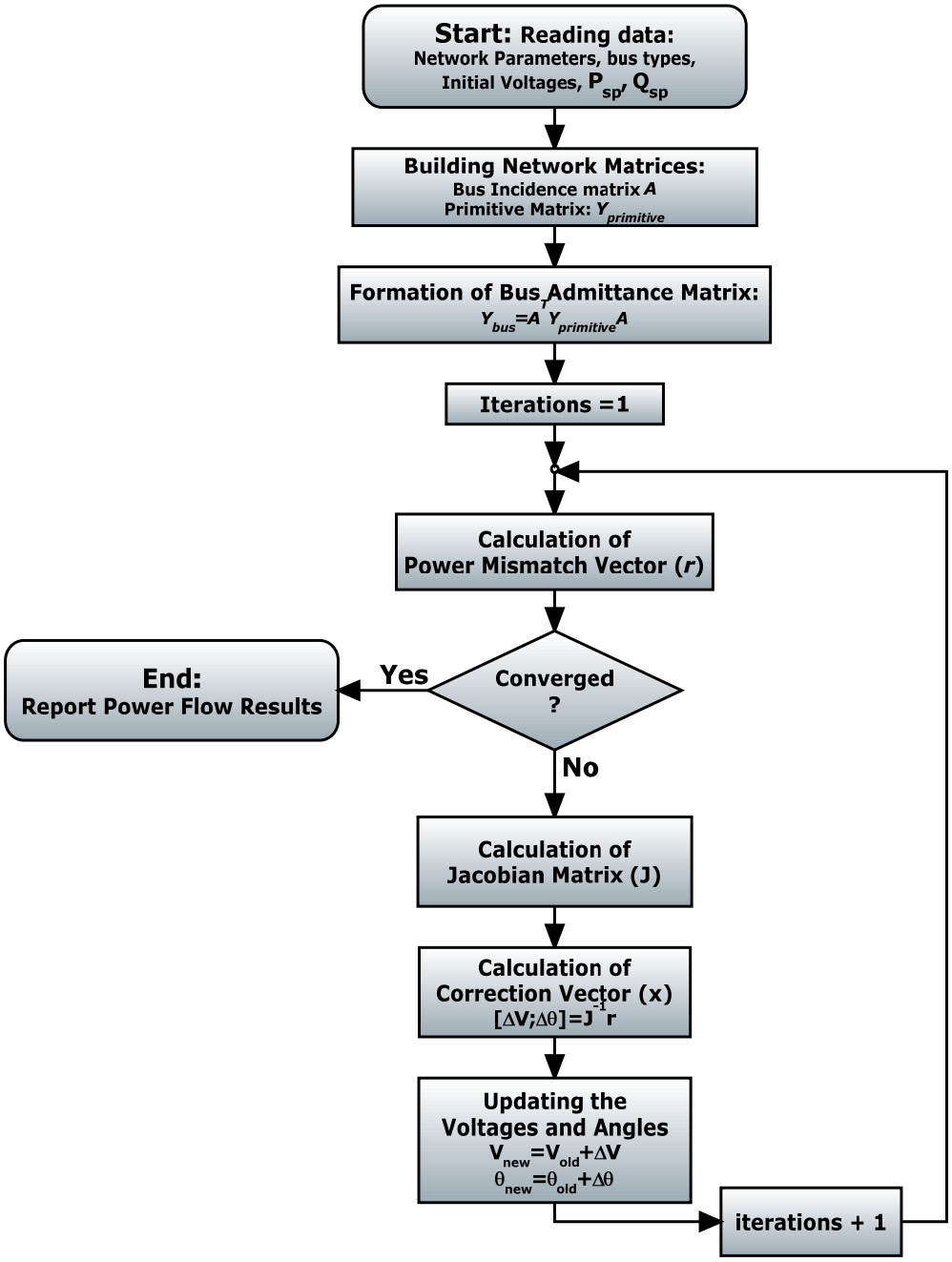

Figure 2.8 Flowchart for implementation of Newton-Raphson Load Flow

CHAPTER 3

Implementation of WLS State Estimator

3.1 Power Equations Using the Physical Admittances

To examine the behavior of the state estimator in the presence of uncertainty in the network parameters, we extract the basic equations that relate the active and reactive power injections to the voltages, angles and the network parameters using the physical admittances. Firstly we describe the equivalent pi-model for a branch and then we write the node power equations.

3.1.1 Complex Power Flow equations

Consider an equivalent pi model for a transfer line as shown in **Figure 3.1**:

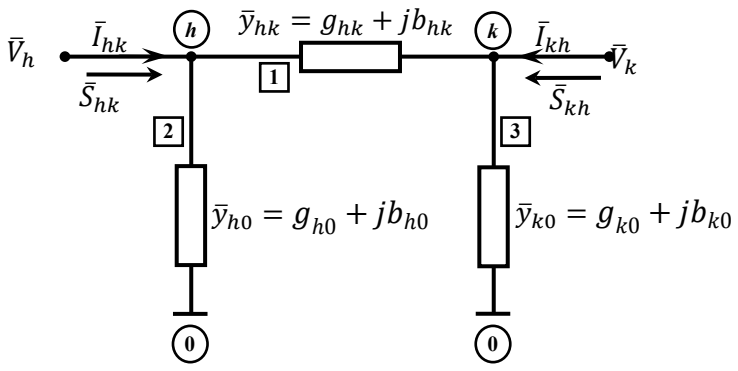

Figure 3.1 Equivalent pi-model for a branch connecting bus h to bus k.

Where:

- $\bar{V}_h$ and $\bar{V}_h$ are the complex voltages in polar form at bus h and k.
- $\bar{y}_{h0}$ and $\bar{y}_{k0}$ are the admittances of the shunt branches connected at bus h and k.
- $\bar{y}_{hk}$ is the admittance of the series branch connecting bus h to bus k.
- $\bar{I}_{hk}$ and $\bar{I}_{kh}$ are the line current flow between bus h and bus k.
- $\bar{S}_{hk}$ and $\bar{S}_{kh}$ are the complex power flows.

The reduced incidence matrix C will be:

$$C = \begin{matrix} \\ (h) \\ (k) \end{matrix} \begin{matrix} \boxed{1} & \boxed{2} & \boxed{3} \end{matrix} \begin{bmatrix} 1 & 1 & 0 \\ -1 & 0 & 1 \end{bmatrix}$$

and the branch admittance matrix is:

$$\bar{y}_b = \begin{bmatrix} \bar{y}_{hk} & 0 & 0 \\ 0 & \bar{y}_{h0} & 0 \\ 0 & 0 & \bar{y}_{k0} \end{bmatrix}.$$

The nodal admittance matrix can be found by:

$$Y = CY_bC^T$$

$$Y = \begin{bmatrix} 1 & 1 & 0 \\ -1 & 0 & 1 \end{bmatrix} \begin{bmatrix} \bar{y}_{hk} & 0 & 0 \\ 0 & \bar{y}_{h0} & 0 \\ 0 & 0 & \bar{y}_{k0} \end{bmatrix} \begin{bmatrix} 1 & -1 \\ 1 & 0 \\ 0 & 1 \end{bmatrix}$$

$$Y = \begin{bmatrix} \bar{y}_{hk} + \bar{y}_{h0} & -\bar{y}_{hk} \\ -\bar{y}_{hk} & \bar{y}_{hk} + \bar{y}_{k0} \end{bmatrix}$$

According to Ohm's law: $I = YV$, the vector of injected currents can be extracted as:

$$\begin{bmatrix} \bar{I}_{hk} \\ \bar{I}_{kh} \end{bmatrix} = \begin{bmatrix} \bar{y}_{hk} + \bar{y}_{h0} & -\bar{y}_{hk} \\ -\bar{y}_{hk} & \bar{y}_{hk} + \bar{y}_{k0} \end{bmatrix} \begin{bmatrix} \bar{V}_h \\ \bar{V}_k \end{bmatrix}$$

$$\begin{cases} \bar{I}_{hk} = (\bar{y}_{hk} + \bar{y}_{h0})\bar{V}_h - \bar{y}_{hk}\bar{V}_k \\ \bar{I}_{kh} = -\bar{y}_{hk}\bar{V}_h + (\bar{y}_{hk} + \bar{y}_{k0})\bar{V}_k \end{cases}$$

Which $\bar{I}_{hk}$ is the current from bus h to k. Finally the complex power $\bar{S}_{hk}$ that flows from bus h to bus k will be:

$$\bar{S}_{hk} = \bar{V}_h \, \bar{I}_{hk}^*$$

$$\bar{S}_{hk} = \bar{V}_h\left((\bar{y}_{hk} + \bar{y}_{h0})\bar{V}_h - \bar{y}_{hk}\bar{V}_k\right)^*$$

$$\bar{S}_{hk} = (\bar{y}_{hk} + \bar{y}_{h0})^*\bar{V}_h\bar{V}_h^* - \bar{y}_{hk}{}^*\bar{V}_h\bar{V}_k^*$$

Substituting the complex power flow $\bar{S}_{hk}$ with the elements of $\bar{y}_{hk} = g_{hk} + jb_{hk}$ yields:

$$\bar{S}_{hk} = (g_{hk} - jb_{hk} + g_{h0} - jb_{h0})|\bar{V}_h|^2 - (g_{hk} - jb_{hk})|\bar{V}_h||\bar{V}_k|e^{j\theta_{hk}}$$

Using Euler rule: $e^{j\theta} = \cos\theta + j\sin\theta$ we will have:

$$\bar{S}_{hk} = \left(g_{hk} + g_{h0} - j(b_{hk} + b_{h0})\right)|\bar{V}_h|^2 - (g_{hk} - jb_{hk})(\cos\theta_{hk} + j\sin\theta_{hk})|\bar{V}_h||\bar{V}_k|$$

$$\begin{aligned}\bar{S}_{hk} = \\ &= \left(g_{hk} + g_{h0} - j(b_{hk} + b_{h0})\right)|\bar{V}_h|^2 - \\ &- [(g_{hk}\cos\theta_{hk} + jg_{hk}\sin\theta_{hk} - jb_{hk}\cos\theta_{hk} + b_{hk}\sin\theta_{hk})]|\bar{V}_h||\bar{V}_k|\end{aligned}$$

$$\begin{aligned}\bar{S}_{hk} = \\ &= (g_{hk} + g_{h0})|\bar{V}_h|^2 - j(b_{hk} + b_{h0})|\bar{V}_h|^2 - (g_{hk}\cos\theta_{hk})|\bar{V}_h||\bar{V}_k| - \\ &- j(g_{hk}\sin\theta_{hk})|\bar{V}_h||\bar{V}_k| + j(b_{hk}\cos\theta_{hk})|\bar{V}_h||\bar{V}_k| - (b_{hk}\sin\theta_{hk})|\bar{V}_h||\bar{V}_k|\end{aligned}$$

$$\begin{aligned}\bar{S}_{hk} = \\ &= (g_{hk} + g_{h0})|\bar{V}_h|^2 - (b_{hk}\sin\theta_{hk})|\bar{V}_h||\bar{V}_k| - (g_{hk}\cos\theta_{hk})|\bar{V}_h||\bar{V}_k| - \\ &- j(g_{hk}\sin\theta_{hk})|\bar{V}_h||\bar{V}_k| + j(b_{hk}\cos\theta_{hk})|\bar{V}_h||\bar{V}_k| - j(b_{hk} + b_{h0})|\bar{V}_h|^2\end{aligned}$$

$$\begin{aligned}\bar{S}_{hk} = \\ &= (g_{hk} + g_{h0})|\bar{V}_h|^2 - (g_{hk}\cos\theta_{hk})|\bar{V}_h||\bar{V}_k| - (b_{hk}\sin\theta_{hk})|\bar{V}_h||\bar{V}_k| + \\ &+ j[-(g_{hk}\sin\theta_{hk})|\bar{V}_h||\bar{V}_k| + (b_{hk}\cos\theta_{hk})|\bar{V}_h||\bar{V}_k| - (b_{hk} + b_{h0})|\bar{V}_h|^2]\end{aligned}$$

$$\begin{aligned}\bar{S}_{hk} = \\ &= (g_{hk} + g_{h0})|\bar{V}_h|^2 - (g_{hk}\cos\theta_{hk} + b_{hk}\sin\theta_{hk})|\bar{V}_h||\bar{V}_k| + j[-(b_{hk} + b_{h0})|\bar{V}_h|^2 - \\ &- (g_{hk}\sin\theta_{hk} - b_{hk}\cos\theta_{hk})|\bar{V}_h||\bar{V}_k|]\end{aligned}$$

The complex power flow can decomposed into its real and imaginary parts:

$$\bar{S}_{hk} = P_{hk} + jQ_{hk}$$

Therefore the active and reactive power flows can be finally extracted as:

$$P_{hk} = (g_{hk} + g_{h0})|\bar{V}_h|^2 - (g_{hk}\cos\theta_{hk} + b_{hk}\sin\theta_{hk})|\bar{V}_h||\bar{V}_k|$$

$$Q_{hk} = -(b_{hk} + b_{h0})|\bar{V}_h|^2 - (g_{hk}\sin\theta_{hk} - b_{hk}\cos\theta_{hk})|\bar{V}_h||\bar{V}_k|$$

3.2 Measurement Model

For a power network the set of measurements $\boldsymbol{z}$ given are by:

$$\boldsymbol{z} = \begin{bmatrix} z_1 \\ z_2 \\ \vdots \\ z_m \end{bmatrix} = \begin{bmatrix} f_1(x_1, \dots, x_n) \\ f_2(x_1, \dots, x_n) \\ \vdots \\ f_m(x_1, \dots, x_n) \end{bmatrix} + \begin{bmatrix} r_1 \\ r_2 \\ \vdots \\ r_m \end{bmatrix} = \boldsymbol{f}(x) + \boldsymbol{r}$$

where:

$f_i(x)$ is the non-linear function relating measurement i to the state vector x

$\boldsymbol{r}$ is the vector of measurement errors

Regarding to the statistical properties of the measurement errors, for $i = 1, \dots, m$ we commonly have $E[r_i] = 0$. Also the measurement errors are considered to be independent, i.e. $E[r_i r_j] = 0$. Furthermore, they are assumed to have a Gaussian distribution with zero mean.

The measurement vector $\boldsymbol{z}$ is composed of the conventional measurements including: Voltage magnitude, Active power injections, Reactive power injections, Active power flows and Reactive power flows along with a set of phase measurements from PMU. The measurement vector is in the following form:

$$\boldsymbol{z} = \begin{bmatrix} |V_1| \\ \vdots \\ |V_{N_v}| \end{bmatrix} Voltage\ Magnitudes \\ \begin{bmatrix} P_1 \\ \vdots \\ P_{N_i} \end{bmatrix} Active\ Power\ Injection \\ \begin{bmatrix} Q_1 \\ \vdots \\ Q_{N_i} \end{bmatrix} Rective\ Power\ Injection \\ \begin{bmatrix} PF_1 \\ \vdots \\ PF_{N_f} \end{bmatrix} Active\ Line\ Power\ Flow \\ \begin{bmatrix} QF_1 \\ \vdots \\ QF_{N_f} \end{bmatrix} Rective\ Line\ Power\ Flow \\ \begin{bmatrix} \varphi_1 \\ \vdots \\ \varphi_{N_\varphi} \end{bmatrix} Phases\ From\ PMU \\ \Big]_{(N_v+2N_i+2N_f+N_\varphi)\times 1}$$

For the non-linear functions relating measurement i to the state vector, the power injection and power flow equations, which are proven in previous chapter and in this chapter, are considered. The equations can be summarized here as:

$$\begin{cases} P_h = |V_h| \sum_{k=1}^{N_{bus}} |V_k|(G_{hk}\cos\theta_{hk} + B_{hk}\sin\theta_{hk}) \\ Q_h = |V_h| \sum_{k=1}^{N_{bus}} |V_k|(G_{hk}\sin\theta_{hk} - B_{hk}\cos\theta_{hk}) \\ P_{hk} = (g_{hk} + g_{h0})|\bar{V}_h|^2 - (g_{hk}\cos\theta_{hk} + b_{hk}\sin\theta_{hk})|\bar{V}_h||\bar{V}_k| \\ Q_{hk} = -(b_{hk} + b_{h0})|\bar{V}_h|^2 - (g_{hk}\sin\theta_{hk} - b_{hk}\cos\theta_{hk})|\bar{V}_h||\bar{V}_k| \end{cases}$$

3.3 Minimization Problem

For obtaining the states (voltages and related phases of the power system) from the measurements, state estimation is applied to $\boldsymbol{r = z - f(x)}$**.** So, the minimization problem will be:

$$\begin{cases} MIN & \boldsymbol{J(x) = r^T r} \\ S.T. & \boldsymbol{r = z - f(x)} \end{cases}$$

Which $\boldsymbol{J(x)}$ is the *objective function* that is going to be minimized. The objective function can be written as:

$$\boldsymbol{J(x) = [z - f(x)]^T [z - f(x)]}$$

To minimize $\boldsymbol{J(x)}$, its first derivative with respect to $\boldsymbol{x}$ is equated to zero:

$$\frac{\boldsymbol{\partial J(x)}}{\boldsymbol{\partial x}} = \boldsymbol{0}$$

$$\frac{\boldsymbol{\partial J(x)}}{\boldsymbol{\partial x}} = \frac{\boldsymbol{\partial [z^T z - z^T f(x) - f(x)^T z + f(x)^T f(x)]}}{\boldsymbol{\partial x}} = \boldsymbol{-2 z^T \frac{\partial f(x)}{\partial x} + 2 f(x)^T \frac{\partial f(x)}{\partial x}}$$

$$\frac{\boldsymbol{\partial J(x)}}{\boldsymbol{\partial x}} = \boldsymbol{-2[z - f(x)]^T \left[\frac{\partial f(x)}{\partial x}\right]}$$

The Jacobian matrix of $\boldsymbol{J(x)}$ is defined by $\boldsymbol{g(x)}$:

$$\boldsymbol{g(x) = \left[\frac{\partial J(x)}{\partial x}\right]^T = -2\left[\frac{\partial f(x)}{\partial x}\right]^T [z - f(x)]}$$

The Jacobian Matrix structure and equations of calculating its components will be described in the next sub-section.

The Hessian matrix of $\boldsymbol{J(x)}$ is the second derivative with respect to $\boldsymbol{x}$ and called *Gain Matrix*:

$$\boldsymbol{H(x)} = \frac{\boldsymbol{\partial g(x)}}{\boldsymbol{\partial x}} = \mathbf{2}\left[\frac{\boldsymbol{\partial f(x)}}{\boldsymbol{\partial x}}\right]^{\boldsymbol{T}}\left[\frac{\boldsymbol{\partial f(x)}}{\boldsymbol{\partial x}}\right]$$

$\boldsymbol{H(x)}$ is symmetric, positive definite and is a matrix populated primarily with zeros (a sparse matrix).

The Taylor Series expansion of the non linear function $\boldsymbol{g(x)}$ around the state vector x^k gives:

$$\boldsymbol{g(x)} = \boldsymbol{g(x_k)} + \frac{\boldsymbol{\partial g(x_k)}}{\boldsymbol{\partial x}}\boldsymbol{(x - x_k)} + \cdots = \mathbf{0}$$

Considering the first order of Taylor Series expansion and neglecting the higher order terms, directs us to an iterative solution of Gauss-Newton method:

$$\boldsymbol{x_{k+1}} = \boldsymbol{x_k} - \left[\boldsymbol{\partial g(x_k)}/_{\boldsymbol{\partial x}}\right]^{-1}\boldsymbol{g(x_k)}$$

Where k is the iteration index and $\boldsymbol{x_k}$ is the state vector at iteration k. Supposing:

$$\boldsymbol{\Delta x_{k+1}} = \boldsymbol{x_{k+1}} - x_k$$

We will have:

$$\boldsymbol{\Delta x_{k+1}} = -[\boldsymbol{H(x_k)}]^{-1}\boldsymbol{g(x_k)}$$

Finding the inverse of $\boldsymbol{H(x_k)}$ in high dimensions for large networks can be an expensive and time consuming operation. In such cases, instead of directly inverting the $\boldsymbol{H(x_k)}$, it's better to calculate the $\boldsymbol{\Delta x_{k+1}}$ as the solution to the system of linear equations:

$$[\boldsymbol{H(x_k)}]\boldsymbol{\Delta x_{k+1}} = -\boldsymbol{g(x_k)}$$

$$[\boldsymbol{H(x_k)}]\boldsymbol{\Delta x_{k+1}} = 2\left[\frac{\boldsymbol{\partial f(x_k)}}{\boldsymbol{\partial x}}\right]^{\boldsymbol{T}}\boldsymbol{[z - f(x_k)]}$$

This can be solved by triangular factorization techniques, like the Cholesky factorization. The set of equation given by $[\boldsymbol{H(x_k)}]\boldsymbol{\Delta x_{k+1}}$ is also mentioned as the Normal Equations.

3.3.1 Jacobian Matrix structure and components

According to the measurement vector structure, the Jacobian matrix will be in the following form:

$$\boldsymbol{g} = \begin{bmatrix} \begin{bmatrix} \boldsymbol{g_{11}} \end{bmatrix} & \begin{bmatrix} \boldsymbol{g_{12}} \end{bmatrix} \\ \begin{bmatrix} \boldsymbol{g_{21}} \end{bmatrix} & \begin{bmatrix} \boldsymbol{g_{22}} \end{bmatrix} \\ \begin{bmatrix} \boldsymbol{g_{31}} \end{bmatrix} & \begin{bmatrix} \boldsymbol{g_{32}} \end{bmatrix} \\ \begin{bmatrix} \boldsymbol{g_{41}} \end{bmatrix} & \begin{bmatrix} \boldsymbol{g_{42}} \end{bmatrix} \\ \begin{bmatrix} \boldsymbol{g_{51}} \end{bmatrix} & \begin{bmatrix} \boldsymbol{g_{52}} \end{bmatrix} \\ \begin{bmatrix} \boldsymbol{g_{61}} \end{bmatrix} & \begin{bmatrix} \boldsymbol{g_{62}} \end{bmatrix} \end{bmatrix}$$

Where the sub-matrices is described in the following:

- $\boldsymbol{g_{11}}$ is the Derivative of Voltage Magnitudes with respect to angles:

$$\boldsymbol{g_{11}} = \frac{\partial |\bar{V}|}{\partial \theta} = \begin{bmatrix} 0 & \cdots & 0 \\ \vdots & \ddots & \vdots \\ 0 & \cdots & 0 \end{bmatrix}_{N_v \times (N_{bus}-1)}$$

  - All the elements are zero.

- $\boldsymbol{g_{12}}$ is the derivative of Voltage Magnitudes with respect to Voltage Magnitudes:

$$\boldsymbol{g_{12}} = \frac{\partial |\bar{V}|}{\partial |\bar{V}|} = \begin{bmatrix} 1 & 0 & 0 & \dots \\ 0 & 1 & 0 & \dots \\ 0 & 0 & 1 & \dots \\ \vdots & \vdots & \vdots & \ddots \end{bmatrix}_{N_v \times (N_{bus})}$$

  - All the elements are zero except the diagonals that are one.

- $\boldsymbol{g_{21}}$ is the derivative of Real Power Injections with respect to Angles:

$$\boldsymbol{g_{21}} = \frac{\partial P}{\partial \theta} = \begin{bmatrix} \frac{\partial P_1}{\partial \theta_2} & \cdots & \frac{\partial P_1}{\partial \theta_{N_{bus}}} \\ \vdots & \ddots & \vdots \\ \frac{\partial P_{N_{pi}}}{\partial \theta_2} & \cdots & \frac{\partial P_{N_{pi}}}{\partial \theta_{N_{bus}}} \end{bmatrix}_{N_{pi} \times (N_{bus}-1)}$$

Equations for calculation of $\boldsymbol{g_{21}}$ components:

$$\frac{\partial P_k}{\partial \theta_k} = -B_{kk}|\bar{V}_k|^2 + \sum_{j=1}^{N_{bus}} |\bar{V}_j|(-G_{kj}\sin\theta_{kj} + B_{kj}\cos\theta_{kj})$$

$$\frac{\partial P_k}{\partial \theta_j} = |\bar{V}_k||\bar{V}_j|(G_{kj}\sin\theta_{kj} - B_{kj}\cos\theta_{kj})$$

- $\boldsymbol{g_{22}}$ is the derivative of Real Power Injections with respect to Voltage Magnitudes:

$$\boldsymbol{g_{22}} = \frac{\partial P}{\partial |\bar{V}|} = \begin{bmatrix} \frac{\partial P_1}{\partial |\bar{V}_1|} & \cdots & \frac{\partial P_1}{\partial |\bar{V}_{N_{bus}}|} \\ \vdots & \ddots & \vdots \\ \frac{\partial P_{N_{pi}}}{\partial |\bar{V}_1|} & \cdots & \frac{\partial P_{N_{pi}}}{\partial |\bar{V}_{N_{bus}}|} \end{bmatrix}_{N_{pi} \times (N_{bus})}$$

Equations for calculation of $\boldsymbol{g_{22}}$ components:

$$\frac{\partial P_k}{\partial |\bar{V}_k|} = G_{kk}|\bar{V}_k| + \sum_{j=1}^{n} |\bar{V}_j|(G_{kj}\cos\theta_{kj} + B_{kj}\sin\theta_{kj})$$

$$\frac{\partial P_k}{\partial |\bar{V}_j|} = |\bar{V}_k|(G_{kj}\cos\theta_{kj} + B_{kj}\sin\theta_{kj})$$

- $\boldsymbol{g_{31}}$ is the derivative of Reactive Power Injections with respect to Angles:

$$\boldsymbol{g_{31}} = \frac{\partial Q}{\partial \theta} = \begin{bmatrix} \frac{\partial Q_1}{\partial \theta_2} & \cdots & \frac{\partial Q_1}{\partial \theta_{N_{bus}}} \\ \vdots & \ddots & \vdots \\ \frac{\partial Q_{N_{qi}}}{\partial \theta_2} & \cdots & \frac{\partial Q_{N_{qi}}}{\partial \theta_{N_{bus}}} \end{bmatrix}_{N_{qi} \times (N_{bus}-1)}$$

Equations for calculation of $\boldsymbol{g_{31}}$ components:

$$\frac{\partial Q_k}{\partial \theta_k} = -G_{kk}|\bar{V}_k|^2 + \sum_{j=1}^{n} |\bar{V}_j|(G_{kj}\cos\theta_{kj} + B_{kj}\sin\theta_{kj})$$

$$\frac{\partial Q_k}{\partial \theta_j} = -|\bar{V}_k||\bar{V}_j|(G_{kj}\cos\theta_{kj} + B_{kj}\sin\theta_{kj})$$

- $\boldsymbol{g_{32}}$ is the derivative of Reactive Power Injections with respect to Voltage Magnitudes:

$$\boldsymbol{g_{32}} = \frac{\partial Q}{\partial |\bar{V}|} = \begin{bmatrix} \frac{\partial Q_1}{\partial |\bar{V}_1|} & \cdots & \frac{\partial Q_1}{\partial |\bar{V}_{N_{bus}}|} \\ \vdots & \ddots & \vdots \\ \frac{\partial Q_{N_{qi}}}{\partial |\bar{V}_1|} & \cdots & \frac{\partial Q_{N_{qi}}}{\partial |\bar{V}_{N_{bus}}|} \end{bmatrix}_{N_{qi}\times(N_{bus})}$$

Equations for calculation of $\boldsymbol{g_{32}}$ components:

$$\frac{\partial Q_k}{\partial |\bar{V}_k|} = -B_{kk}|\bar{V}_k| + \sum_{j=1}^{n} |\bar{V}_j|(G_{kj}\sin\theta_{kj} - B_{kj}\cos\theta_{kj})$$

$$\frac{\partial Q_k}{\partial |\bar{V}_j|} = |\bar{V}_k|(G_{kj}\sin\theta_{kj} - B_{kj}\cos\theta_{kj})$$

- $\boldsymbol{g_{41}}$ is the derivative of Real Power Flows with respect to Angles:

$$\boldsymbol{g_{41}} = \frac{\partial P_{fl}}{\partial \theta} = \begin{bmatrix} \frac{\partial P_{fl_1}}{\partial \theta_2} & \cdots & \frac{\partial P_{fl_1}}{\partial \theta_{N_{bus}}} \\ \vdots & \ddots & \vdots \\ \frac{\partial P_{fl_{N_{pf}}}}{\partial \theta_2} & \cdots & \frac{\partial P_{fl_{N_{pf}}}}{\partial \theta_{N_{bus}}} \end{bmatrix}_{N_{pf}\times(N_{bus}-1)}$$

Equations for calculation of $\boldsymbol{g_{41}}$ components:

$$\frac{\partial P_{fl}{}_{hk}}{\partial \theta_h} = |\bar{V}_h||\bar{V}_k|(g_{hk}\sin\theta_{hk} - b_{hk}\cos\theta_{hk})$$

$$\frac{\partial P_{fl}{}_{hk}}{\partial \theta_k} = -|\bar{V}_h||\bar{V}_k|(g_{hk}\sin\theta_{hk} - b_{hk}\cos\theta_{hk})$$

- $\boldsymbol{g_{42}}$ is the derivative of Real Power Flows with respect to Voltage Magnitudes:

$$\boldsymbol{g_{42}} = \frac{\partial P_{fl}}{\partial |\bar{V}|} = \begin{bmatrix} \frac{\partial P_{fl_1}}{\partial |\bar{V}_1|} & \cdots & \frac{\partial P_{fl_1}}{\partial |\bar{V}_{N_{bus}}|} \\ \vdots & \ddots & \vdots \\ \frac{\partial P_{fl_{N_{pf}}}}{\partial |\bar{V}_1|} & \cdots & \frac{\partial P_{fl_{N_{pf}}}}{\partial |\bar{V}_{N_{bus}}|} \end{bmatrix}_{N_{pf} \times (N_{bus})}$$

Equations for calculation of $\boldsymbol{g_{42}}$ components:

$$\frac{\partial P_{fl_{hk}}}{\partial |\bar{V}_h|} = -|\bar{V}_k|(g_{hk}\cos\theta_{hk} + b_{hk}\sin\theta_{hk}) + 2(g_{hk} + g_{h0})|\bar{V}_h|$$

$$\frac{\partial P_{fl_{hk}}}{\partial |\bar{V}_k|} = -|\bar{V}_h|(g_{hk}\cos\theta_{hk} + b_{hk}\sin\theta_{hk})$$

- $\boldsymbol{g_{51}}$ is the derivative of Reactive Power Flows with respect to Angles:

$$\boldsymbol{g_{51}} = \frac{\partial Q_{fl}}{\partial \theta} = \begin{bmatrix} \frac{\partial Q_{fl}}{\partial \theta_2} & \cdots & \frac{\partial Q_{fl_1}}{\partial \theta_{N_{bus}}} \\ \vdots & \ddots & \vdots \\ \frac{\partial Q_{fl_{N_{qf}}}}{\partial \theta_2} & \cdots & \frac{\partial Q_{fl_{N_{qf}}}}{\partial \theta_{N_{bus}}} \end{bmatrix}_{N_{qf} \times (N_{bus}-1)}$$

Equations for calculation of $\boldsymbol{g_{51}}$ components:

$$\frac{\partial Q_{fl_{hk}}}{\partial \theta_h} = -|\bar{V}_h||\bar{V}_k|(g_{hk}\cos\theta_{hk} + b_{hk}\sin\theta_{hk})$$

$$\frac{\partial Q_{fl_{hk}}}{\partial \theta_k} = |\bar{V}_h||\bar{V}_k|(g_{hk}\cos\theta_{hk} + b_{hk}\sin\theta_{hk})$$

- $\boldsymbol{g_{52}}$ is the derivative of Reactive Power Flows with respect to Voltage Magnitudes:

$$\boldsymbol{g_{52}} = \frac{\partial Q_{fl}}{\partial |\bar{V}|} = \begin{bmatrix} \frac{\partial Q_{fl_1}}{\partial |\bar{V}_1|} & \cdots & \frac{\partial Q_{fl_1}}{\partial |\bar{V}_{N_{bus}}|} \\ \vdots & \ddots & \vdots \\ \frac{\partial Q_{fl_{N_{qf}}}}{\partial |\bar{V}_1|} & \cdots & \frac{\partial Q_{fl_{N_{qf}}}}{\partial |\bar{V}_{N_{bus}}|} \end{bmatrix}_{N_{qf} \times (N_{bus})}$$

Equations for calculation of $\boldsymbol{g_{52}}$ components:

$$\frac{\partial Q_{fl_{hk}}}{\partial |\bar{V}_h|} = -|\bar{V}_k|(g_{hk}\sin\theta_{hk} - b_{hk}\cos\theta_{hk}) - 2(b_{hk} + b_{h0})|\bar{V}_h|$$

$$\frac{\partial Q_{fl_{hk}}}{\partial |\bar{V}_k|} = -|\bar{V}_h|(g_{hk}\sin\theta_{hk} - b_{hk}\cos\theta_{hk})$$

- $\boldsymbol{g_{61}}$ is the derivative of PMU Angles with respect to Angles:

$$\boldsymbol{g_{61}} = \frac{\partial\theta}{\partial\theta} = \begin{bmatrix} all\ zeros \\ except \\ one\ (-1)\ in\ each\ row \end{bmatrix}_{N_\theta \times (N_{bus}-1)}$$

  - In each row there is only a (-1) corresponding to the PMU bus number and the other elements are zero.

- $\boldsymbol{g_{62}}$ is the derivative of PMU Angles with respect to Voltage Magnitudes:

$$\boldsymbol{g_{62}} = \frac{\partial\theta}{\partial|\bar{V}|} = \begin{bmatrix} 0 & \cdots & 0 \\ \vdots & \ddots & \vdots \\ 0 & \cdots & 0 \end{bmatrix}_{N_\theta \times (N_{bus})}$$

  - All the elements are zero.

3.4 Minimization Problem Considering the Measurements Uncertainty

In realistic networks, all the measurements are not accurate and have deviation from the real values. Besides some values of measurement vector z are not practically measured and some predictive statistics and history are used to determine them (e.g. some power fluxes) [Valenzuela 2000]. So the measurements are depend upon uncertain quantities and can be considered as random variables.

To extract the states of the system (voltages and related phases) from the measurements, Weighted Least Squares (WLS) estimation is applied to $\big(\boldsymbol{z} - \boldsymbol{f}(x)\big)$. WLS state estimation will minimize the weighted sum of the squares of the measurement residuals.

$$\boldsymbol{z} = \begin{bmatrix} z_1 \\ z_2 \\ \vdots \\ z_m \end{bmatrix} = \begin{bmatrix} f_1(x_1, \dots, x_n) \\ f_2(x_1, \dots, x_n) \\ \vdots \\ f_m(x_1, \dots, x_n) \end{bmatrix} + \begin{bmatrix} r_1 \\ r_2 \\ \vdots \\ r_m \end{bmatrix} = \boldsymbol{f}(x) + \boldsymbol{r}$$

The minimization problem will be:

$$\begin{cases} MIN & \boldsymbol{J(x) = r^T \Sigma_z^{-1} r} \\ S.T. & \boldsymbol{r = z - f}(x) \end{cases}$$

The $\boldsymbol{\Sigma_z}$ is the variance-covariance matrix of measurement errors. Its inverse represents the weighting matrix that is the inverse of measurement covariance matrix. The elements of weighting matrix $\boldsymbol{\Sigma_z^{-1}}$ cause to be connected with the influence of measurements [Huang 2003].

$$\boldsymbol{\Sigma_z} = cov(\boldsymbol{r}) = E[\boldsymbol{r}.\boldsymbol{r}^T]$$

$$\boldsymbol{\Sigma_z^{-1}} = \begin{bmatrix} \sigma_1^2 & 0 & \cdots & 0 \\ 0 & \sigma_2^2 & & \vdots \\ \vdots & & \ddots & 0 \\ 0 & \cdots & 0 & \sigma_m^2 \end{bmatrix}^{-1}$$

Which σ_m^2 is the variance, and σ_m is the standard deviation of m^{th} measurement. Standard deviation of each measurement is deliberated to reflect the expected accuracy of the corresponding meter used.

The objective function can be written as:

$$\boldsymbol{J}(x) = [\boldsymbol{z - f}(x)]^T \boldsymbol{\Sigma_z^{-1}} [\boldsymbol{z - f}(x)]$$

For minimization, the first derivative with respect to x is equated to zero:

$$\frac{\partial \boldsymbol{J(x)}}{\partial \boldsymbol{x}} = 0$$

The Jacobian matrix of $\boldsymbol{J(x)}$ is defined by $\boldsymbol{g(x)}$:

$$\boldsymbol{g}(x) = \left[\frac{\boldsymbol{\partial J(x)}}{\boldsymbol{\partial x}}\right]^T = -2\left[\frac{\boldsymbol{\partial f(x)}}{\boldsymbol{\partial x}}\right]^T \boldsymbol{\Sigma_z^{-1}} [\boldsymbol{z - f(x)}] = 0$$

All the proofs for $\boldsymbol{g(x)}$ can be found in the appendices.

The Hessian matrix of $\boldsymbol{J(x)}$ is the second derivative with respect to $\boldsymbol{x}$:

$$\boldsymbol{H(x)} = \frac{\boldsymbol{\partial g(x)}}{\boldsymbol{\partial x}} \cong \boldsymbol{2}\left[\frac{\boldsymbol{\partial f(x)}}{\boldsymbol{\partial x}}\right]^{\boldsymbol{T}} \boldsymbol{\Sigma_z^{-1}} \left[\frac{\boldsymbol{\partial f(x)}}{\boldsymbol{\partial x}}\right]$$

All the proofs for $\boldsymbol{H(x)}$ also can be found in the appendices.

The Taylor Series expansion of the non linear function $\boldsymbol{g}(\boldsymbol{x})$ around the state vector $\boldsymbol{x}^k$ gives:

$$\boldsymbol{g}(\boldsymbol{x}) = \boldsymbol{g}(\boldsymbol{x}_k) + \frac{\partial \boldsymbol{g}(\boldsymbol{x}_k)}{\partial \boldsymbol{x}}(\boldsymbol{x} - \boldsymbol{x}_k) + \cdots = 0$$

Considering the first order of Taylor Series expansion and neglecting the higher order terms, directs us to an iterative solution of Gauss-Newton method:

$$\boldsymbol{x}_{k+1} = \boldsymbol{x}_k - \left[\frac{\partial \boldsymbol{g}(\boldsymbol{x}_k)}{\partial \boldsymbol{x}}\right]^{-1} \boldsymbol{g}(\boldsymbol{x}_k)$$

Where k is the iteration index and x_k is the state vector at iteration k. Supposing:

$$\boldsymbol{\Delta x}_{k+1} = \boldsymbol{x}_{k+1} - \boldsymbol{x}_k$$

We will have:

$$\boldsymbol{\Delta x}_{k+1} = -[\boldsymbol{H}(\boldsymbol{x}_k)]^{-1}\boldsymbol{g}(\boldsymbol{x}_k)$$

$\boldsymbol{H}(\boldsymbol{x}_k)$ is symmetric, positive definite, sparse matrix and called the *Gain Matrix*. Finding the inverse of $\boldsymbol{H}(\boldsymbol{x}_k)$ in high dimensions for large networks can be an expensive and time consuming operation. In such cases, instead of directly inverting the $\boldsymbol{H}(\boldsymbol{x}_k)$, it's better to calculate the $\boldsymbol{\Delta x}_{k+1}$ as the solution to the system of linear equations:

$$[\boldsymbol{H}(\boldsymbol{x}_k)]\boldsymbol{\Delta x}_{k+1} = -\boldsymbol{g}(\boldsymbol{x}_k)$$

$$[\boldsymbol{H}(\boldsymbol{x}_k)]\boldsymbol{\Delta x}_{k+1} = 2\left[\frac{\partial \boldsymbol{f}(\boldsymbol{x}_k)}{\partial \boldsymbol{x}}\right]^{T} \boldsymbol{\Sigma}_z^{-1}[\boldsymbol{z} - \boldsymbol{f}(\boldsymbol{x}_k)]$$

This can be solved by Cholesky factorization. The set of equation given by $[\boldsymbol{H}(\boldsymbol{x}_k)]\boldsymbol{\Delta x}_{k+1}$ is also mentioned as the Normal Equations.

The conditions for stopping the iterations are firstly if the number of iterations is enough or the difference in two successive state variables is less than a satisfactory tolerance, i.e. $\max|\boldsymbol{\Delta x}_{k+1}| < Tolerance$.

The variance covariance matrix of the estimates can be extracted by:

$$\boldsymbol{\Sigma}_x = \left[\left[\frac{\partial \boldsymbol{f}(\boldsymbol{x})}{\partial \boldsymbol{x}}\right]^{T} \boldsymbol{\Sigma}_z^{-1} \left[\frac{\partial \boldsymbol{f}(\boldsymbol{x})}{\partial \boldsymbol{x}}\right]\right]^{-1}$$

As it can be seen in the last equation, the parameters uncertainty does not have any contribution to the computation of variance covariance matrix of the estimates. In the next chapter a method is proposed to consider both the contribution of measurement and parameters uncertainty on variance covariance matrix of estimates.

CHAPTER 5

Algorithm Development

The flowchart of implementation is depicted in Figure 4.1. In the following, the sub-blocks and the steps are described in detail.

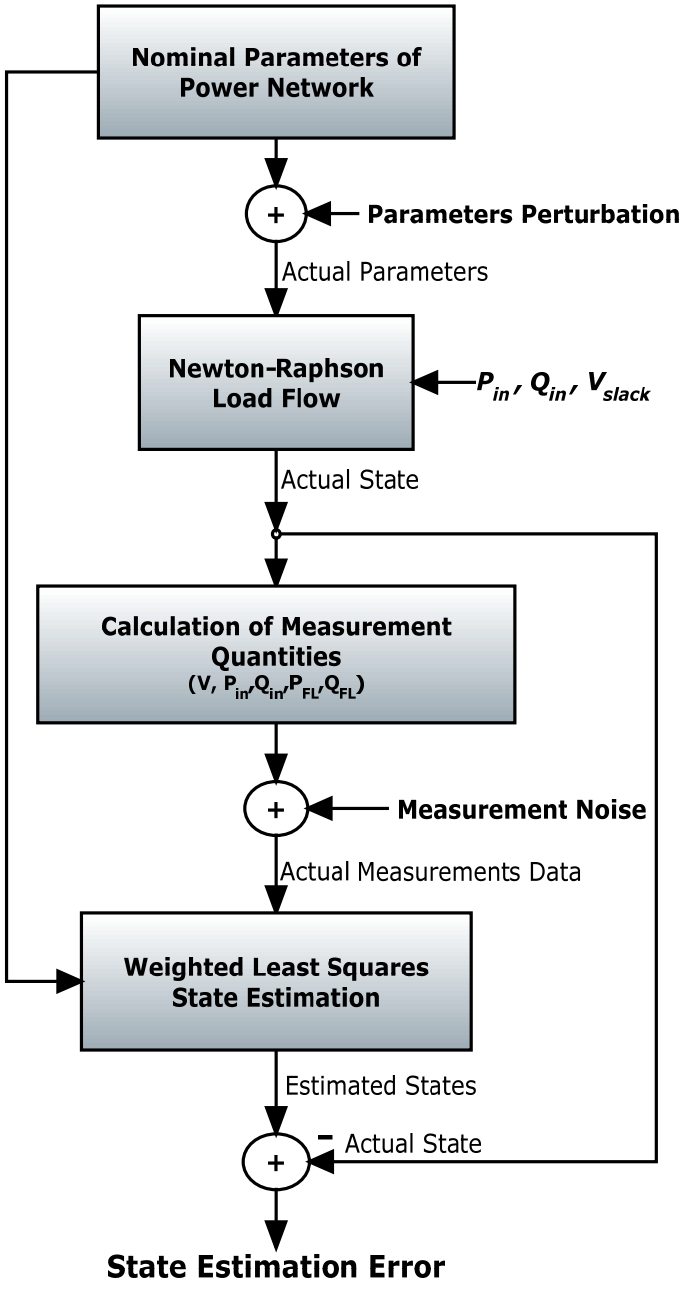

Figure 4.1 Flowchart of the Algorithm Implementation

4.1 Parameters Model

In our study, nominal values of resistance, reactance and susceptance characterizing the network elements are randomly perturbed extracting their values from a multivariate Gaussian distribution. The mean vector μ of the distribution was represented by the nominal values of the parameters, and the variance-covariance matrix was build considering a standard deviation as a fixed percentage α of the nominal value, i.e. for the i^{th} parameter $\sigma_i = \alpha \times \mu_i$ and assigning a prescribed correlation coefficient ρ_{ij} for each couple *i,j* of parameters. Furthermore the parameters with zero nominal values were not perturbed.

Since all these parameters, for physical reason, are defined by positive real numbers, it is important to avoid perturbations so wide resulting in negative parameters. For this reasons it was evaluated the probability to get negative results for such extraction for standard deviations less than 25% of the nominal values. Surprisingly it was found that this probability is independent from the nominal values but it is just a function of α. The authors were not able to find in literature a demonstration of such a property of the Normal multivariate distribution but we just verified this property numerically computing the probability $\boldsymbol{P}$ of getting at least one negative value among *N* parameter as:

$$\boldsymbol{P} = \boldsymbol{P}(\boldsymbol{\alpha}) = \boldsymbol{p}\left\{\bigcup_{\boldsymbol{i=1}}^{\boldsymbol{N}}(\boldsymbol{\pi_i} \leq \boldsymbol{0})\right\} =$$
$$= \sum_{\boldsymbol{i=1}}^{\boldsymbol{N}} \boldsymbol{p}\{\boldsymbol{\pi_i} \leq \boldsymbol{0}\} - \sum_{\boldsymbol{i=1}}^{\boldsymbol{N}}\sum_{\boldsymbol{j=i}}^{\boldsymbol{N}} \boldsymbol{p}\left\{(\boldsymbol{\pi_i} \leq \boldsymbol{0}) \bigcap (\boldsymbol{\pi_j} \leq \boldsymbol{0})\right\} +$$
$$+ \sum_{\boldsymbol{i=1}}^{\boldsymbol{N}}\sum_{\boldsymbol{j=i}}^{\boldsymbol{N}}\sum_{\boldsymbol{k=j}}^{\boldsymbol{N}} \boldsymbol{p}\left\{(\boldsymbol{\pi_i} \leq \boldsymbol{0}) \bigcap (\boldsymbol{\pi_j} \leq \boldsymbol{0}) \bigcap (\boldsymbol{\pi_k} \leq \boldsymbol{0})\right\} + (\boldsymbol{-1})^{\boldsymbol{N+1}} \boldsymbol{p}\left\{\bigcap_{\boldsymbol{i=1}}^{\boldsymbol{N}}(\boldsymbol{\pi_i} \leq \boldsymbol{0})\right\}$$

The probability of the intersecting events in the previous equation was computed marginalizing the known multivariate Normal distribution, e.g. the probability of the event $p\{(\pi_i \leq 0) \cap (\pi_j \leq 0) \cap (\pi_k \leq 0)\}$ was computed as:

$$\boldsymbol{p}\left\{(\boldsymbol{\pi_i} \leq \boldsymbol{0}) \bigcap (\boldsymbol{\pi_j} \leq \boldsymbol{0}) \bigcap (\boldsymbol{\pi_k} \leq \boldsymbol{0})\right\} = \int_{-\infty}^{\boldsymbol{0}}\int_{-\infty}^{\boldsymbol{0}}\int_{-\infty}^{\boldsymbol{0}} \boldsymbol{N}(\boldsymbol{\pi_i}, \boldsymbol{\pi_j}, \boldsymbol{\pi_k}) \boldsymbol{d_{\pi_i}} \boldsymbol{d_{\pi_j}} \boldsymbol{d_{\pi_k}}$$

with

$$N(\pi_i, \pi_j, \pi_k) = \int_{\mathbb{R}^{N-3}} N(\pi_1, \dots, \pi_N) \prod_{m \neq i,j,k}^{N} d_{\pi_m}$$

and N(•) being the multivariate Normal probability density function.

As a numeric example, let's consider the values of network parameters in IEEE 14 bus test case. With a parameter standard deviation of 0.25 which is the greatest standard deviation used in the simulations of this paper, the probability of reaching to a negative number for resistance, reactance or susceptance will be $P = 0.5 \times 10^{-5}$ that is negligible for the number of Monte Carlo trials we have considered. Practically, in the simulations if a negative value is observed, until getting a positive value, the program will repeat the parameter perturbation, without affecting the parameters probability density function.

4.2 Sub-blocks Details

4.2.1 Newton Raphson Load Flow

The realistic parameters along with the power injections are used to get the actual states which are the voltage and phases of power network for each bus using power flow solution by Newton Raphson (NR) method [Tinney 1967]. Since 1970s the load flow methods continue to develop and among them the most successful is the Fast Decoupled method [Wood 1996]. Comparing with the NR method, this method is faster and simpler and more efficient algorithmically and needs less storage, but it may fail to converge when some of the basic assumptions do not hold. Therefore the NR load flow is chosen because it is the most robust power flow algorithm that widely used in practice.

The states that are generated by NR load flow are used for the next part that is the calculation of exact measurement data. NR states are also taken as the reference (actual states) for comparing the results of State Estimator afterwards.

4.2.2 Calculation of Measurement Quantities

The exact measurement data can be calculated using Newton-Raphson load flow states to extract the measured quantities. To convert the exact measurement data to realistic

measurement data (which always affected by uncertainty), Normal random numbers with zero mean and variances according to the measurement devices' uncertainty are added.

4.2.3 WLS State Estimation

In the last stage the nominal network parameters and the realistic (perturbed) measurement data are used as inputs to WLS State Estimator to get the State Estimator's states and compared to the NR states to get the State Estimation Error.

4.3 Monte Carlo Procedure

Monte Carlo simulation method is based on probability and statistics theory and methodology. For numerical problems in a large number of dimensions, Monte Carlo experiments are often more efficient than conventional numerical methods on the other hand Monte Carlo experiments needs sampling from high dimensional probability distributions [Hastings 1970]. In Monte Carlo simulation method, the state of each component in the system is determined by sampling [Wang 2009]. Monte Carlo experiments rely on repeated random sampling to compute their results when it is infeasible to compute an exact result with a deterministic algorithm.

In this thesis the uncertainty analysis is performed by Monte Carlo simulation and the steps are described more in detail in the following:

Step1: Read and preprocess the data:

The data pertaining to network parameters (transmission line's nominal data), measurement locations and the standard deviations of measurement instruments are read. The nominal bus admittance matrix is built.

Step2: Repeat for $i = 1$ to P sigmas defined per parameters uncertainty (sampling of parameters noise):

1. Repeat for *j=1* to *MC_tests* defined per maximum number of Monte Carlo trials:

   I. Perturb each of the parameters by i^{th} sigma.

   II. Repeat I if we get negative values.

III. Create the perturbed bus admittance matrix using perturbed network parameters.

IV. Perform Newton-Raphson load flow using bus power injections and perturbed bus admittance matrix and collect NR states.

V. Calculate the exact measurement data using NR states, perturbed bus admittance matrix and measurement locations.

VI. Perform WLS State Estimation (SE) using the nominal bus admittance matrix and perturbed measurements and collect the SE states.

VII. Subtract the NR states from SE states to get the SE error.

2. Calculate the RMS of SE errors and the standard deviations for all Monte Carlo trials.

Step3: Show the results using statistical indices.

In the next chapter, the algorithm is implemented on different IEEE power test cases and the numerical results are shown.

CHAPTER 6

Simulation Results

To analyze the effects of parameter and measurement uncertainties on the power system state estimation results, the algorithm is tested on several IEEE power network test cases such as: 14-bus, 30-bus, 57-bus and 118-bus test cases. The network data files can be downloaded from Power Systems Test Case Archive in [Christie 1999].

In the following sections firstly it is briefly described that how the measurement set is chosen and then the general criteria for evaluation of simulation results are defined. Finally for each IEEE test case, the inputs (network data and measurements) are reported and the simulations results are shown.

For each test case a set of measurement chosen to avoid an unobservable network. Degree of redundancy (η) is generally expressed as the ratio of number of meters by the number of states and is a very important quantity because the more redundant measurements, the more chances for bad data to be detected [Clements 1988]. The measurement redundancy ratio is defined by:

$$\eta = \frac{\text{Number of Measurements}}{\text{Number of States}}$$

Which the number of states is $(2N_{bus} - 1)$ for N_{bus} network buses. In fact for practical implementation, there should be enough redundancy in measurement all over the network [Pajic 2007].

The measurement set is chosen by calculating "perfect measurements" from the data available (IEEE test cases come with both network parameters and true states). The measurement set includes almost all the PV buses (voltage and power injection measurements) together with some active and reactive power flow measurements.

Choosing of measurement locations are inspired from the literature; for instance for IEEE 14-bus from [Lukomski 2008] [Baran 1995], for IEEE 30-bus from [Kerdchuen 2009], for IEEE 57-bus from [Chen 2006] and for IEEE 118-bus from [Rakpenthai 2005]. Some of them altered by the author because of algorithm stability issues according to the experience.

In reality, actual measurements are not exact and there is a level of uncertainty present in the measurements. Therefore measurement error must be considered. For instance for the test cases, the uncertainty for of voltage measurement considered as 0.1 percent of read value and for power measurement considered as 1 percent of read value:

- $\sigma_V = 0.001$
- $\sigma_{P_{inj}} = \sigma_{Q_{inj}} = \sigma_{P_{fl}} = \sigma_{Q_{fl}} = 0.01$

These quantities represent the expected accuracy of the meters used and are expressed in the diagonal elements of the weighting matrix since measurement errors are considered independent.

In the simulations, the following samples of uncertainty for network parameters are assigned:

- $\sigma_{param} = 0.00,\ 0.05,\ 0.10,\ 0.15,\ 0.20$ and 0.25.

The number of Monte Carlo trials is chosen so that the population of samples is sufficient amount and experimentally it is seen that, for each parameter uncertainty, 1000 Monte Carlo Trials are sufficient for our analysis. Besides, for most of our simulations the increase of trials does not affect the results remarkably or extraordinary but for some of the test cases, the trials are increased up to 5000 to have more reliable data (in the simulations any change in the number of trials are reported clearly).

For each network parameter uncertainty, the following actions are done:

- The developed algorithm that described in previous chapter is run on test cases. Thus for N_{MC} Monte Carlo Trials, N_{MC} values for each state are extracted.
- Then all of these values are formed a new matrix of size $N_{MC} \times N_{bus}$ for voltage magnitude and another matrix of size $N_{MC} \times (N_{bus} - 1)$ for angles.
- Then for each state, the mean is computed (mean of each column).
- Finally the mean and standard deviation of all the buses is computed.

The mean and standard deviation of voltage magnitudes and angles of each IEEE test case are used in order to evaluate the State Estimator's output accuracy according to the criteria that is described in the next section.

5.1 General Criteria for Evaluation of the Simulation Results

In this section a general criteria is defined according to the desirable properties of a power state estimator, to evaluate the simulation results. These measures include evaluation of the mean and standard deviation, biasness and root mean square of state estimator.

In addition, another simulation is performed to show how much the State Estimator's results are mutually connected to each other taking into account that there exists network parameters uncertainty. The simulations are also repeated for the test networks including PMU measurement data.

5.1.1 Mean and Standard Deviation of State Estimator

The error bars plots are used to illustrate the mean and standard deviation of voltage magnitude and voltage angles versus all the network parameters uncertainty samples.

Please note that the states are shown separately in two different figures and the voltage magnitudes are in Per Unit and the angles are in degrees.

As already described, in WLS State Estimation the theoretical standard deviations of State Estimator errors can be extracted by taking the square root of the diagonal elements

of the variance covariance matrix of the estimates. In the figures the distribution of the theoretical standard deviations are depicted as two horizontal lines (1σ above and below the mean).

As will be seen, in the figures the mean of errors for both voltage magnitudes and angles don't start from zero that it implies the effect of the measurement uncertainty.

5.1.2 Bias Test for State Estimator

Another important analysis that can be performed is to check for which network parameters uncertainties the State Estimator is biased. It is done by using the ratio of absolute value of voltage error Means by the related Standard Deviations versus the network parameters uncertainty.

To determine if the State Estimator is biased or not, a threshold can be defined. To have a vision of this threshold, a horizontal dashed line is also depicted in the figures. It means that the state estimator is not biased for the network parameters uncertainty range below this line. To illustrate the dashed line, the value of the Mean of state errors over the standard deviation is calculated by performing a hypothesis testing considering the threshold.

5.1.3 Correlation of State Estimator's Errors

This analysis is intended to show how much the State Estimator's results are mutually connected to each other taking into account that there exists network parameters uncertainty. The State Estimator's Error correlation coefficient matrix describes the normalized measure of the strength of linear relationship between State Estimator's Errors. Correlation coefficients are given by:

$$R(i,j) = \frac{Cov\_SE(i,j)}{\sqrt{Cov\_SE(i,i)Cov\_SE(j,j)}}$$

where Cov_SE is the covariance matrix of State Estimator's errors. The diagonals of Correlation coefficients matrix are equal to 1 and the other elements of correlation coefficients matrix will be in the range between -1 to 1.

For each network case, the correlation coefficients of State Estimator's errors are plotted versus parameters uncertainty for Voltage errors and Phase errors.

The values close to 0 suggest there is no linear relationship between the data. Values close to 1 suggest that there is a positive linear relationship between the data and the values close to -1 suggest that there is a negative linear relationship between the data (anti-correlation).

5.1.4 Parameter's Correlation Effect

Another analysis about the correlation effect that is performed in this section is the evaluation effects of parameter's correlation on different IEEE test cases.

For this aim, firstly the nominal values of line resistances are correlated with a correlation coefficient (the line resistances with zero nominal values were not correlated).

Then the ratio of the mean of voltage magnitudes errors (and angles errors separately) by standard deviations for each test case is displayed versus the network parameter uncertainties.

Having parameters correlated, a threshold again is set by a horizontal dashed line in the figures to determine if the State Estimator is biased or not.

5.1.5 The Results with PMU

In this analysis, the bias testing of State Estimator is performed when PMU measurements are also included in the measurement set.

5.2 Test of Algorithm on IEEE 14-Bus Case

The one-line diagram of the IEEE 14-Bus test case with measurement locations is illustrated in Figure 5.1. This network has been used in many references that are cited in this thesis and in many examples during the research. The original network and data files can be found in [Christie 1999].

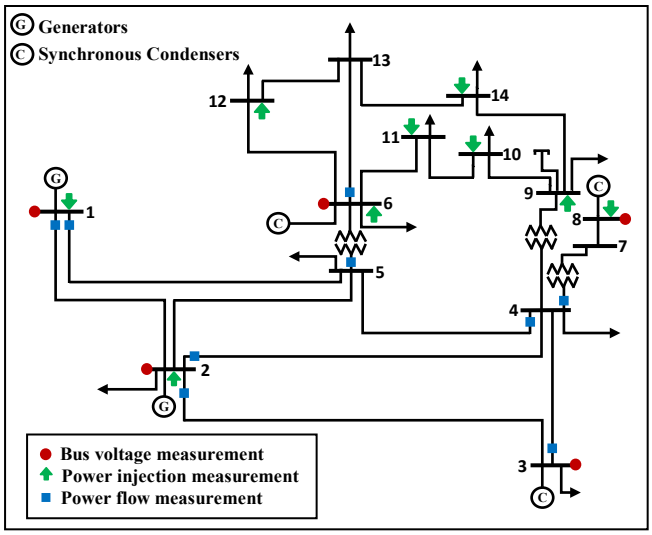

Figure 5.1 IEEE 14-Bus Test Case with Measurement locations

For not experiencing the observability problem, totally 41 measurements are selected. For 14 buses, there are $(2 \times 14 - 1)$ states, so the measurement redundancy ratio will be:

$\eta \approx 1.5$

The measurement set for this test case almost includes all the PV buses (voltage and power injection measurements) together with some power flow measurements as the following:

- Voltage magnitudes at buses 1, 2, 3, 6 and 8.
- 9 active and reactive power injections at buses 1, 2, 6, 8, 9, 10, 11, 12 and 14.
- 9 active and reactive power flows on branches 1–2, 1–5, 2–3, 2–4, 3–4, 4–5, 4–7, 5–6, and 6–13.

For each σ_{param}, the actions that are done could be summarized as:

- The developed algorithm that described in previous chapter is run on this test case. Thus 1000 values for each state are extracted which divided into one matrix

of 1000 by 14 for voltage magnitude and another matrix of size 1000 by 13 for phases.

- Then for each state, the mean is computed.
- Then the mean and standard deviation of all buses for each parameter uncertainty is computed.

5.2.1 Mean and Standard Deviation of State Estimator

The error bars plots for mean and standard deviation of voltage magnitude and voltage angles versus all the network parameters uncertainty samples are shown respectively in Figure 5.2 and Figure 5.3.

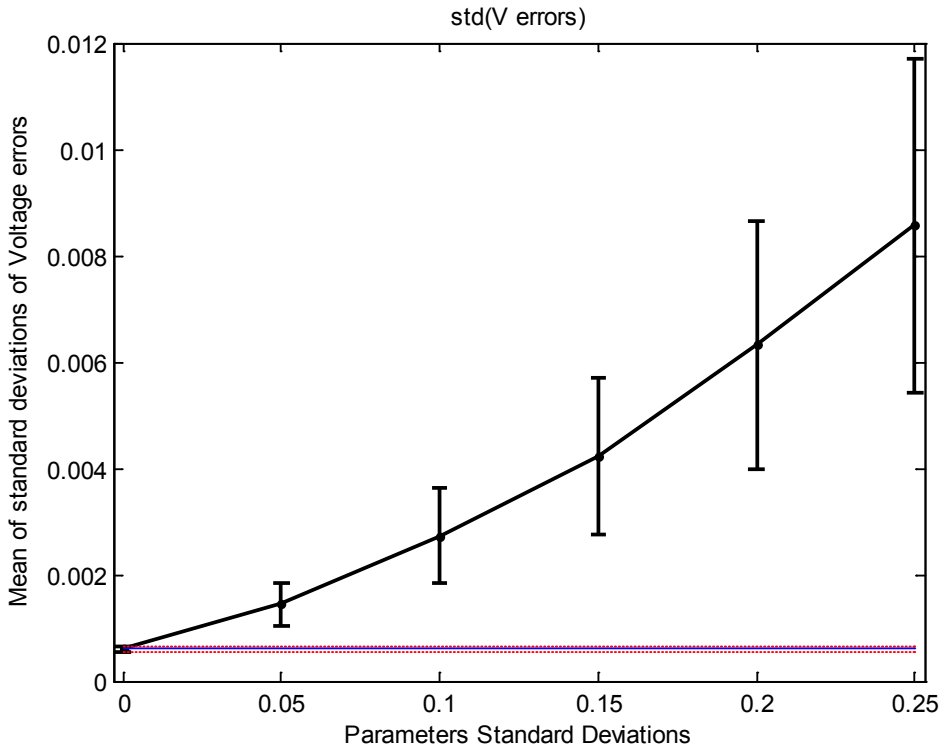

Figure 5.2 Mean and Standard Deviation of Voltage Magnitude Errors for IEEE 14-Bus test case.

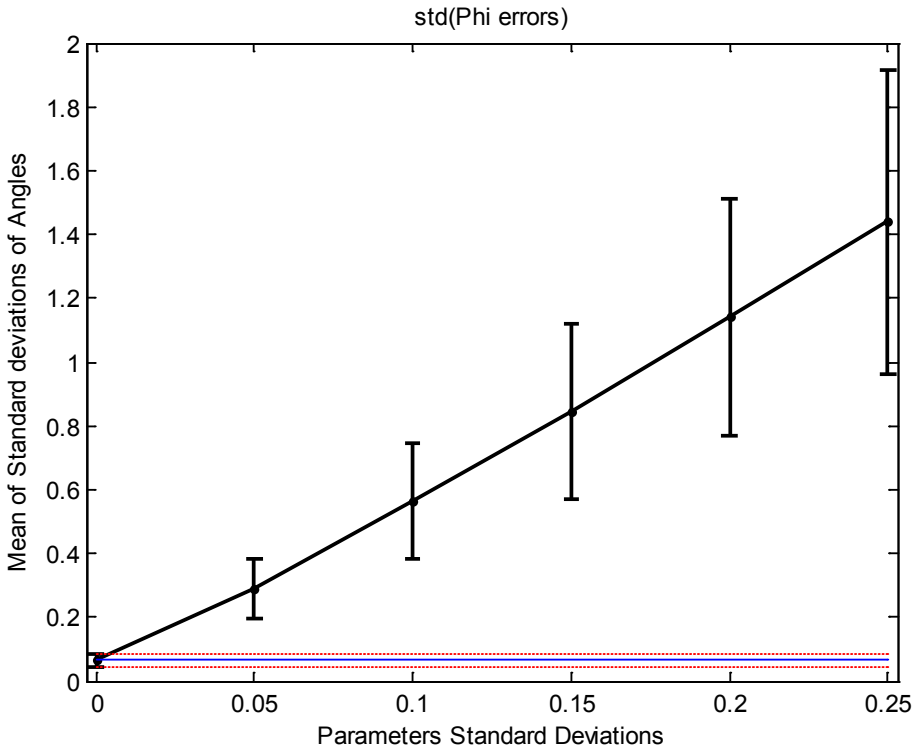

Figure 5.3 Mean and Standard Deviation of Voltage Angle Errors for IEEE 14-Bus test case.

In the figures the mean of errors for both voltage magnitudes and angles don't start from zero point showing the effect of the measurement uncertainty.

The figures clearly show that by growth of the network parameters uncertainty, the mean and standard deviation of errors will considerably grow.

Therefore the State Estimation's standard deviation is underestimated enormously, if just the theoretical standard deviations are taken into consideration.

To see how much the mean standard deviation and deviation of State Estimator errors are affected by measurement uncertainty, the same procedure is done for different measurement uncertainties. In Figure 5.4 and Figure 5.5 using different line styles displaying different measurement uncertainties, the error bar plots for mean and standard deviation of voltage magnitude and voltage angles versus all the network parameters uncertainty are shown respectively. These figures are only shown for IEEE 14-Bus test case.

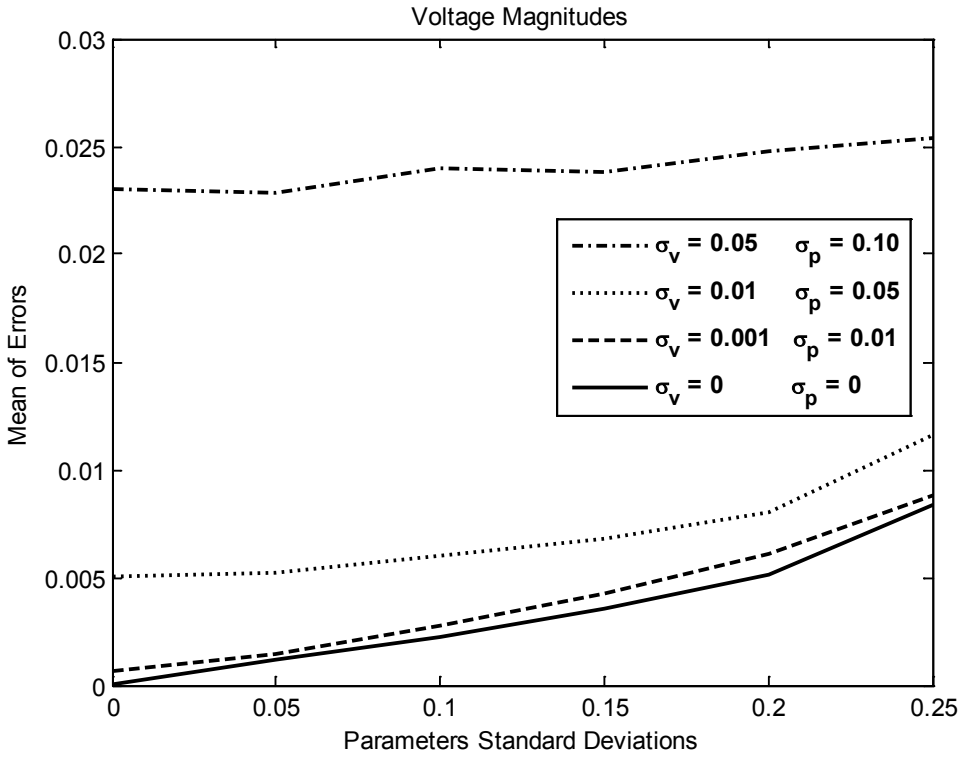

Figure 5.4 Mean and Standard Deviation of Voltage Magnitude Errors for Different Measurement Uncertainties for IEEE 14-Bus test case

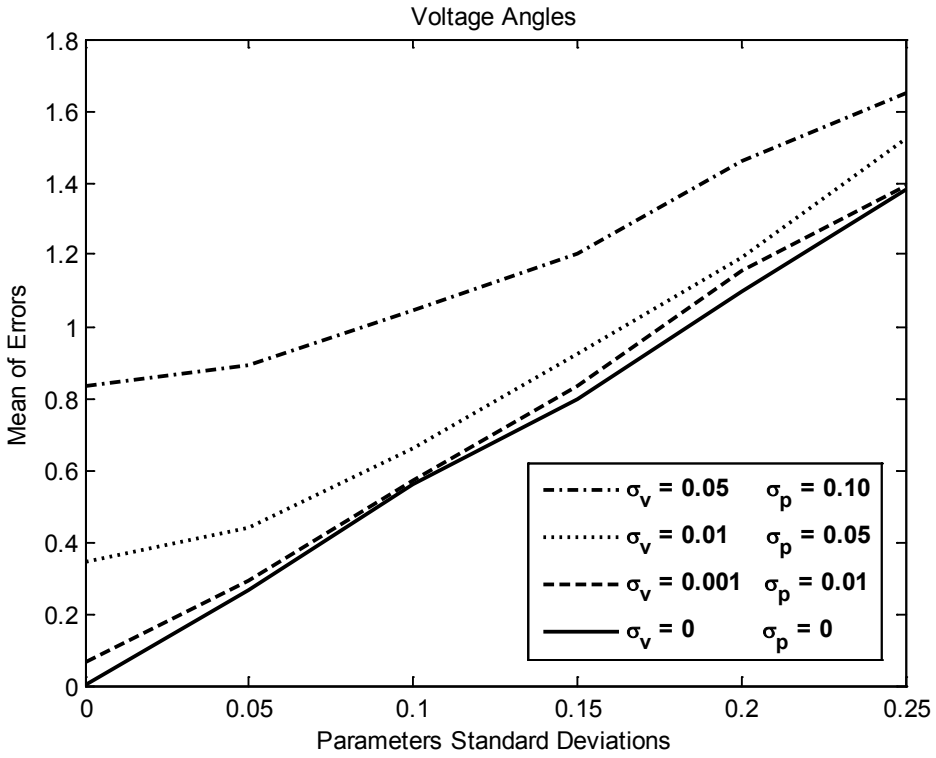

Figure 5.5 Mean and Standard Deviation of Voltage Angles Errors for Different Measurement Uncertainties for IEEE 14-Bus test case

As seen in the figures above, when the measurement uncertainty grows, the starting point goes farther from zero and the error mean shifts upward.

5.2.2 Bias Testing for State Estimator

Figure 5.6 and Figure 5.7 show the ratio of absolute value of voltage error Means by the related Standard Deviations versus the network parameters uncertainty respectively for voltage magnitudes and angles for IEEE 14-bus test case.

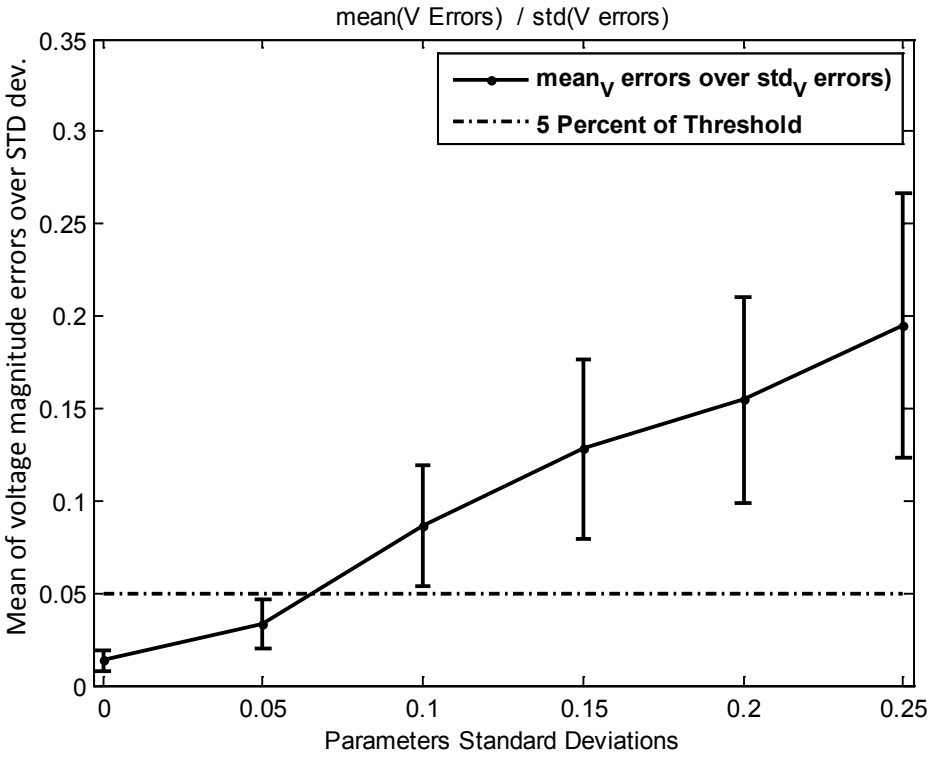

Figure 5.6 Ratio of the Mean of voltage magnitude errors by related Standard Deviations for IEEE 14-Bus test case.

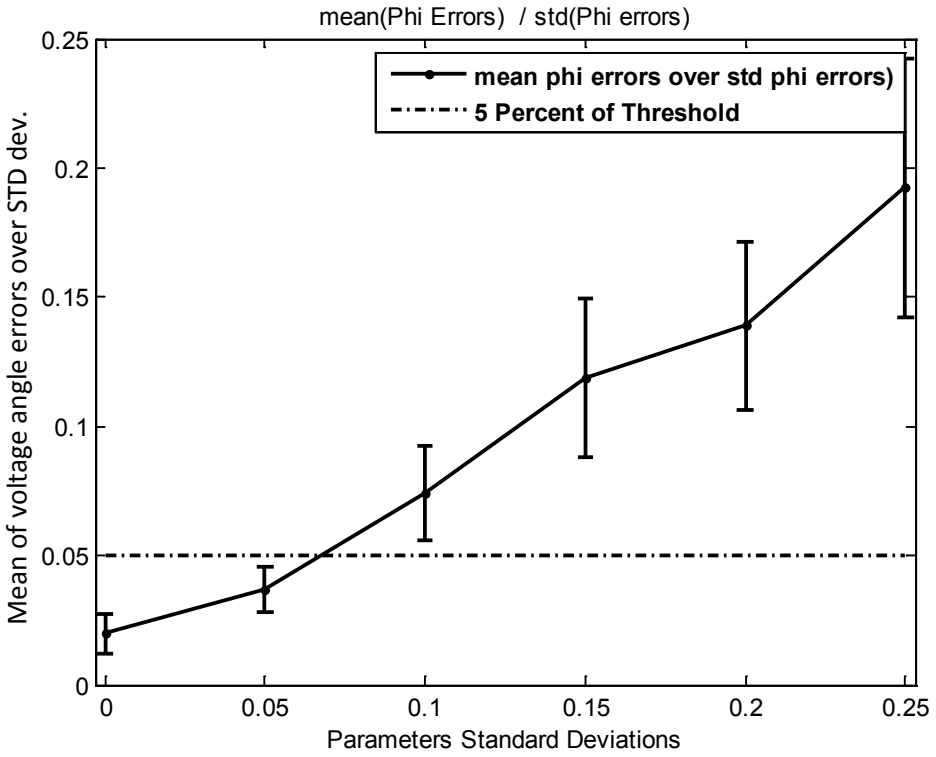

Figure 5.7 Ratio of the Mean of voltage angle errors by related Standard Deviations for IEEE 14-Bus test case.

A horizontal dashed line is also depicted in the figures to give an idea about the 5 percent of threshold, meaning that the state estimator is not biased for the network parameters uncertainty range below this line.

According to the figures, it is apparent that the State Estimator is not biased for the parameters uncertainties up to nearly 7 percent.

5.2.3 Correlation of State Estimator's Errors

In Figure 5.8 and Figure 5.9 the correlation coefficients of State Estimator's errors versus parameters uncertainty are shown for Voltage errors and Phase errors respectively.

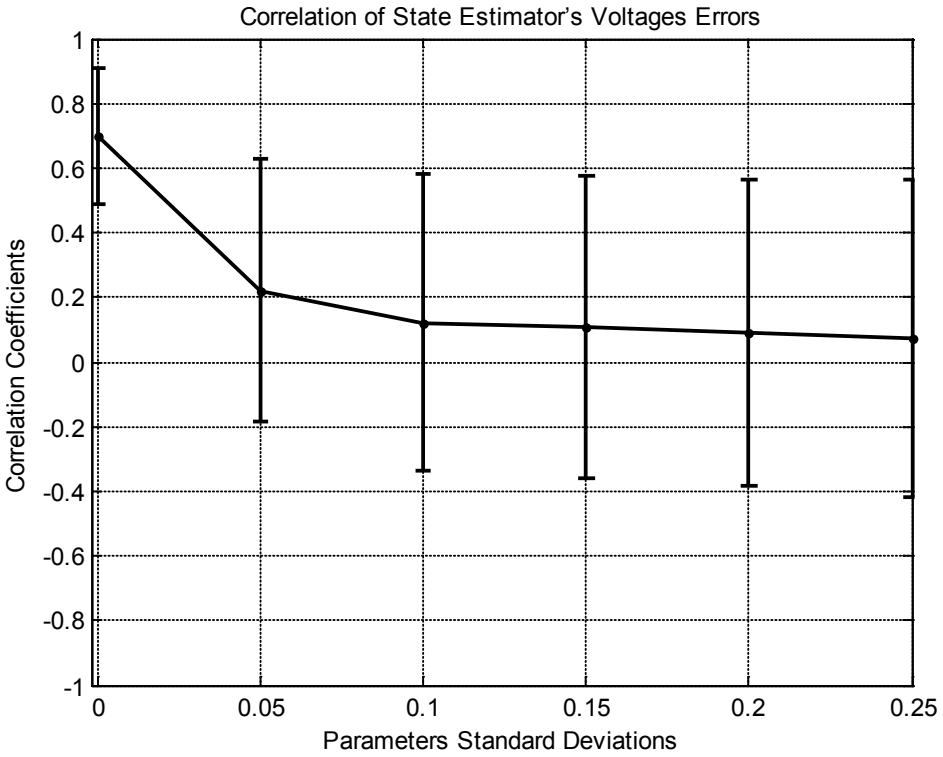

Figure 5.8 Correlation of State Estimator's Errors (Voltage) of IEEE 14-Bus test case.

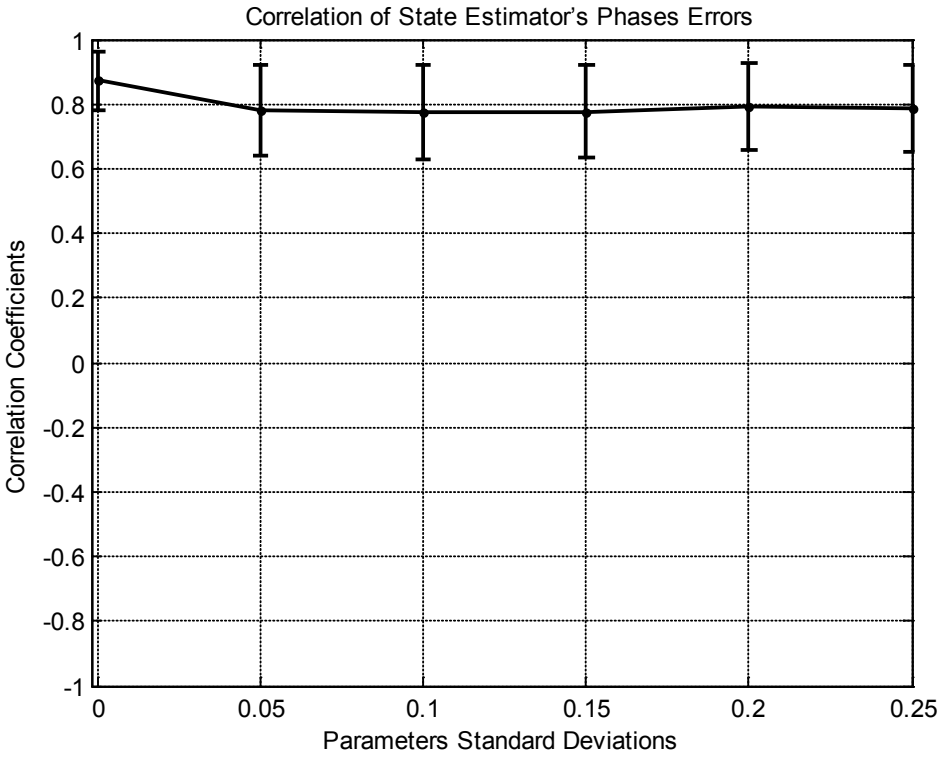

Figure 5.9 Correlation of State Estimator's Errors (Phase) of IEEE 14-Bus test case.

In Figure 5.8 and Figure 5.9 it is noticeable that the State Estimator's Errors are correlated so much when there is no parameters uncertainty. By increasing the network parameters uncertainty up to about 10%, the estimated voltage errors will be roughly uncorrelated but the estimated voltage phases will be still correlated even for large parameters uncertainties up to 25%.

5.2.4 Parameter's Correlation Effect on IEEE 14-Bus case

To perform this analysis, the nominal values of line resistances are correlated with the correlation coefficient of 0.8 and the line resistances with zero nominal values were not correlated.

With having parameters correlation, the ratio of the mean of voltage magnitudes and angles errors by Standard Deviations for IEEE 14-Bus test case are shown in Figure 5.10 and Figure 5.11.

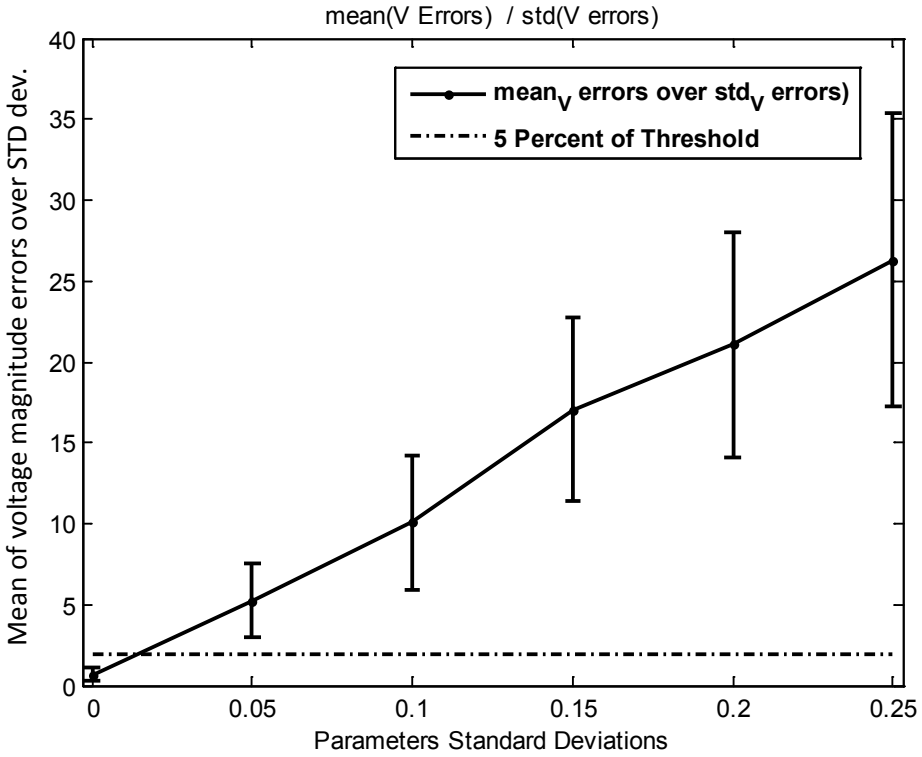

Figure 5.10 Ratio of the Mean of voltage magnitudes errors by Standard Deviations with parameters correlation for IEEE 14-Bus test case.

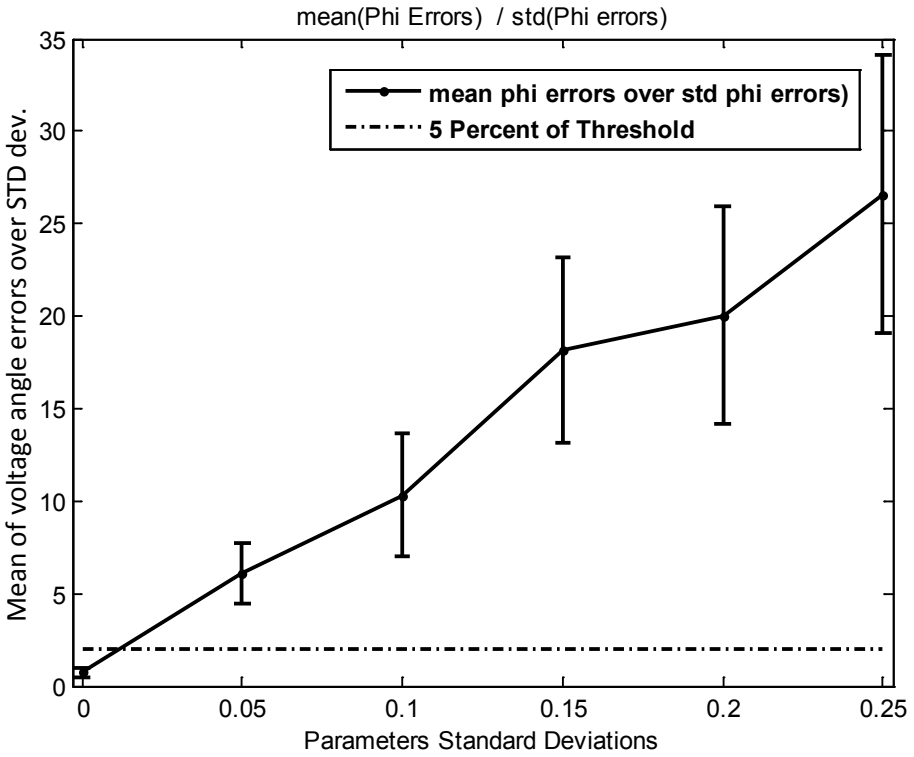

Figure 5.11 Ratio of the Mean of voltage angles errors by Standard Deviations with parameters correlation for IEEE 14-Bus test case.

By comparing the Figure 5.6 and Figure 5.7 with above figures (Figure 5.10 and Figure 5.11), it can be concluded that when the network parameters are correlated, the State Estimator is more biased (for smaller parameters uncertainties).

5.2.5 The Results with PMU

Figure 5.12 and Figure 5.13 show the bias tests for voltage magnitudes and phases respectively when there exist two PMUs on bus number 6 and 9.

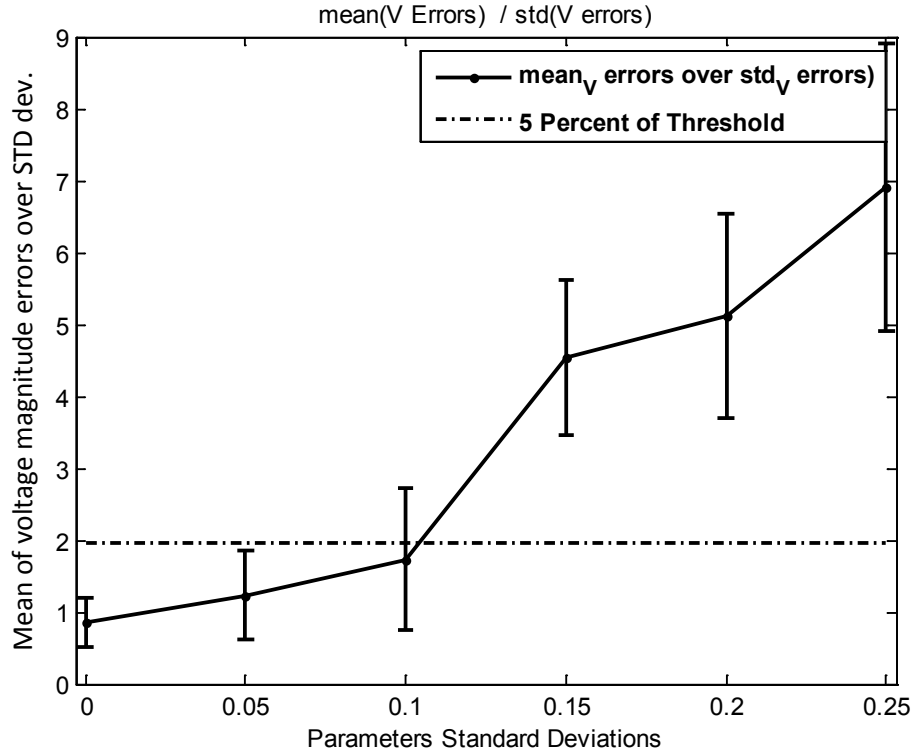

Figure 5.12 Ratio of the Mean of voltage magnitude errors by related Standard Deviations with the presence of PMU measurements for IEEE 14-Bus test case.

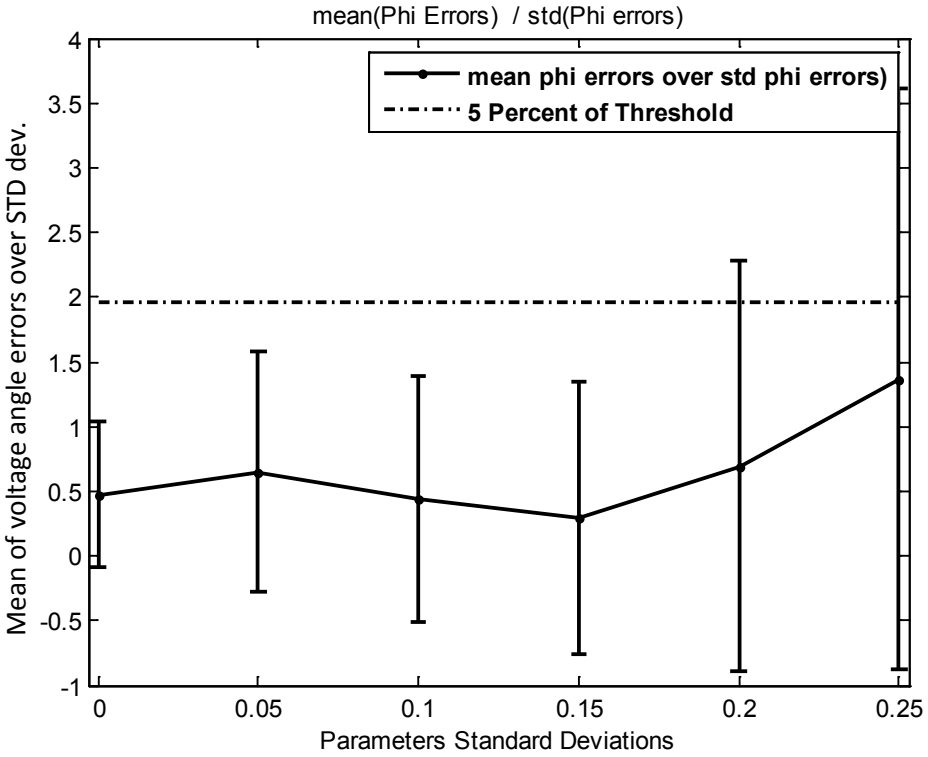

Figure 5.13 Ratio of the Mean of voltage Angle errors by related Standard Deviations with the presence of PMU measurements for IEEE 14-Bus test case.

As it is clear in the figures, when there is PMU installed, the output of SE voltage magnitudes are less biased (for bigger range of network parameters) and the SE output of phases are totally not biased.

5.3 Test of Algorithm on IEEE 30-Bus Case

The one-line diagram of the IEEE 30-Bus test case is illustrated in Figure 5.14. The original network and data files can be found in [Christie 1999].

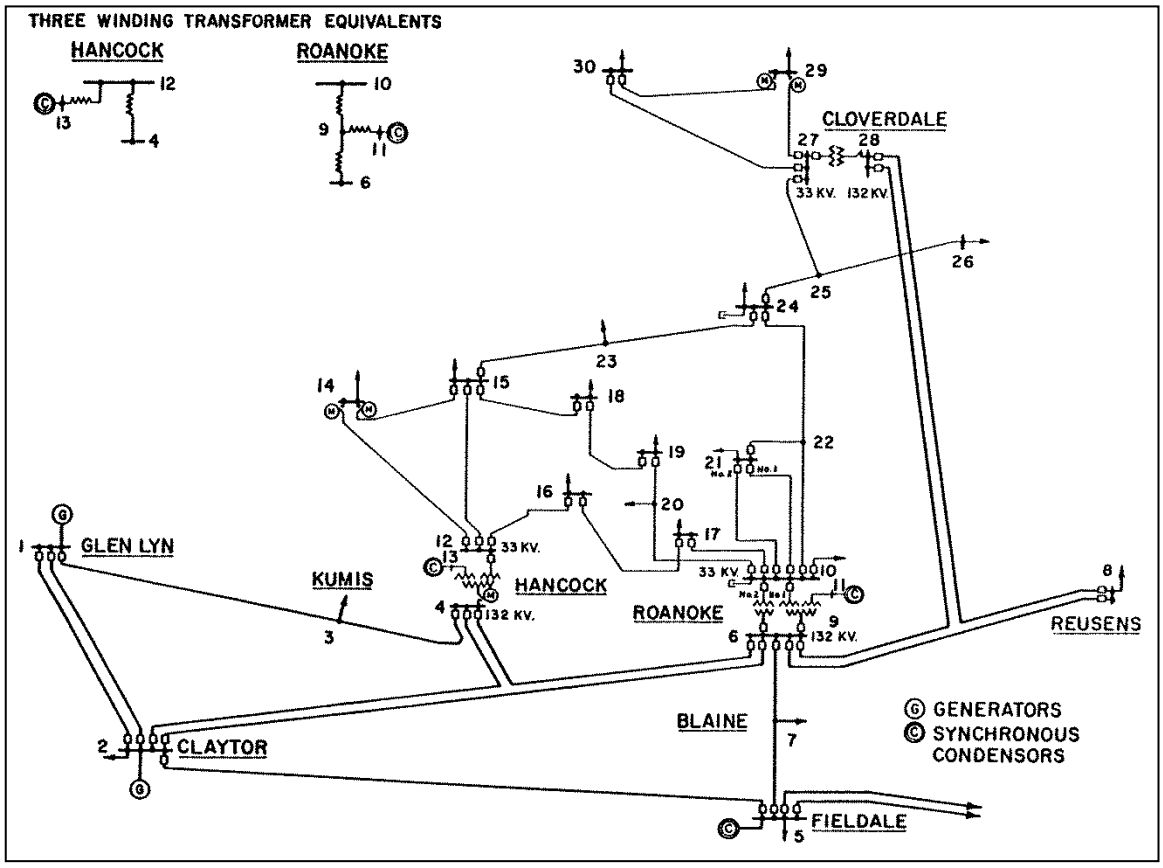

Figure 5.14 IEEE 30-Bus Test Case One-Line Diagram

For not experiencing the observability problem, totally 83 measurements are selected. The measurement redundancy ratio will be:

$\eta \approx 1.4$

The measurement set for this test case almost includes all the PV buses (voltage and power injection measurements) together with power flow measurements as the following:

- Voltage magnitudes at buses 1, 2, 3, 4, 5, 6, 7, 8, 9, 10 and 11.
- Active and reactive power injections at buses: 2, 3, 5, 8, 9, 11, 12, 13, 17, 20, 25, 27, 28 and 29.
- Active and reactive power flows on branches: 1-3, 2-6, 2-4, 7-5, 4-6, 6-28, 6-8, 6-9, 10-6,12-13, 12-15, 10-20, 10-17, 10-21, 14-15, 15-23, 15-18, 22-24, 25-26, 25-27, 28-27 and 29-30.

5.3.1 Mean and Standard Deviation of State Estimator

The error bars plots for mean and standard deviation of voltage magnitude and voltage angles versus all the network parameters uncertainty samples are shown respectively in the Figure 5.15 and Figure 5.16.

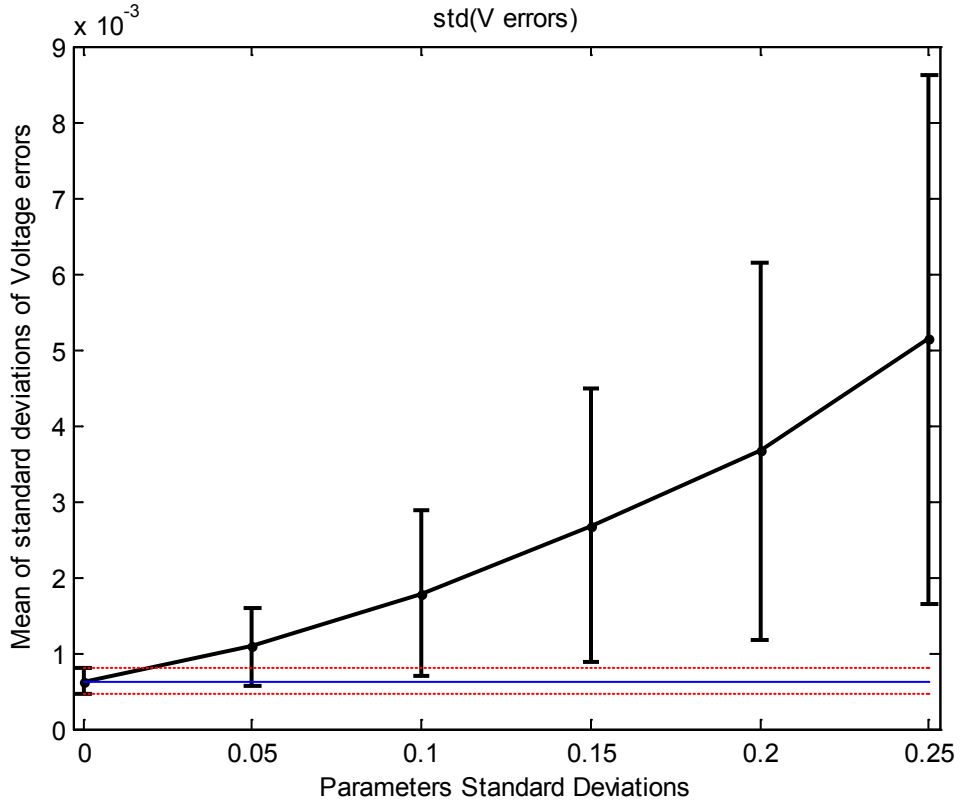

Figure 5.15 Mean and Standard Deviation of Voltage Magnitude Errors for IEEE 30-Bus test case.

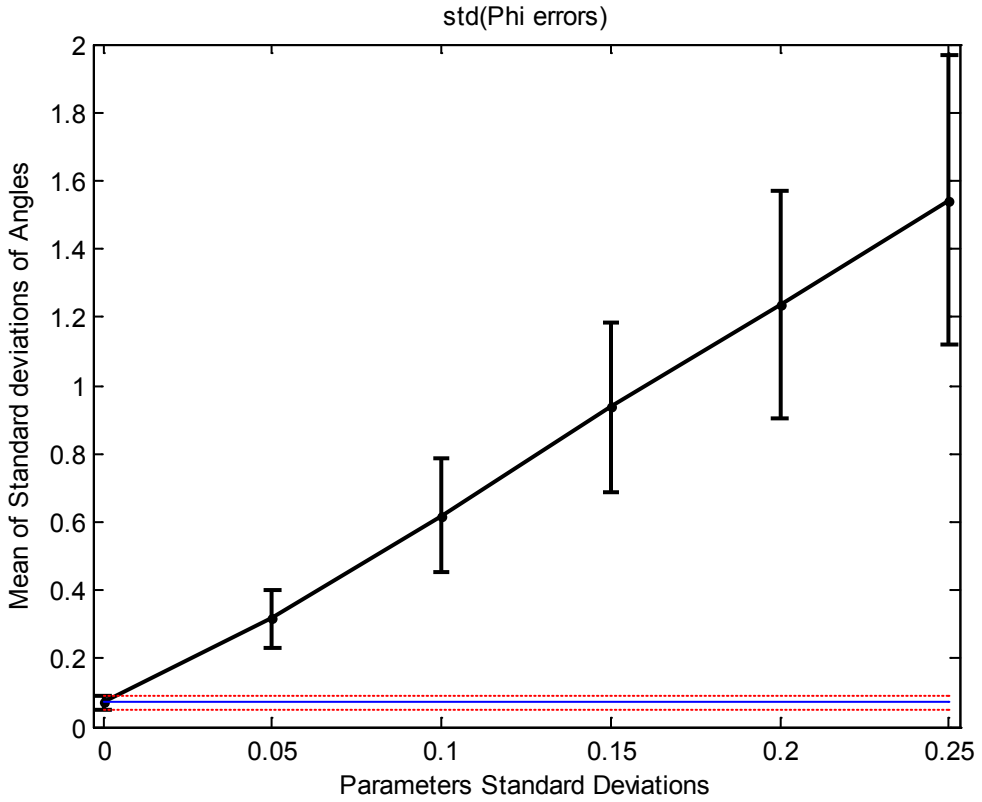

Figure 5.16 Mean and Standard Deviation of Voltage Angle Errors for IEEE 30-Bus test case.

In the figures, the mean of errors for both voltage magnitudes and angles don't start from zero point showing the effect of the measurement uncertainty.

The figures clearly show that by growth of the network parameters uncertainty, the mean and standard deviation of errors will considerably grow.

Therefore the State Estimation's standard deviation is underestimated enormously, if just the theoretical standard deviations are taken into consideration.

5.3.2 Bias Testing for State Estimator

Figure 5.17 and Figure 5.18 show the ratio of absolute value of voltage error Means by the related Standard Deviations versus the network parameters uncertainty respectively for voltage magnitudes and angles for IEEE 30-bus test case.

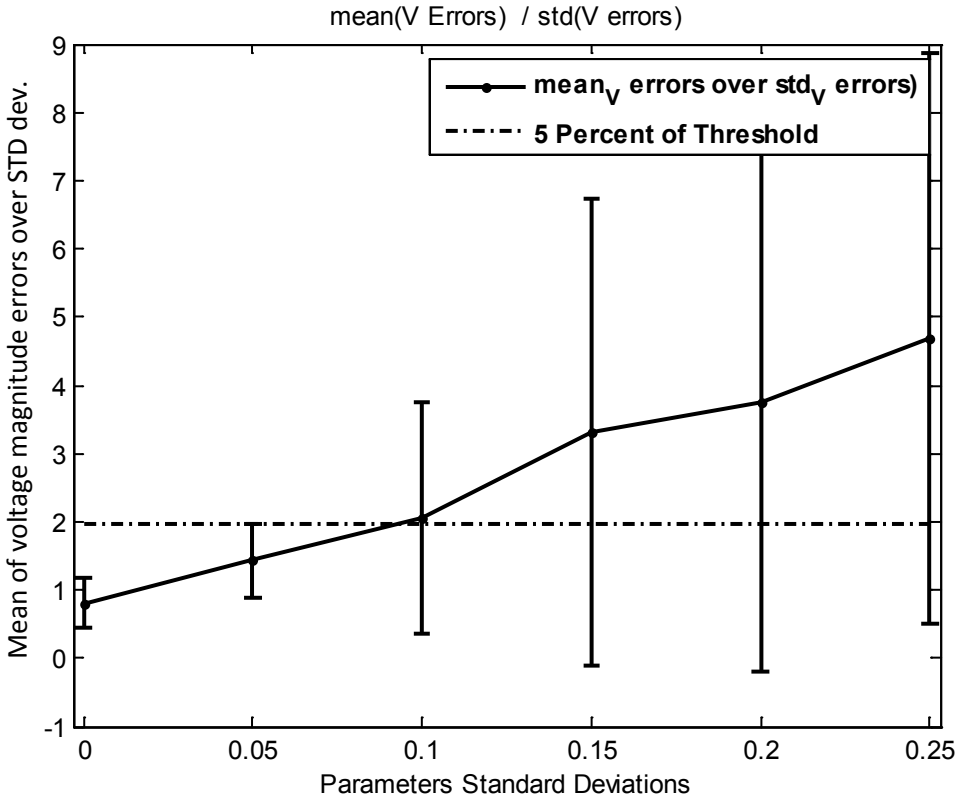

Figure 5.17 Mean and Standard Deviation of Voltage Magnitude Errors for IEEE 30-Bus test case.

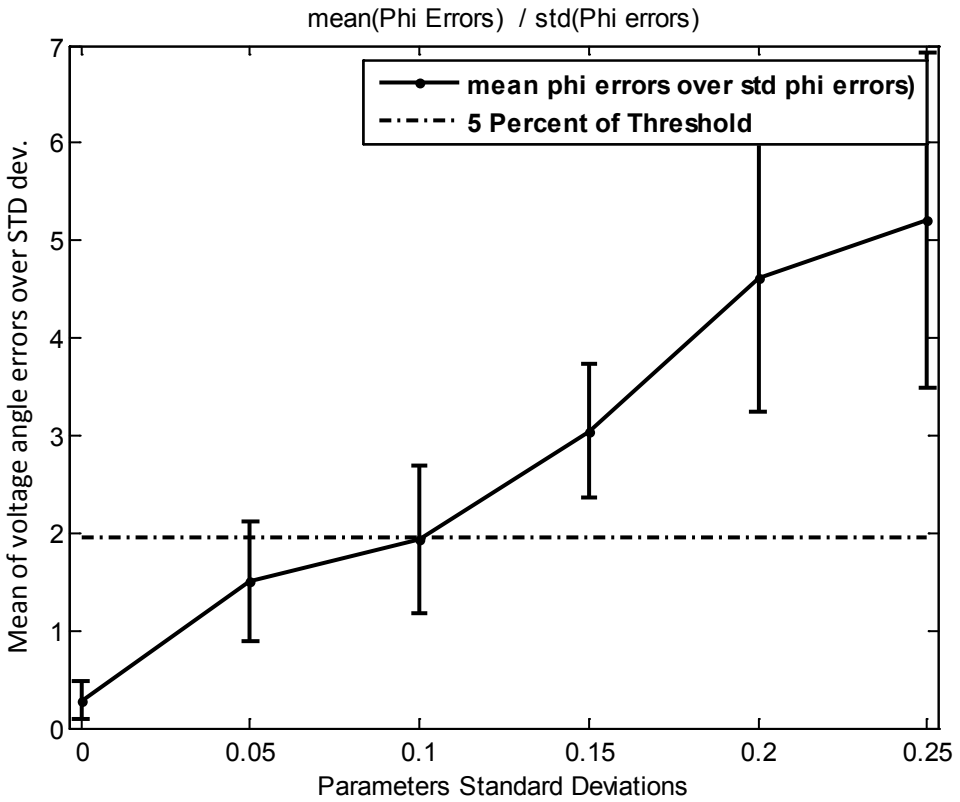

Figure 5.18 Mean and Standard Deviation of Voltage Angle Errors for IEEE 30-Bus test case.

A horizontal dashed line is also depicted in the figures to give an idea about the 5 percent of threshold, meaning that the state estimator is not biased for the network parameters uncertainty range below this line.

According to the figures, it is apparent that the State Estimator is not biased for the parameters uncertainties up to nearly 10 percent.

5.3.3 Correlation of State Estimator's Errors

In Figure 5.19 and Figure 5.20 the correlation coefficients of State Estimator's errors versus parameters uncertainty are shown for Voltage errors and Phase errors respectively.

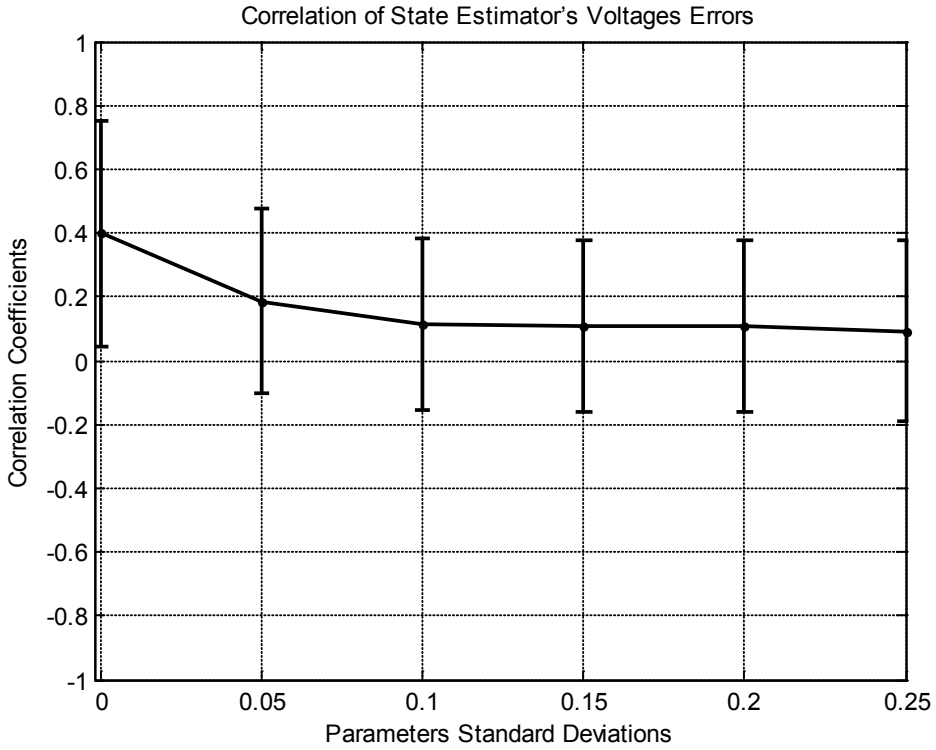

Figure 5.19 Correlation of State Estimator's Errors (Voltage Magnitude) of IEEE 30-Bus test case.

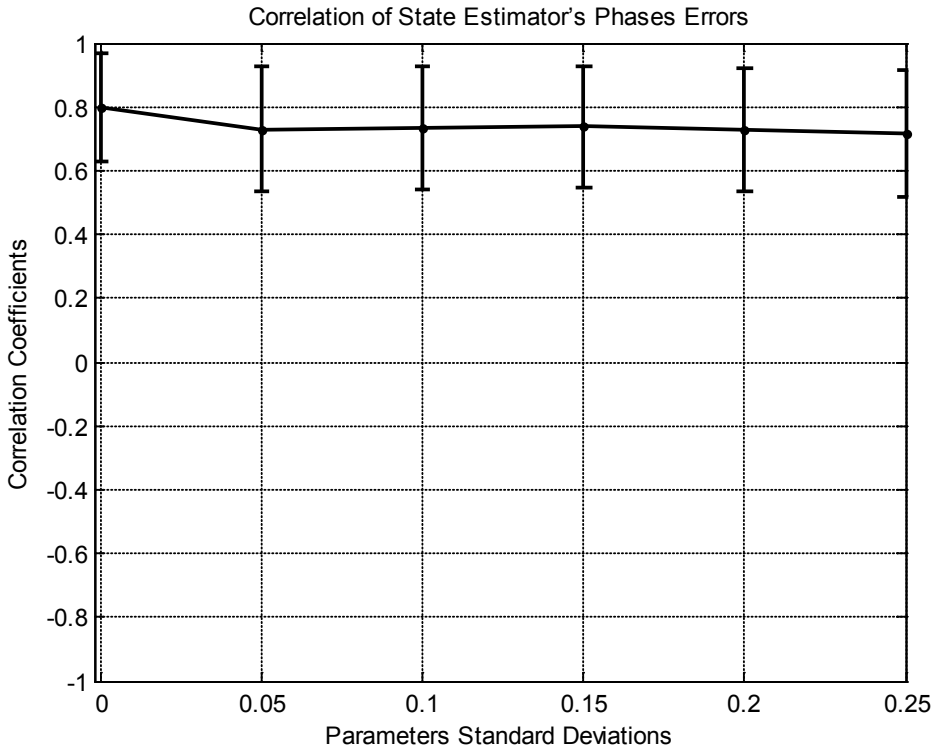

Figure 5.20 Correlation of State Estimator's Errors (Angles) of IEEE 30-Bus test case.

In Figure 5.19 it is noticeable that the State Estimator's Voltage Magnitude Errors are a little bit correlated and by increment of network uncertainty, the correlation goes even lesser. This behavior is because of the voltage measurement locations that are less compared to IEEE case 14-bus.

The Figure 5.20 shows that the State Estimator's Angles Errors are correlated so much when there is no parameters uncertainty and the Angles errors will be still correlated even for large parameters uncertainties up to 25%.

5.3.4 Parameter's Correlation Effect on IEEE 30-Bus case

To perform this analysis, the nominal values of line resistances are correlated with the correlation coefficient of 0.8 and the line resistances with zero nominal values were not correlated.

With having parameters correlation, the ratios of the mean of voltage magnitudes and angles errors by Standard Deviations for IEEE 30-Bus test case are shown in Figure 5.21 and Figure 5.22.

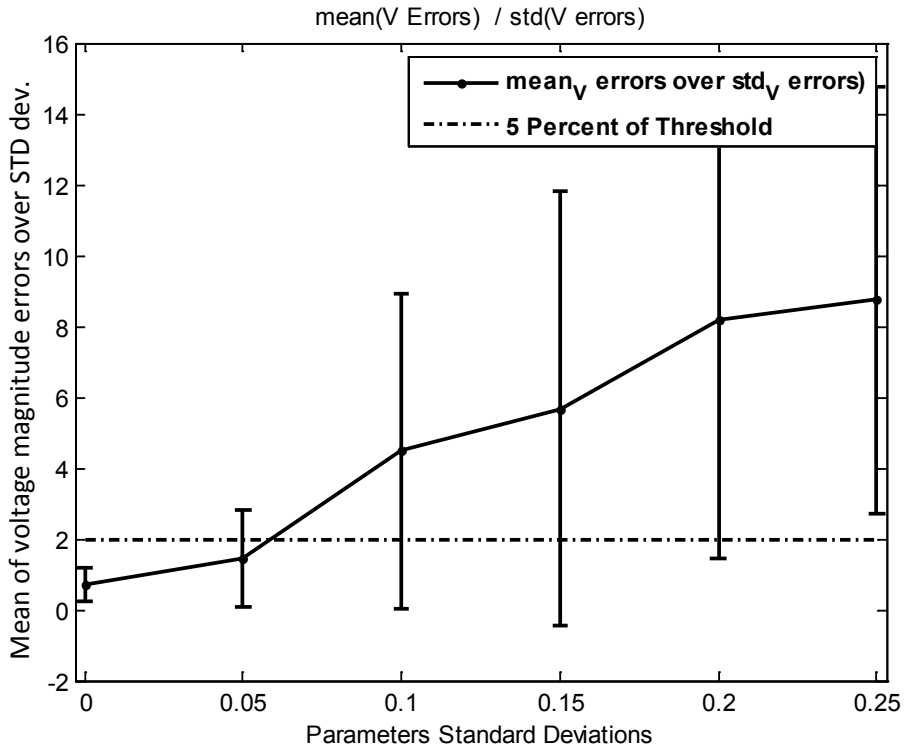

Figure 5.21 Ratio of the Mean of voltage magnitudes errors by Standard Deviations with parameters correlation for IEEE 30-Bus test case.

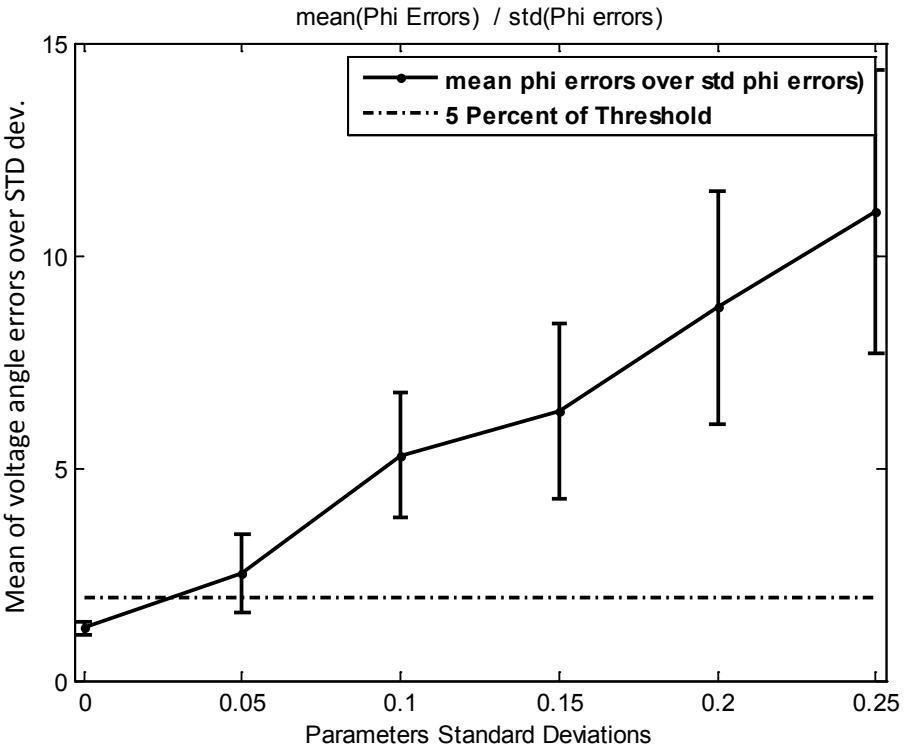

Figure 5.22 Ratio of the Mean of voltage angles errors by Standard Deviations with parameters correlation for IEEE 30-Bus test case.

By comparing the Figure 5.21 and Figure 5.22 with the bias testing figures without parameter correlation for this test case in Figure 5.17 and Figure 5.18, it can be concluded that when the network parameters are correlated, the State Estimator is more biased (for smaller parameters uncertainties).

5.3.5 The Results with PMU

According to the optimal PMU locations developed in [Chakrabarti 2009], for this test case PMU are placed on 5 buses that shown in Table 5.1.

Table 5.1 PMU locations for IEEE 30-Bus test case

PMU placed on bus number:
2
4
6
10
12

Figure 5.23 and Figure 5.24 show the bias tests for voltage magnitudes and phases respectively.

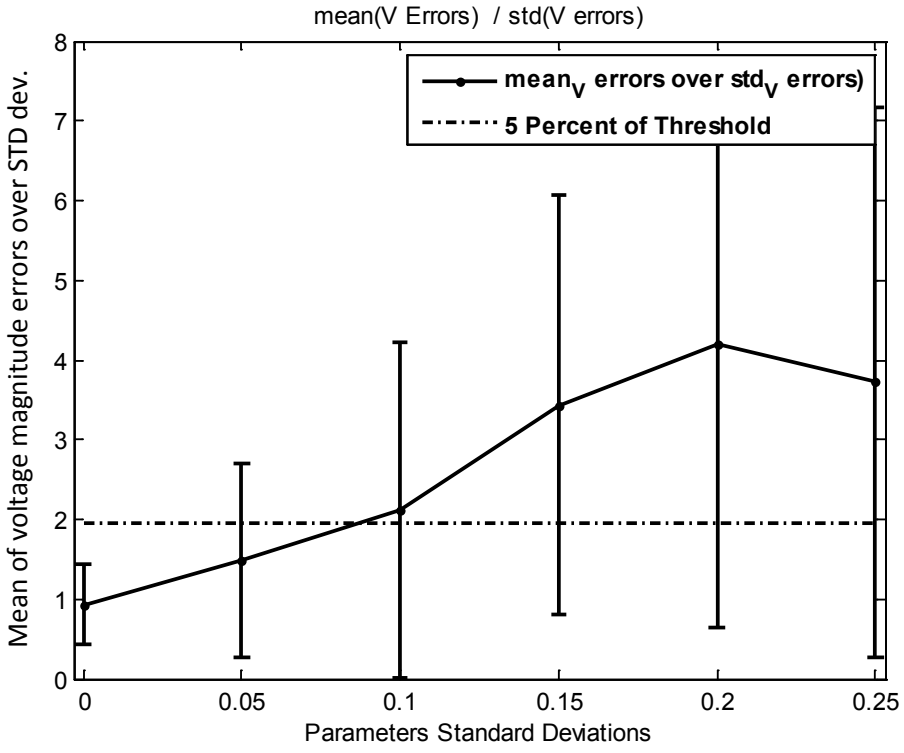

Figure 5.23 Ratio of the Mean of voltage magnitude errors by related Standard Deviations with the presence of PMU measurements for IEEE 30-Bus test case.

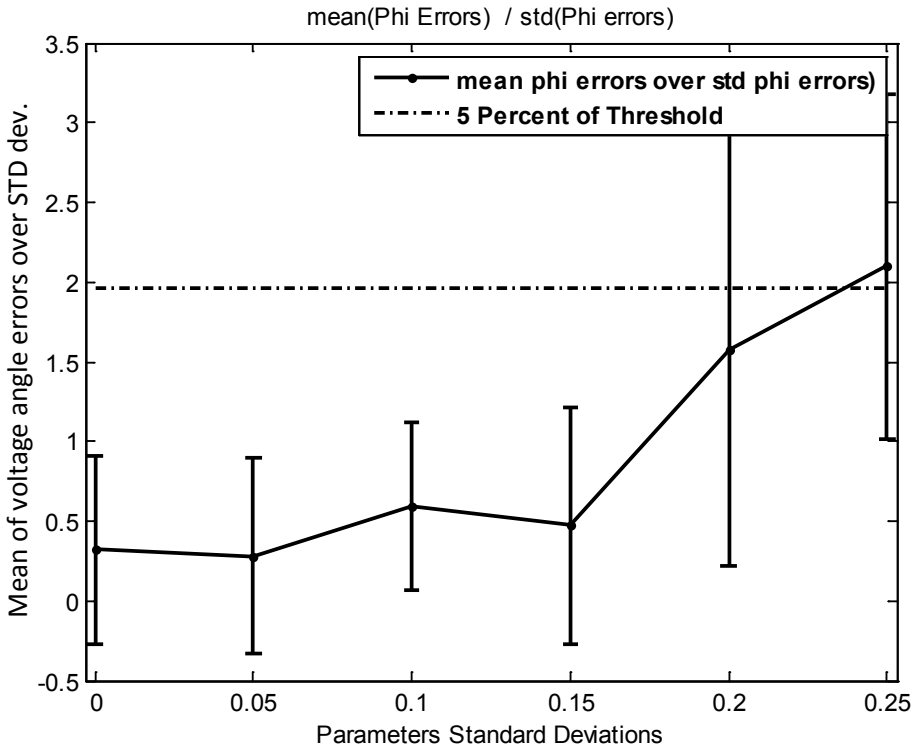

Figure 5.24 Ratio of the Mean of voltage Angle errors by related Standard Deviations with the presence of PMU measurements for IEEE 30-Bus test case.

As it is clear in Figure 5.24, when there are PMUs installed, the output of State Estimator's voltage Angles are not biased for the network parameter uncertainties up to 25%.

It is mentionable that in Figure 5.23, the bias behavior is not affected significantly in this test case, it is mostly because the PMUs are placed on the buses that there was already voltage meter available.

5.4 Test of Algorithm on IEEE 57-Bus Case

The one-line diagram of the IEEE 57-Bus test case is illustrated in Figure 5.25. The original network and data files can be found in [Christie 1999].

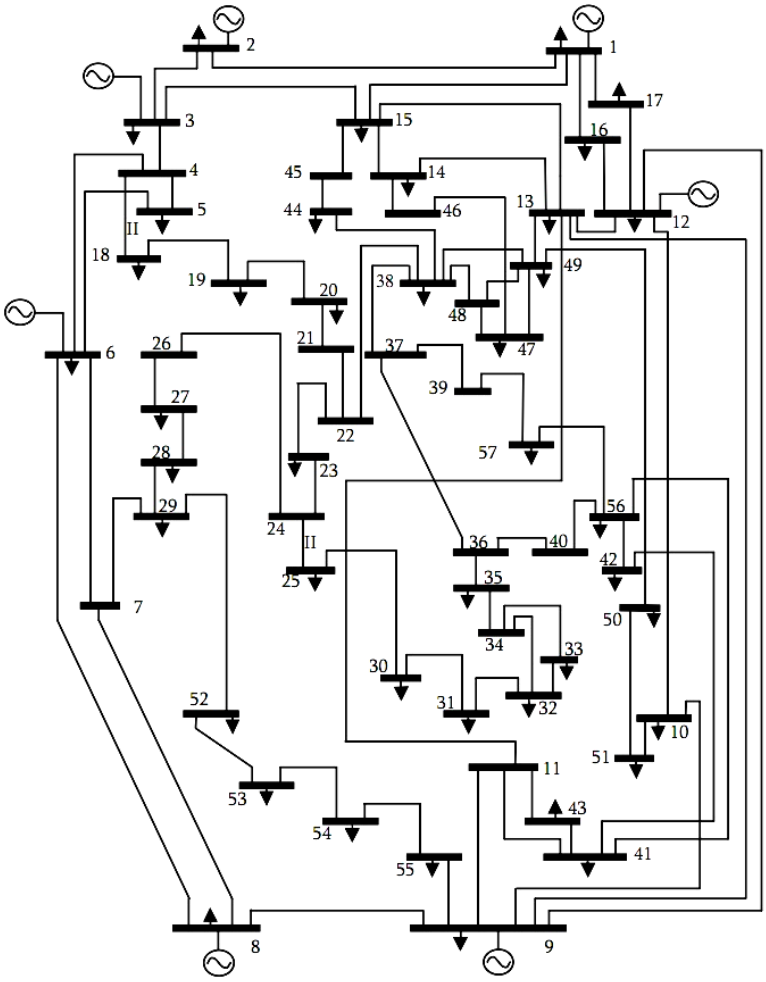

Figure 5.25 IEEE 57-Bus Test Case One-Line Diagram

For this test case, totally 166 measurements are selected. The measurement redundancy ratio will be:

$\eta \approx 1.47$

The measurement set for this test case almost includes all the PV buses (voltage and power injection measurements) together with power flow measurements as the following:

- Voltage magnitudes at PV buses: 1, 2, 3, 6, 8 and 9.
- Active and reactive power injections at buses: 1, 2, 3, 5, 6, 7, 8, 9, 11, 17, 20, 21, 25, 29, 30, 31, 33, 34, 37, 38, 39, 40, 44, 45, 46, 48, 49, 52, 54, 55, 56 and 57.
- Active and reactive power flows on branches: 1-2, 1-15, 2-3, 3-4, 4-5, 7-6, 8-6, 8-9, 9-13, 11-9, 11-13, 12-13, 13-49, 14-15, 19-18, 20-19, 23-22, 24-23, 24-25, 24-26, 27-26, 27-28, 30-25, 30-31, 31-32, 32-34, 32-33, 34-35, 36-

35, 36-37, 36-40, 37-38, 38-22, 38-40, 40-49, 40-56, 41-43, 42-41, 45-15, 46-47, 47-48, 48-49, 49-50, 50-51, 52-53, 53-54, 54-55 and 55-9.

5.4.1 Mean and Standard Deviation of State Estimator

The error bars plots for mean and standard deviation of voltage magnitude and voltage angles versus all the network parameters uncertainty samples are shown respectively in the Figure 5.26 and Figure 5.27.

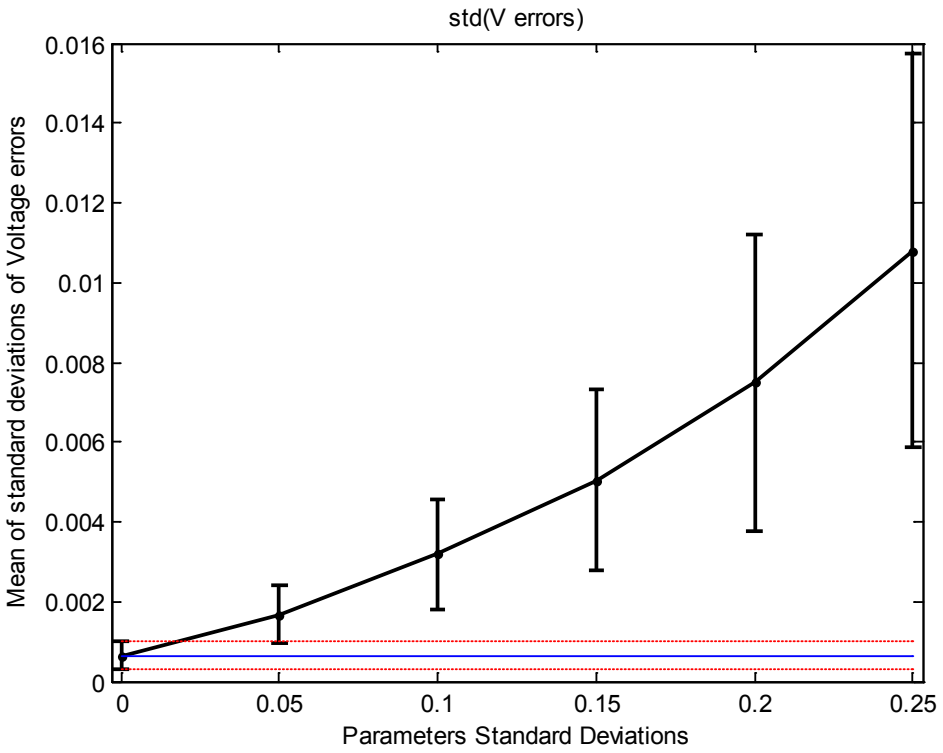

Figure 5.26 Mean and Standard Deviation of Voltage Magnitude Errors for IEEE 57-Bus test case.

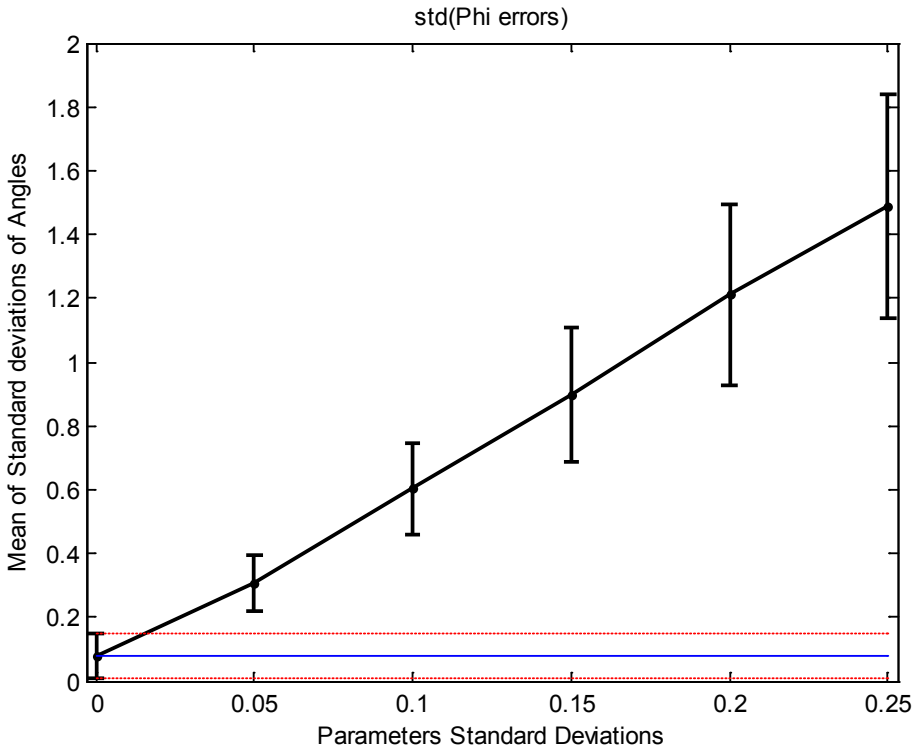

Figure 5.27 Mean and Standard Deviation of Voltage Angle Errors for IEEE 57-Bus test case.

In the figures, the mean of errors for both voltage magnitudes and angles don't start from zero point showing the effect of the measurement uncertainty.

The figures clearly show that by growth of the network parameters uncertainty, the mean and standard deviation of errors will considerably grow. Therefore if just the theoretical standard deviations are taken into consideration, the State Estimation's standard deviation is underestimated enormously.

5.4.2 Bias Testing for State Estimator

Figure 5.28 and Figure 5.29 show the ratio of absolute value of voltage error Means by the related Standard Deviations versus the network parameters uncertainty respectively for voltage magnitudes and angles for IEEE 57-bus test case.

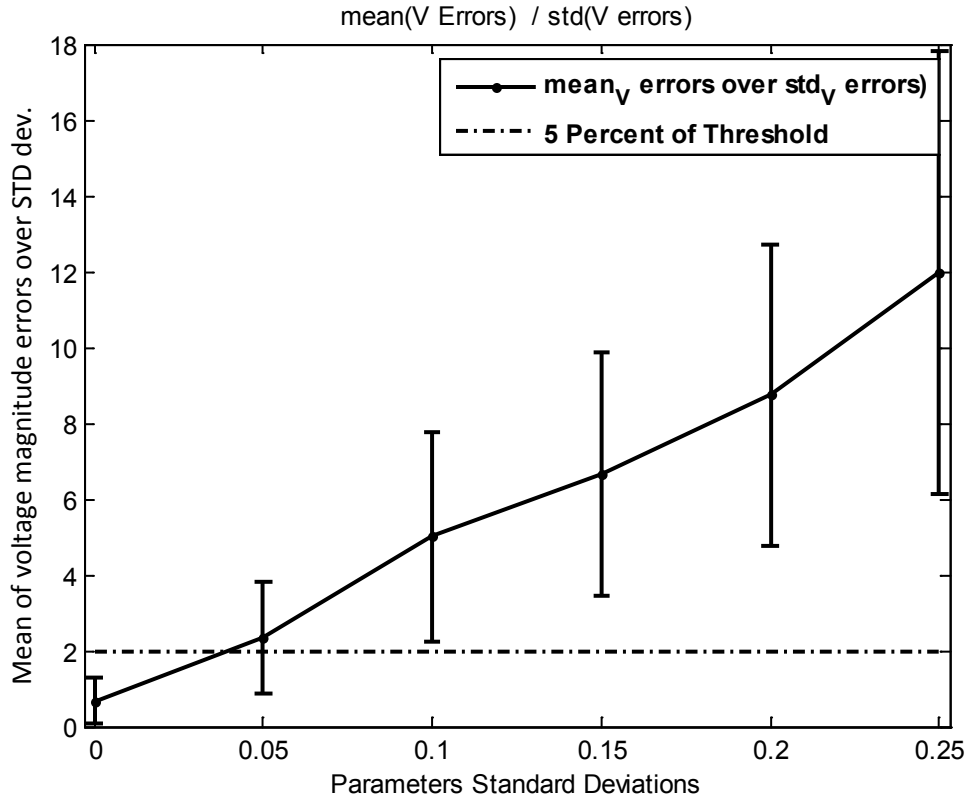

Figure 5.28 Mean and Standard Deviation of Voltage Magnitude Errors for IEEE 57-Bus test case.

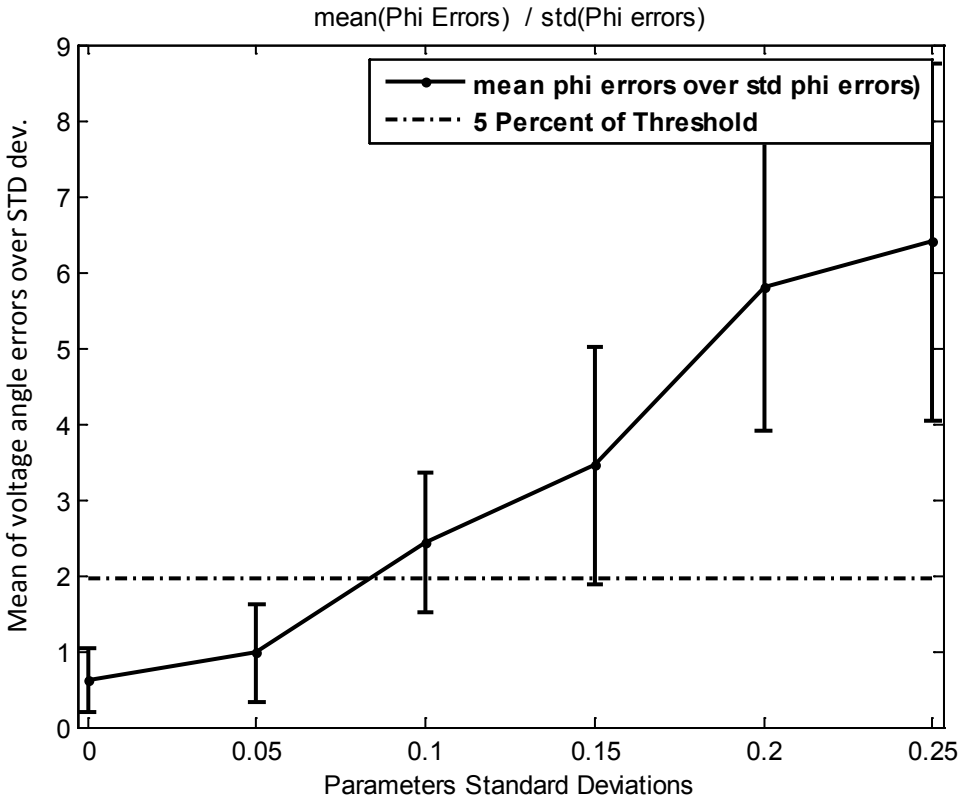

Figure 5.29 Mean and Standard Deviation of Voltage Angle Errors for IEEE 57-Bus test case.

A horizontal dashed line is also depicted in the figures to give an idea about the 5 percent of threshold, meaning that the state estimator is not biased for the network parameters uncertainty range below this line.

According to the figures, it is apparent that for this power network test case the State Estimator's Voltage Magnitude and Voltage Angle outputs are not biased for the parameters uncertainties up to nearly 4 percent and 8 percent respectively.

5.4.3 Correlation of State Estimator's Errors

In Figure 5.30 and Figure 5.31 the correlation coefficients of State Estimator's errors versus parameters uncertainty are shown for Voltage errors and Phase errors respectively.

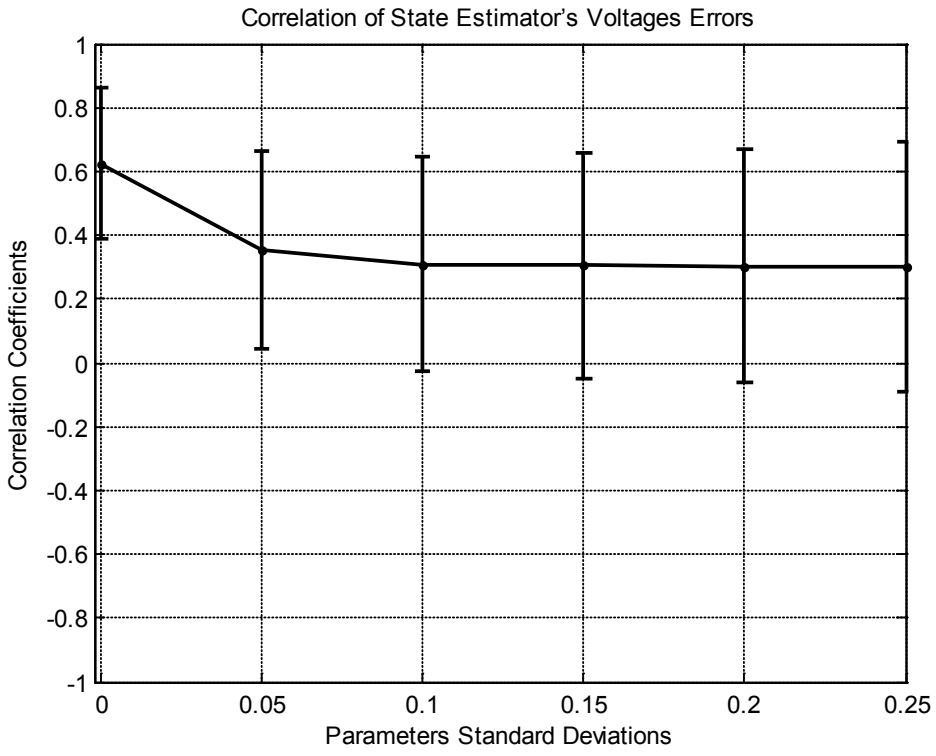

Figure 5.30 Correlation of State Estimator's Errors (Voltage Magnitude) of IEEE 57-Bus test case.

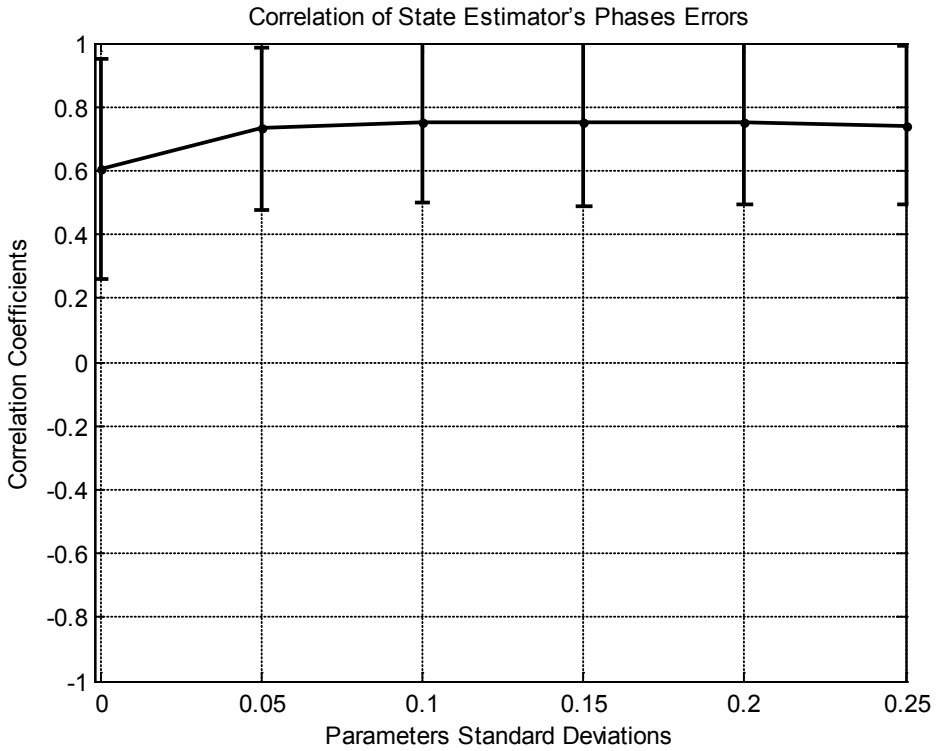

Figure 5.31 Correlation of State Estimator's Errors (Angles) of IEEE 57-Bus test case.

In Figure 5.30 it is noticeable that the State Estimator's Voltage Magnitude Errors are a little bit correlated and by increment of network uncertainty, the correlation goes even lesser. This behavior is because of the voltage measurement locations that are less compared to IEEE case 14-bus.

The Figure 5.31 shows that the State Estimator's Angles Errors are correlated considerably when there is parameters uncertainty and the Angles errors will be still correlated even for large parameters uncertainties up to 25%. State Estimator's Angles Errors are less correlated when there is no parameters uncertainty.

5.4.4 Parameter's Correlation Effect on IEEE 57-Bus case

To perform this analysis, the nominal values of line resistances are correlated with the correlation coefficient of 0.8 and the line resistances with zero nominal values were not correlated.

With having parameters correlation, the ratio of the mean of voltage magnitudes and angles errors by Standard Deviations for IEEE 57-Bus test case are shown in Figure 5.32 and Figure 5.33.

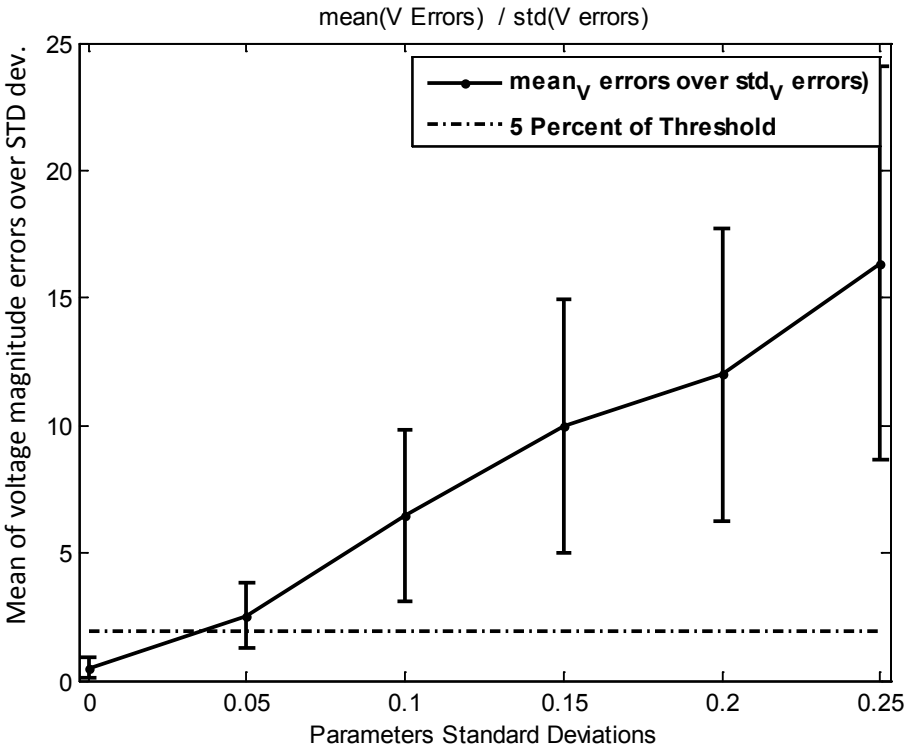

Figure 5.32 Ratio of the Mean of voltage magnitudes errors by Standard Deviations with parameters correlation for IEEE 57-Bus test case.

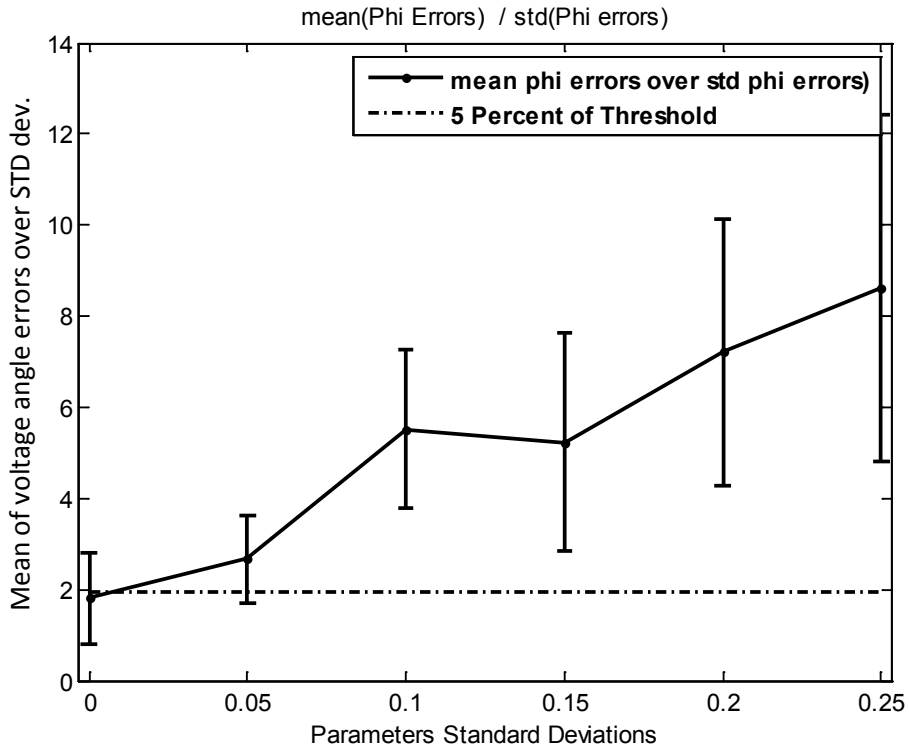

Figure 5.33 Ratio of the Mean of voltage angles errors by Standard Deviations with parameters correlation for IEEE 57-Bus test case.

By comparing Figure 5.32 and Figure 5.33 with the figures of bias testing without parameter correlation for this test case (Figure 5.28 and Figure 5.29), it is evident that when the network parameters are correlated, the State Estimator is more biased and.

This test case showed this effect prominently after increasing the number of Monte Carlo trials to 5000.

5.4.5 The Results with PMU

According to the optimal PMU locations developed in [Chakrabarti 2009], for this test case 7 PMUs are placed on the buses that shown in Table 5.2.

Table 5.2 PMU locations for IEEE 57-Bus test case

PMU placed on bus number:
4
9
15
20
24
53
57

Figure 5.34 and Figure 5.35 show the bias tests for voltage magnitudes and phases respectively.

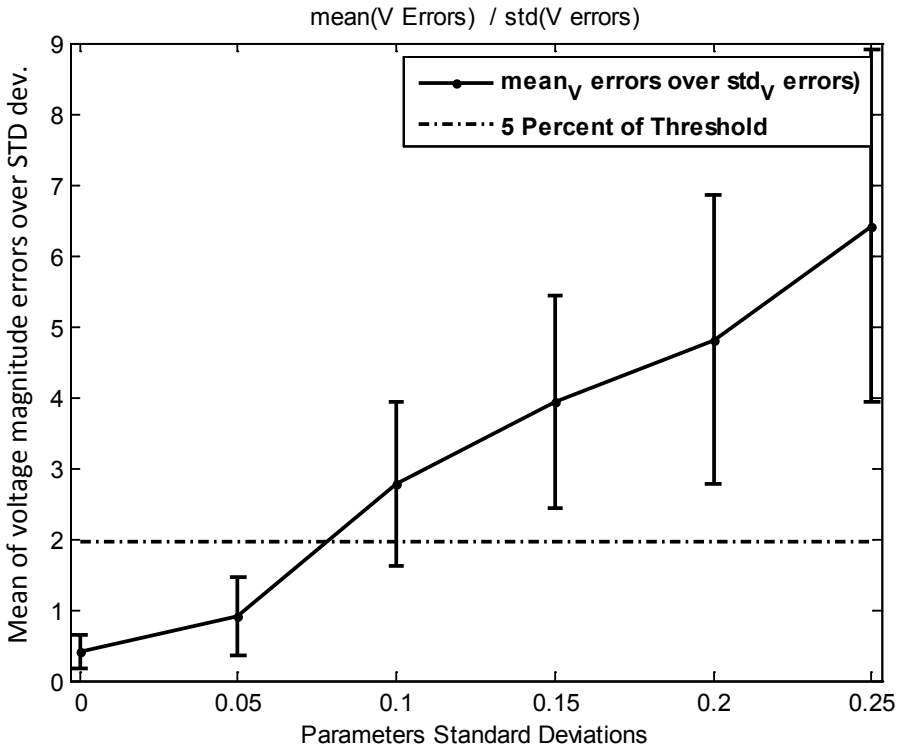

Figure 5.34 Ratio of the Mean of voltage magnitude errors by related Standard Deviations with the presence of PMU measurements for IEEE 57-Bus test case.

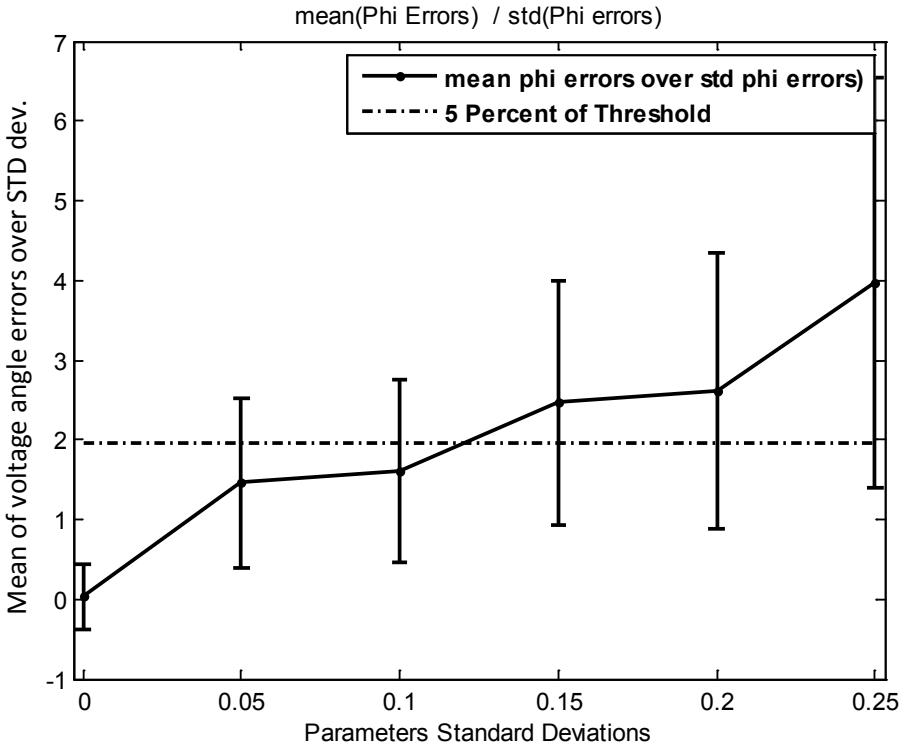

Figure 5.35 Ratio of the Mean of voltage Angle errors by related Standard Deviations with the presence of PMU measurements for IEEE 57-Bus test case.

According to the Figure 5.34 and Figure 5.35, when there are PMU measurements for this test case, the output of State Estimator's voltage Magnitudes and Angles are less biased (for bigger range of network parameters).

5.5 Test of Algorithm on IEEE 118-Bus Case

The one-line diagram of the IEEE 118-Bus test case is illustrated in Figure 5.36. Network parameters and Bus data for this test case can be found in [Christie 1999].

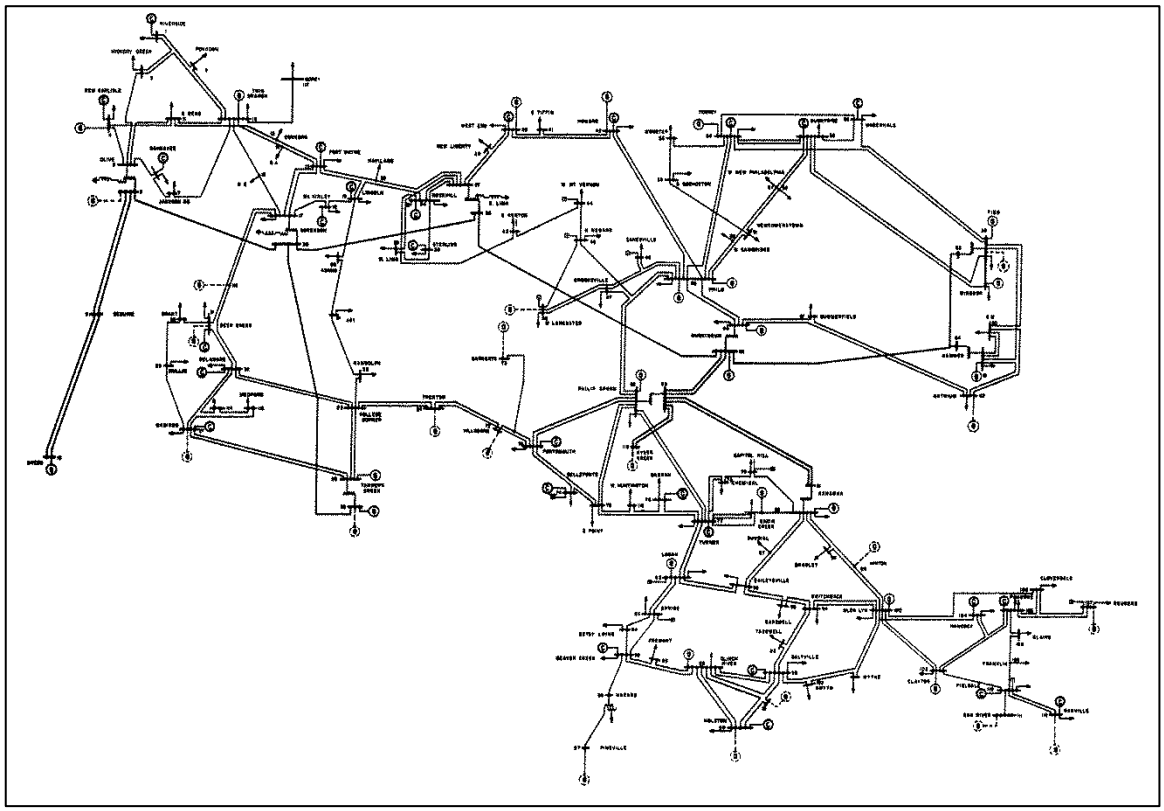

Figure 5.36 IEEE 118-Bus Test Case One-Line Diagram

For this test case, totally 365 measurements are selected. The measurement redundancy ratio will be:

$\eta \approx 1.55$

The measurement set for this test case almost includes all the PV buses (voltage and power injection measurements) together with power flow measurements as the following:

- Voltage magnitudes at PV buses: 1, 2, 3, 4, 5, 6, 7, 8, 9, 10, 11, 12, 13, 14, 15, 16, 17, 18, 19, 20, 21, 22, 23, 24, 25, 26, 27, 28, 29, 30, 31, 32, 33, 34, 35, 36, 37, 38,

39, 40, 41, 42, 43, 44, 45, 46, 47, 48, 49, 50, 51, 52, 53, 54, 55, 56, 57, 58, 59, 60, 61, 62, 63, 64, 65, 66, 67, 68, 69, 70, 71, 72, 73, 74, 75, 76, 77, 78, 79, 80, 81, 82, 83, 84, 85, 86, 87, 88, 89, 90, 91, 92, 93, 94, 95, 96, 97, 98, 99, 100, 101, 102, 103, 104, 105, 106, 107, 108, 109, 110, 111, 112 and 113.

- Active and reactive power injections at buses: 2, 3, 7, 8, 10, 12, 13, 15, 16, 17, 18, 21, 22, 23, 24, 27, 28, 29, 31, 33, 38, 41, 43, 44, 45, 46, 47, 48, 50, 51, 52, 63, 65, 69, 70, 71, 73, 74, 75, 81, 82, 83, 84, 86, 88, 90, 91, 92, 93, 94, 95, 96, 97, 100, 101, 102, 103, 104, 105, 106, 110, 111, 112, 113, 115, 116 and 118.
- Active and reactive power flows on branches: 1-2, 1-3, 3-5, 5-6, 7-12, 8-5, 8-9, 9-10, 11-4, 12-14, 17-15, 17-30, 18-17, 19-20, 25-26, 29-31, 31-32, 32-114, 34-36, 35-36, 35-37, 37-39, 37-40, 38-37, 38-65, 39-40, 40-41, 49-54, 50-49, 51-49, 51-52, 51-58, 52-53, 54-55, 54-59, 59-55, 59-56, 59-60, 59-61, 61-60, 63-59, 64-61, 65-68, 66-49, 66-62, 66-67, 69-68, 71-70, 77-78, 80-77, 80-79, 80-98, 81-68, 83-84, 85-86, 86-87, 95-96, 96-97 and 105-108.

5.5.1 Mean and Standard Deviation of State Estimator

The error bars plots for mean and standard deviation of voltage magnitude and voltage angles versus all the network parameters uncertainty samples are shown respectively in the Figure 5.37 and Figure 5.38.

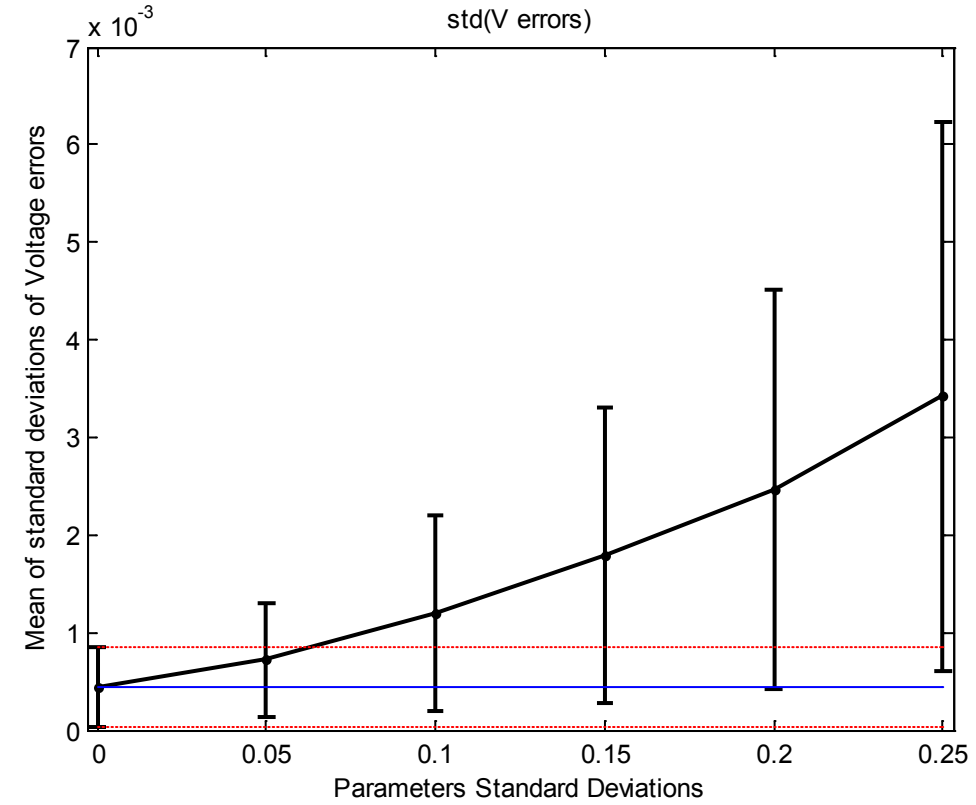

Figure 5.37 Mean and Standard Deviation of Voltage Magnitude Errors for IEEE 118-Bus test case.

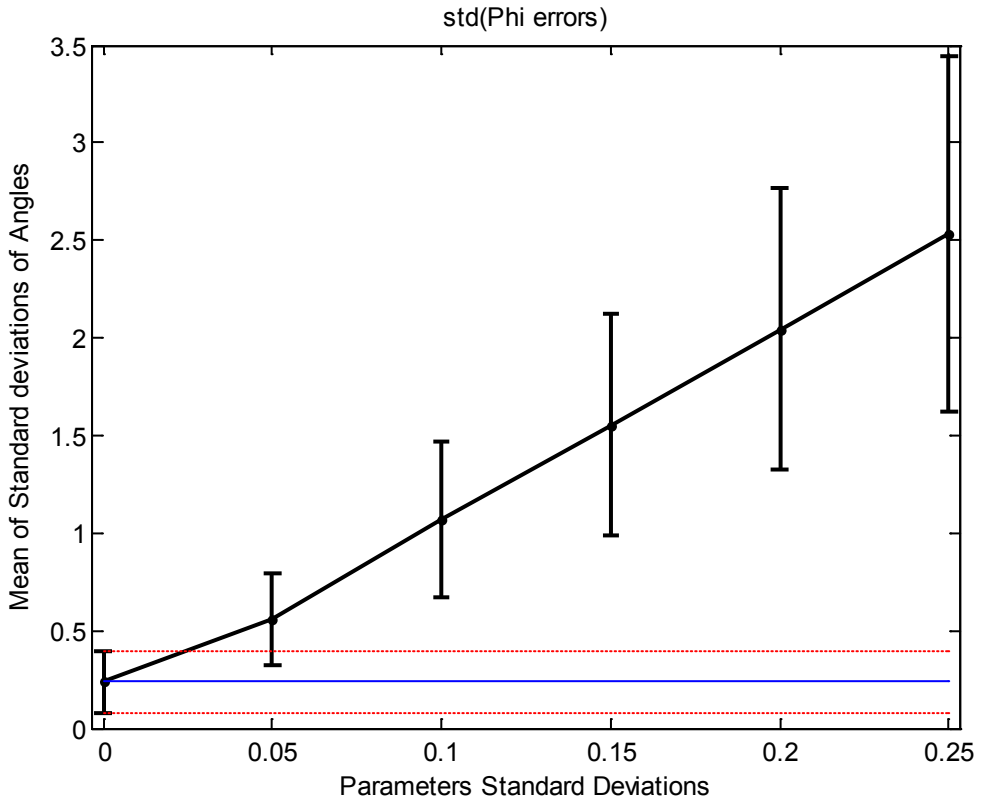

Figure 5.38 Mean and Standard Deviation of Voltage Angle Errors for IEEE 118-Bus test case.

The figures clearly show that by growth of the network parameters uncertainty, the mean and standard deviation of errors will considerably grow. Therefore if just the theoretical standard deviations are taken into consideration, the State Estimation's standard deviation is underestimated enormously. The results are based on 5000 Monte Carlo Trials.

In the figures, the mean of errors for both voltage magnitudes and angles don't start from zero point showing the effect of the measurement uncertainty.

5.5.2 Bias Testing for State Estimator

Figure 5.39 and Figure 5.40 show the ratio of absolute value of voltage error Means by the related Standard Deviations versus the network parameters uncertainty respectively for voltage magnitudes and angles for IEEE 118-bus test case.

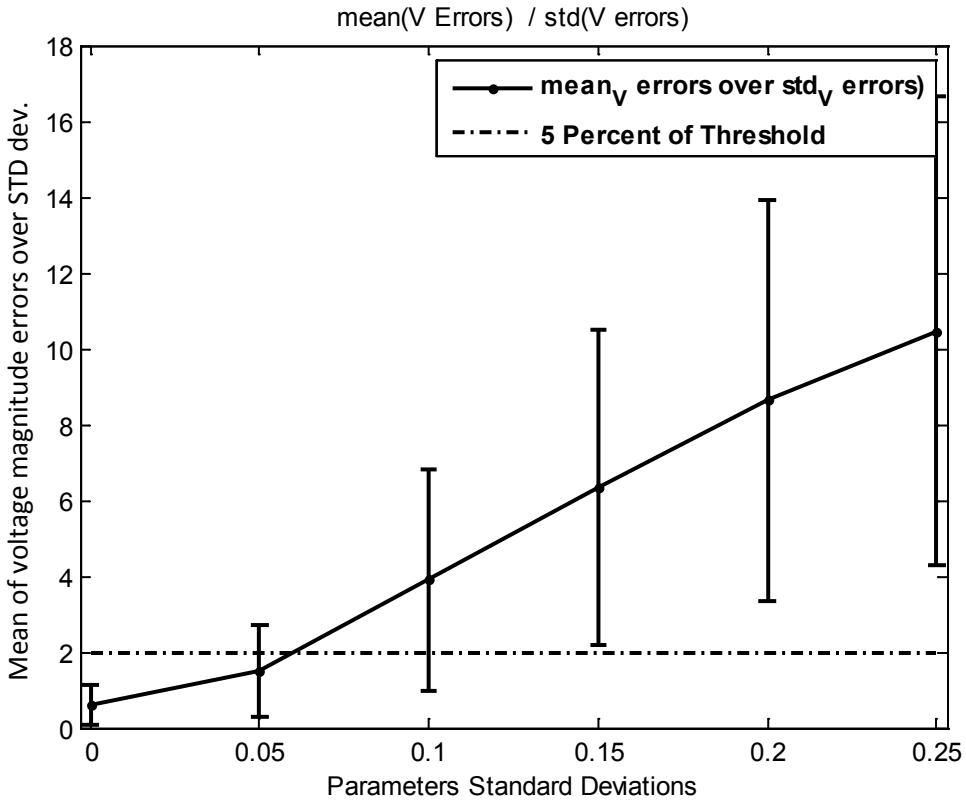

Figure 5.39 Mean and Standard Deviation of Voltage Magnitude Errors for IEEE 118-Bus test case.

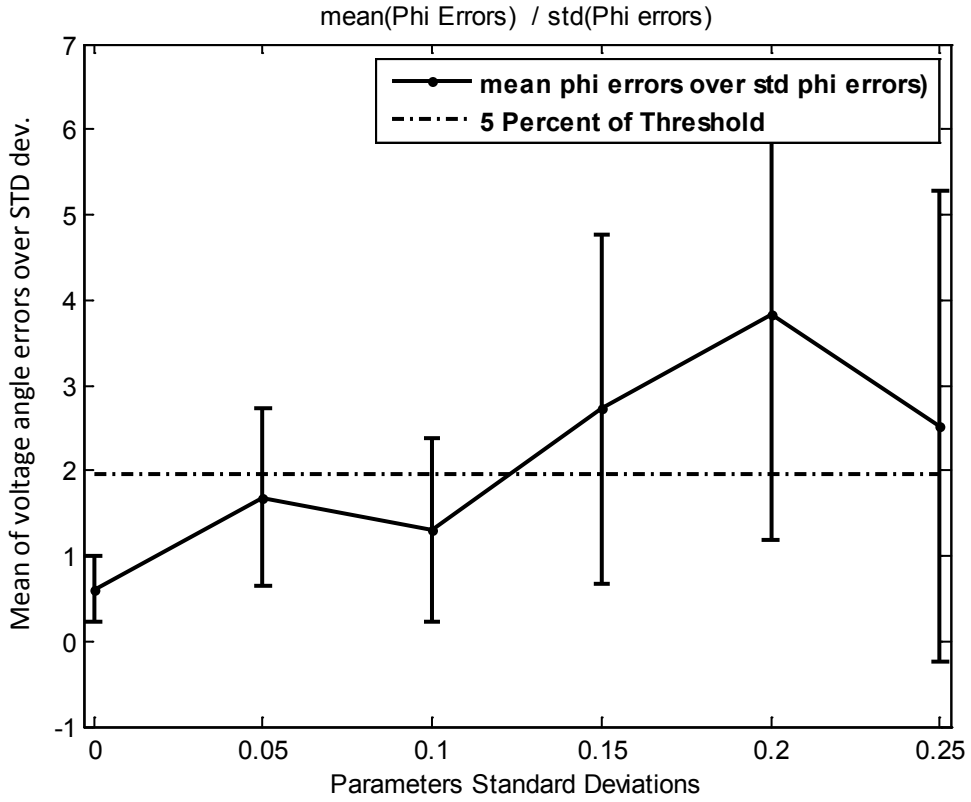

Figure 5.40 Mean and Standard Deviation of Voltage Angle Errors for IEEE 118-Bus test case.

A horizontal dashed line is also depicted in the figures to give an idea about the 5 percent of threshold, meaning that the state estimator is not biased for the network parameters uncertainty range below this line.

According to the figures, it is apparent that for this test case the State Estimator's Voltage Magnitude and Voltage Angle outputs are not biased for the parameters uncertainties up to nearly 6 percent and 12 percent respectively.

5.5.3 Correlation of State Estimator's Errors

In Figure 5.41 and Figure 5.42 the correlation coefficients of State Estimator's errors versus parameters uncertainty are shown for Voltage errors and Phase errors respectively.

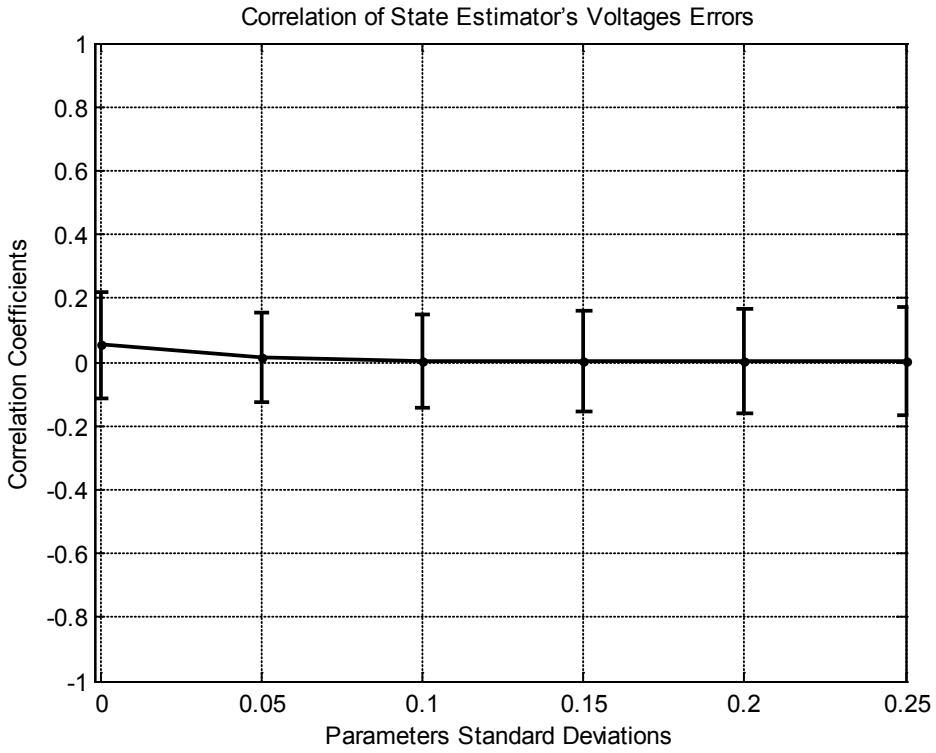

Figure 5.41 Correlation of State Estimator's Errors (Voltage Magnitude) of IEEE 118-Bus test case.

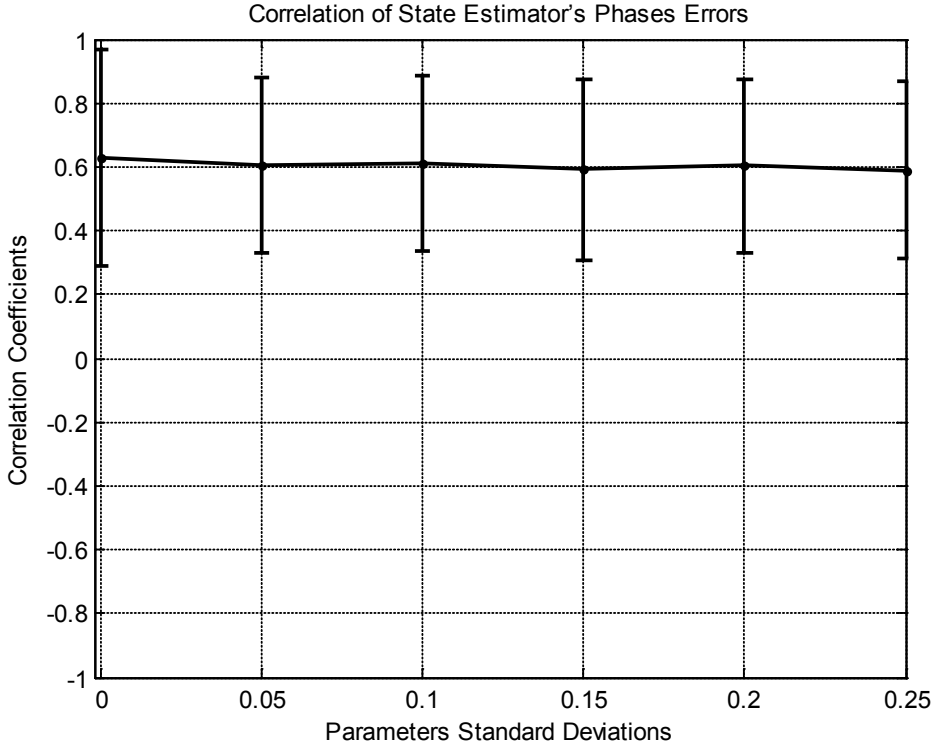

Figure 5.42 Correlation of State Estimator's Errors (Angles) of IEEE 118-Bus test case.

In Figure 5.41 it is noticeable that the State Estimator's Voltage Magnitude Errors are almost not correlated to each other and by increment of network uncertainty it remains uncorrelated. This behavior is mostly because of choosing too many Voltage Magnitudes measurements. The Figure 5.42 shows that the State Estimator's Angles Errors are moderately correlated and when there is parameters uncertainty, the Angles errors will be still correlated even for large parameters uncertainties up to 25%.

5.5.4 Parameter's Correlation Effect on IEEE 118-Bus case

To perform this analysis, the nominal values of line resistances are correlated with the correlation coefficient of 0.8 and the line resistances with zero nominal values were not correlated.

With having parameters correlation, the ratios of the mean of voltage magnitudes and angles errors by Standard Deviations for IEEE 118-Bus test case are shown in Figure 5.43 and Figure 5.44.

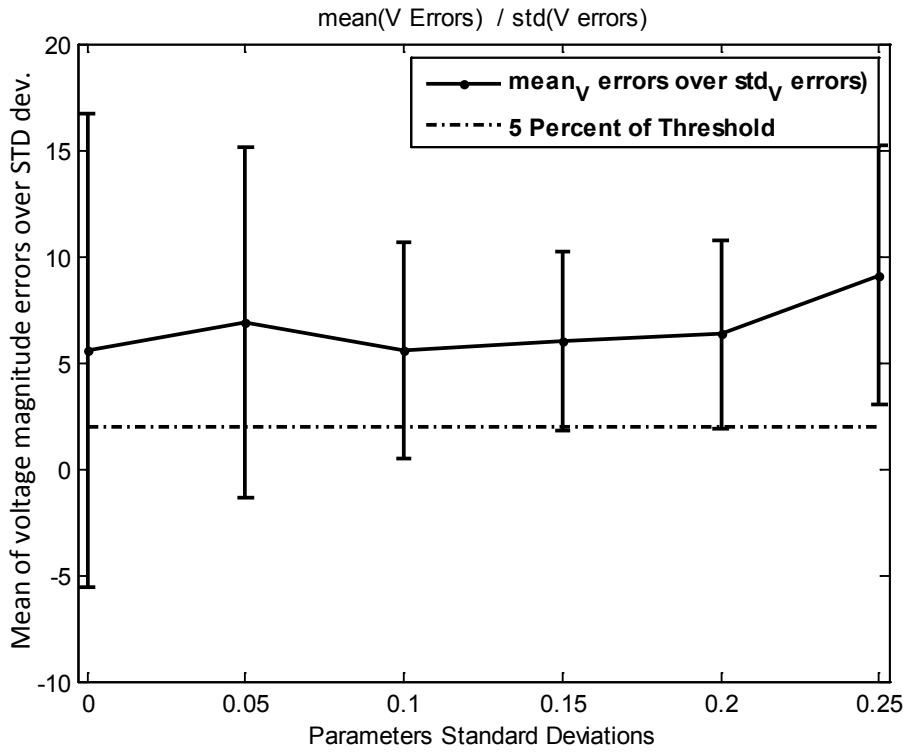

Figure 5.43 Ratio of the Mean of voltage magnitudes errors by Standard Deviations with parameters correlation for IEEE 118-Bus test case.

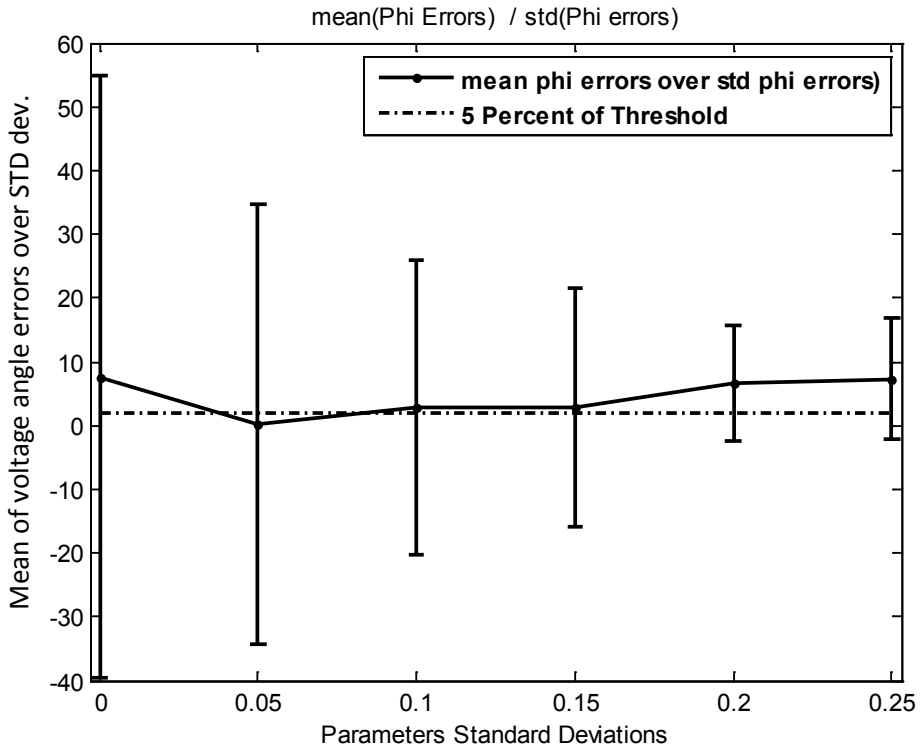

Figure 5.44 Ratio of the Mean of voltage angles errors by Standard Deviations with parameters correlation for IEEE 118-Bus test case.

By comparing Figure 5.43 and Figure 5.44 with the figures of bias testing without parameter correlation for this test case (Figure 5.39 and Figure 5.40), it is evident that when the network parameters are correlated, the State Estimator's Voltage magnitude errors are totally biased and the State Estimator's Voltage magnitude errors is on the edge of biasness for different network parameters.

5.5.5 The Results with PMU

According to the optimal PMU locations developed in [Chakrabarti 2009], for this test case 13 PMUs are placed on the buses that shown in Table 5.3.

Table 5.3 PMU locations for IEEE 118-Bus test case

PMU placed on bus number:
3
12
21
30
37
45
56

64
75
85
94
105
114

Figure 5.45 and Figure 5.46 show the bias tests for voltage magnitudes and phases respectively.

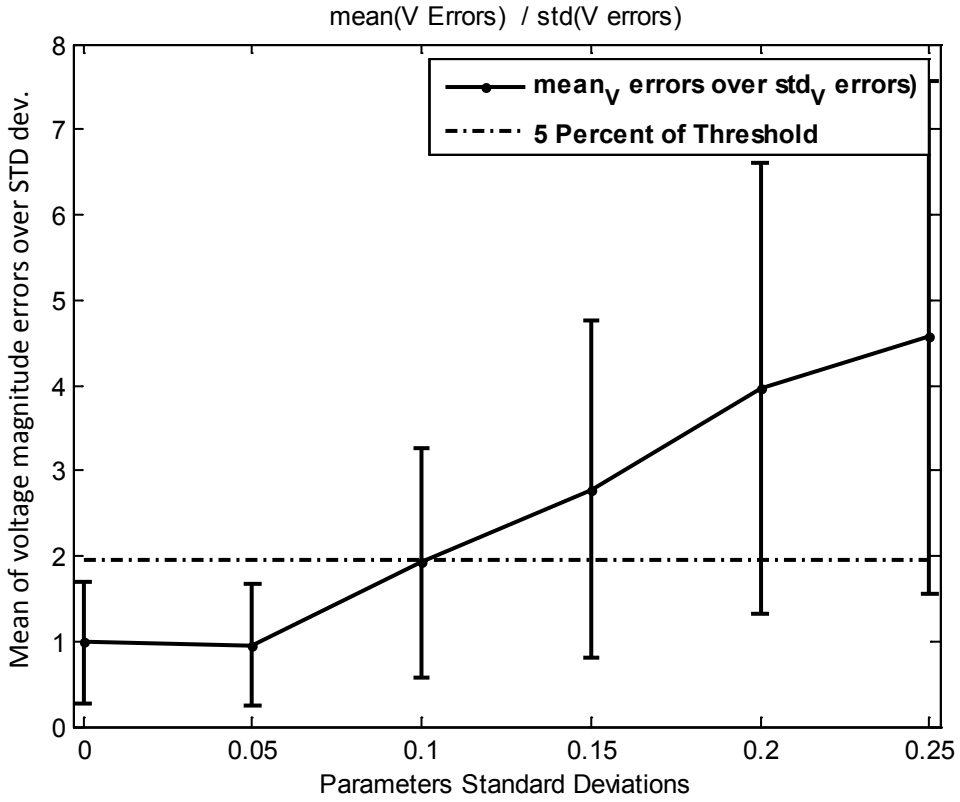

Figure 5.45 Ratio of the Mean of voltage magnitude errors by related Standard Deviations with the presence of PMU measurements for IEEE 118-Bus test case.

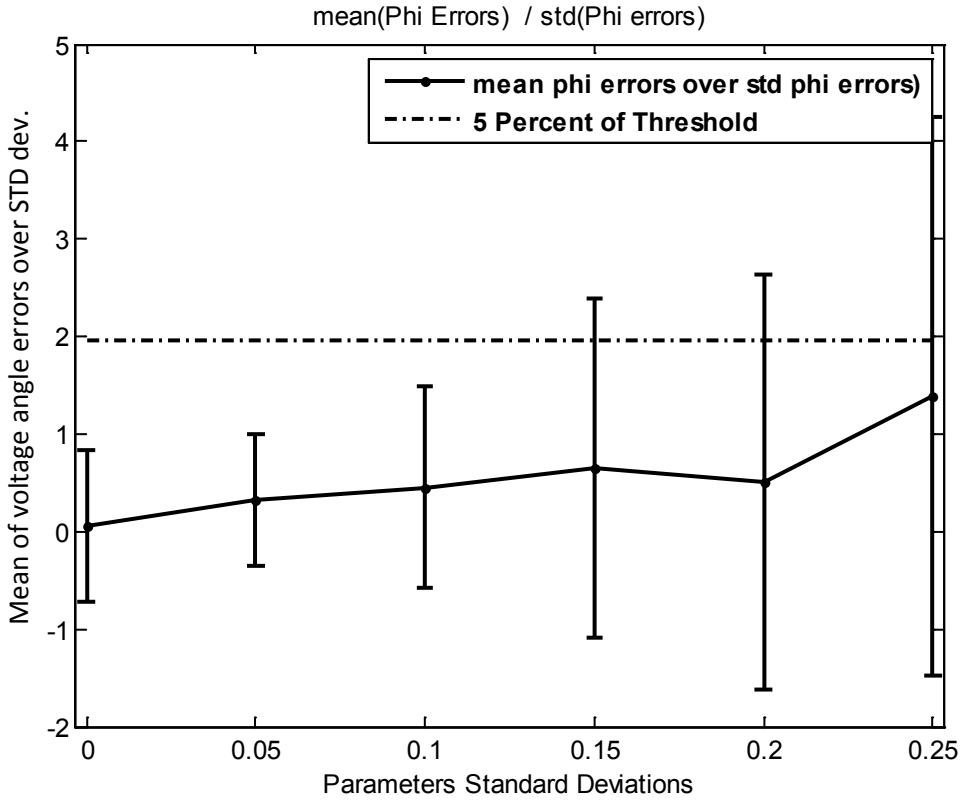

Figure 5.46 Ratio of the Mean of voltage Angle errors by related Standard Deviations with the presence of PMU measurements for IEEE 118-Bus test case.

Considering the Figure 5.45 and Figure 5.46 and comparing them with Figure 5.39 and Figure 5.40, it is apparent when there are PMU measurements for this test case, the output of State Estimator's voltage Magnitudes are less biased (for bigger range of network parameters) and the output of State Estimator's voltage Angles are not biased at least for the parameters uncertainty up to 25%.

Conclusions

In this thesis an algorithm for analyzing both the effects of network parameters uncertainty along with the measurement uncertainty on WLS state estimator is proposed and simulated on IEEE 14-Bus, 30-Bus, 57-Bus and 118-Bus test cases in Matlab simulation environment. The results of simulations show that the state estimator's accuracy is affected considerably according to the network parameters uncertainty and the amount of variations are illustrated by means of state errors distribution (in terms of error bars representing the distribution mean and 1σ standard deviation) versus the network parameters uncertainty for the test cases.

The lack of literature studies about the analysis of network parameters effects on WLS State Estimator's bias performance led us to perform a new prominent analysis to find how network parameters uncertainty can affect the state estimator's bias (for a given measurement uncertainly). Hence it is done by using the ratio of absolute value of state error means by the related standard deviations versus the network parameters uncertainty and comparing it with a predefined threshold.

WLS State Estimation provides a mathematical expression for calculating the variance covariance matrix of State Estimates and when there is network parameters uncertainty, the simulations confirm that the State Estimation's standard deviation is underestimated enormously because only the uncertainty of measurement data is considered.

Phasor Measurement Unit (PMU) can be used to make the state estimates less sensitive to the network parameters uncertainty, because the analysis show that when PMU measurement data are included in the traditional measurement set, the outputs of

State estimator are comparatively much less biased so that in some test cases, the State estimator's phases are totally unbiased for huge range of network parameters.

Lastly an analysis is carried out to illustrate how much the State Estimator's results are mutually connected to each other when the network parameters have uncertainty. The results reveal that when there is no parameters uncertainty the State Estimator's Angle errors are correlated considerably and by increment of network parameter uncertainty, the correlation effect will be a little bit smaller. While the State Estimator's Voltage Magnitude errors are correlated moderately when there is no parameters uncertainty and by increment of network parameter uncertainty, the correlation effect will significantly goes smaller.

Bibliography

[Andreich 1968] R. G. Andreich, H. E. Brown, H. H. Happ, C.E. Person, “The Piecewise Solution Of The Impedance Matrix Load Flow”, IEEE Transactions On Power Apparatus And Systems, 87(10), 1877-1882, 1968.

[Baran 1995] Baran, M.E., Jinxiang Zhu, Hongbo Zhu, Garren, K.E., "A Meter Placement Method For State Estimation", IEEE Transactions On Power Systems, Vol.10, No.3, pp.1704-1710, Aug 1995.

[Bi 2008] T.S. Bi, X.H. Qin, Q.X. Yang, “A Novel Hybrid State Estimator For Including Synchronized Phasor Measurements”, Electric Power Syst. Res., 78, pp. 1343–1352, 2008.

[Brown 1963] H. E. Brown, G. K. Carter, II. H. Happ, And C. E. Person, "Power Flow Solution By Impedance Matrix Iterative Method," IEEE Trans. Power Apparatus And System, Vol. 82, pp. 1-10, April 1963.

[Chakrabarti 2009] Saikat Chakrabarti, Elias Kyriakides, “Placement Of Synchronized Measurements For Power System Observability”, IEEE TRANSACTIONS ON POWER DELIVERY, VOL. 24, NO. 1, JANUARY 2009.

[Chan 2000] W.L. Chan, A.T.P. So, L.L. Lai, “Initial Applications Of Complex Artificial Neural Networks To Load-Flow Analysis”, IEE Proceedings Of Generation Transmission Distribution, 147(6), 361–366, 2000.

[Chen 2006] Jian Chen, Abur, A., "Placement Of Pmus To Enable Bad Data Detection In State Estimation,", IEEE Transactions On Power Systems, Vol.21, No.4, pp.1608-1615, Nov. 2006.

[Christie 1999] Richard D. Christie, "Data For The IEEE 14, 30, 57, 118, 300-Bus Test System", University Of Washington 1999, Online Available: Http://Www.Ee.Washington.Edu/Research/Pstca/

[Clarkson 1993] Peter M. Clarkson, "Optimal And Adaptive Signal Processing", CRC Press, 1993.

[Clements 1988] K. A. Clements, P. W. Davis, "Detection And Identification Of Topology Errors In Electric Power Systems", IEEE Trans. Power System, Vol. 3, No. 4, pp. 1748–1753, Nov. 1988.

[Crow 2007] Mariesa L. Crow, "Computational Methods For Electric Power Systems," In Electric Power Engineering Handbook: Power Systems, 2nd Ed By Leonard L. Grigsby, CRC Press, 2007, Ch. 1, Sec. 5.

[Grainger 1994] J. Grainger, W. Stevenson: "Power System Analysis", Mcgraw-Hill, ISBN 0-07-061293-5, 1994.

[Hastings 1970] W. K. Hastings, "Monte Carlo Sampling Methods Using Markov Chains And Their Applications," Biometrika, Vol. 57, No. 1, pp. 97-109, 1970.

[Huang 2003] Shyh-Jier Huang, Jeu-Min Lin "A Changeable Weighting Matrix Applied For State Estimation Of Electric Power", PEDS 2003.

[Kerdchuen 2009] T. Kerdchuen, "Measurement Scheme Improving For State Estimation Using Stochastic Tabu Search", International Journal Of Electrical And Electronics Engineering, pp.3-9, 2009.

[Li 2011] Wei-Guo Li, Jin Li, Ao Gao And Jin-Hong Yand, "Review And Research Trends On State Estimation Of Electrical Power Systems", Power And Energy Engineering Conference (APPEEC), 2011 Asia-Pacific , Vol., No., pp.1-4, 25-28, March 2011.

[Lo 1999] K.L. Lo, Y.J. Lin, W.H. Siew, "Fuzzy-Logic Method For Adjustment Of Variable Parameters In Load Flow Calculation", IEE Proceedings Of Generation Transmission Distribution, 146(3), 276–282, 1999.

[Lukomski 2008] Robert Lukomski, Kazimierz Wilkosz, "Methods Of Measurement Placement Design For Power System State Estimation", POWER SYSTEM MODELING AND CONTROL, AT&P Journal PLUS2, 2008.

[Meliopoulos 2001] A. P. Sakis Meliopoulos, Bruce Fardanesh, Shalom Zelingher, “Power System State Estimation: Modeling Error Effects And Impact On System Operation”, Hawaii International Conference On System Sciences, January 2001.

[Murty 2011] P. S. R. Murty, "Operation And Control In Power Systems", Taylor And Francis, ISBN: 9780415665650, 2011.

[Muscas 2007a] C. Muscas, F. Pilo, G. Pisano And S. Sulis, "Optimal Measurement Devices Allocation For Harmonic State Estimation Considering Parameters Uncertainty In Distribution Networks”, EPQU’07, 9th International Conference Electrical Power Quality And Utilization, Spain, October 2007.

[Muscas 2007b] C. Muscas, F. Pilo, G. Pisano And S. Sulis, "Considering The Uncertainty On The Network Parameters In The Optimal Planning Of Measurement Systems For Distribution State Estimation”, IEEE IMTC/2007, Poland, May 2007.

[Nguyen 1995] T. Nguyen, “Neural Network Load-Flow”, IEE Proceedings Of Generation Transmission Distribution, 142(1), 51–58, 1995.

[Pajic 2007] Slobodan Pajic, “Power System State Estimation And Contingency Constrained Optimal Power Flow - A Numerically Robust Implementation”, Phd Dissertation, Worcester Polytechnic Institute, April 2007.

[Priestly 1981] M. B. Priestly, “Spectral Analysis And Time Series”, Vol 1, Academic Press, 1981.

[Rakpenthai 2005] Chawasak Rakpenthai, Suttichai Premrudeepreechacharn, Sermsak Uatrongjit, Neville R. Watson, “Measurement Placement For Power System State Estimation Using Decomposition Technique”, Electric Power Systems Research, Volume 75, Issue 1, Pages 41-49, July 2005.

[Rakpenthai 2012] Chawasak Rakpenthai, Sermsak Uatrongjit And Suttichai Premrudeepreechacharn, “State Estimation Of Power System Considering Network Parameter Uncertainty Based On Parametric Interval Linear Systems”, IEEE Transactions On Power Systems, Vol. 27, No. 1, pp. 305-313, Feb. 2012.

[Schweppe 1970a] F. C. Schweppe And J. Wildes, “Power System Static-State Estimation, Part I: Exact Model,” IEEE Trans. On Power Apparatus And Systems, Vol. 89, No. 1, pp. 120-125, January 1970.

[Schweppe 1970b] F. C. Schweppe And D. B. Rom, “Power System Static-State Estimation,Part II: Approximate Model,” IEEE Trans. On Power Apparatus And Systems, Vol. 89, No. 1, pp. 125-130, January 1970.

[Schweppe 1970c] F. C. Schweppe, “Power System Static-State Estimation, Part III: Implementation,” IEEE Trans. On Power Apparatus And Systems, Vol. 89, No. 1, pp. 130-135, January 1970.

[Scott 1974] B. Scott, O. Alsac, “Fast Decoupled Load Flow”, IEEE Transactions On Power Apparatus And Systems, 93(3), 859–869, 1974.

[Stagg 1968] G. W. Stagg, A. H. El-Abiad: “Computer Methods In Power Systems”, Mcgraw-Hill, 1968.

[Tinney 1967] W. F. Tinney, C. E. Hart, “Power Flow Solution By Newton’s Method”, IEEE Transactions On Power Apparatus And Systems, 86(4), 1449–1460, Nov. 1967.

[Valenzuela 2000] Jorge Valenzuela, Mainak Mazumdar: “Statistical Analysis Of Electric Power Production Costs”, IIE 2000.

[Wang 2009] Xi-Fan Wang, Yonghua Song, Malcolm Irving: “Modern Power Systems Analysis”, ISBN 978-0-387-72852-0, 2009.

[Wong 1999] K.P. Wong, A. Li, T.M.Y. Law, “Advanced Constrained Genetic Algorithm Load Flow Method”, Proceedings Of Generation Transmission Distribution, 146(6), 609–616, 1999.

[Wood 1996] Allen J. Wood, Bruce F. Wollenberg, "Power Generation, Operation, And Control", Wiley, ISBN: 978-0471586999, 1996.

[Zimmerman 2011] R. D. Zimmerman, C. E. Murillo-Sanchez And R. J. Thomas, “Matpower: Steady-State Operations, Planning And Analysis Tools For Power Systems Research And Education", IEEE Transactions On Power Systems, Vol. 26, No. 1, pp. 12-19, Feb. 2011.

Appendices

Proof of the Jacobian of $J(x)$

The first derivative of $J(x)$ with respect to x is:

$$\frac{\partial J(x)}{\partial x} = \frac{\partial [y^T \Sigma_y^{-1} y - y^T \Sigma_y^{-1} f(x) - f(x)^T \Sigma_y^{-1} y + f(x)^T \Sigma_y^{-1} f(x)]}{\partial x}$$

$$\frac{\partial J(x)}{\partial x} = -y^T \Sigma_y^{-1} \frac{\partial f(x)}{\partial x} - y^T \Sigma_y^{-1^T} \frac{\partial f(x)}{\partial x} + f(x)^T \Sigma_y^{-1^T} \frac{\partial f(x)}{\partial x} + f(x)^T \Sigma_y^{-1} \frac{\partial f(x)}{\partial x}$$

The variance-covariance matrix of measurements Σ_y^{-1} is symmetrical so we can simplify:

$$\frac{\partial J(x)}{\partial x} = -2y^T \Sigma_y^{-1} \frac{\partial f(x)}{\partial x} + 2f(x)^T \Sigma_y^{-1} \frac{\partial f(x)}{\partial x}$$

$$\frac{\partial J(x)}{\partial x} = -2[y - f(x)]^T \Sigma_y^{-1} \left[\frac{\partial f(x)}{\partial x}\right]$$

The Jacobian matrix of $J(x)$ is defined by $g(x)$:

$$g(x) = \left[\frac{\partial J(x)}{\partial x}\right]^T$$

$$g(x) = -2\left[\frac{\partial f(x)}{\partial x}\right]^T \Sigma_y^{-1}[y - f(x)]$$

Proof of the Hessian of $J(x)$

The Hessian matrix of $J(x)$ is the second derivative with respect to x:

$$H(x) = \frac{\partial g(x)}{\partial x}$$

$$H(x) = \frac{\partial \left[-2 \left[\frac{\partial f(x)}{\partial x} \right]^T \Sigma_y^{-1} [y - f(x)] \right]}{\partial x}$$

$$H(x) = \frac{\partial \left[-2 \left[\frac{\partial f(x)}{\partial x} \right]^T \Sigma_y^{-1} y + 2 \left[\frac{\partial f(x)}{\partial x} \right]^T \Sigma_y^{-1} f(x) \right]}{\partial x}$$

$$H(x) = -2y^T \Sigma_y^{-1} \frac{\partial^2 f(x)}{\partial x^2} + 2f(x)^T \Sigma_y^{-1} \frac{\partial^2 f(x)}{\partial x^2} + 2 \left[\frac{\partial f(x)}{\partial x} \right]^T \Sigma_y^{-1} \left[\frac{\partial f(x)}{\partial x} \right]$$

$$H(x) = 2[f(x)^T - y^T] \Sigma_y^{-1} \frac{\partial^2 f(x)}{\partial x^2} + 2 \left[\frac{\partial f(x)}{\partial x} \right]^T \Sigma_y^{-1} \left[\frac{\partial f(x)}{\partial x} \right]$$

$$H(x) = 2[-r]^T \Sigma_y^{-1} \frac{\partial^2 f(x)}{\partial x^2} + 2 \left[\frac{\partial f(x)}{\partial x} \right]^T \Sigma_y^{-1} \left[\frac{\partial f(x)}{\partial x} \right]$$

By neglecting the first part of above equation, we can write the Hessian matrix of $J(x)$ as:

$$H(x) \cong 2 \left[\frac{\partial f(x)}{\partial x} \right]^T \Sigma_y^{-1} \left[\frac{\partial f(x)}{\partial x} \right]$$

Derivation of power network equations using a sample network

In this section the equations for the power calculations for a node will be inspected. Let's consider a sample power network as shown in the figure below:

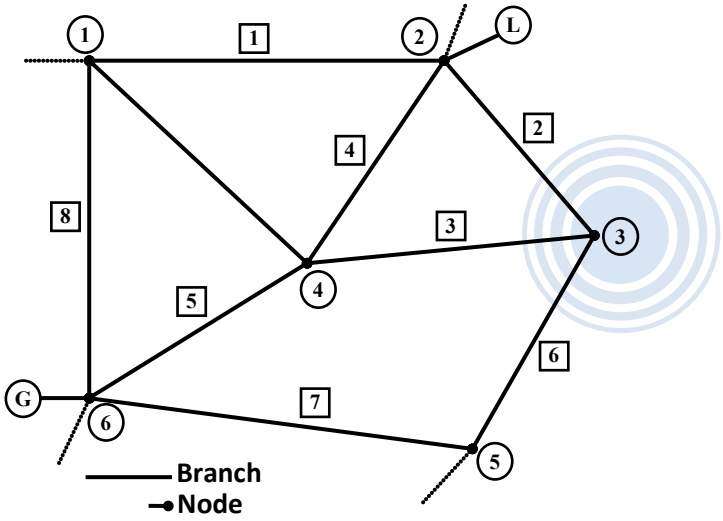

Figure 5.47 Tree of the connected graph of a sample power network

Here all the complex power injections for one node are going to be written and it could be applied to all the nodes in the network. We consider node 3 and all the branches connected to it (Figure below):

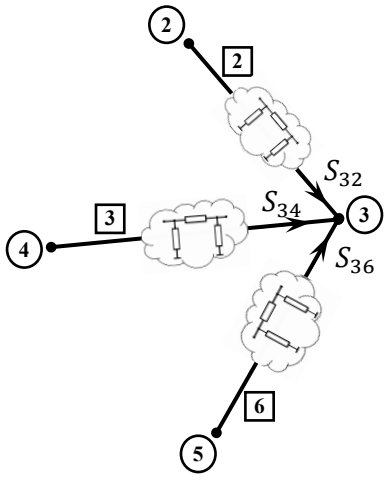

Figure 5.48 The Node 3 in the sample power network along with the all branches connected and the illustration of equivalent pi model for each branch

To find the power injections S_2 and S_3 and S_6 we use the equivalent pi model described in the previous section. The power injection equations will be:

$\bar{S}_{32} = (\bar{y}_2 + \bar{y}_{30})^* \bar{V}_3 \bar{V}_3^* - \bar{y}_2{}^* \bar{V}_3 \bar{V}_2^*$

$\bar{S}_{34} = (\bar{y}_3 + \bar{y}_{30})^* \bar{V}_3 \bar{V}_3^* - \bar{y}_3{}^* \bar{V}_3 \bar{V}_4^*$

$\bar{S}_{36} = (\bar{y}_6 + \bar{y}_{30})^* \bar{V}_3 \bar{V}_3^* - \bar{y}_6{}^* \bar{V}_3 \bar{V}_6^*$

The relationship between the injected complex powers in a node is $\sum \bar{S} = 0$. For node 3 it will be:

$\bar{S}_{32} + \bar{S}_{34} + \bar{S}_{36} = 0$

$(\bar{y}_2 + \bar{y}_{30})^* \bar{V}_3 \bar{V}_3^* - \bar{y}_2{}^* \bar{V}_3 \bar{V}_2^* + (\bar{y}_3 + \bar{y}_{30})^* \bar{V}_3 \bar{V}_3^* - \bar{y}_3{}^* \bar{V}_3 \bar{V}_4^* + (\bar{y}_6 + \bar{y}_{30})^* \bar{V}_3 \bar{V}_3^* - \bar{y}_6{}^* \bar{V}_3 \bar{V}_6^* = 0$

$(\bar{y}_2 + \bar{y}_3 + \bar{y}_6 + 3\bar{y}_{30})^* |\bar{V}_3|^2 - [\bar{y}_2{}^* \bar{V}_2^* + \bar{y}_3{}^* \bar{V}_4^* + \bar{y}_6{}^* \bar{V}_6^*] \bar{V}_3 = 0$

The last equation is the desired non-linear function that relates the states to the physical admittances for the sample power network.

Generalization of Power Equations

The total power fluxes equation for the sample network will be written in order to conclude the equations for a general network easier. The injected powers in nodes are the measured quantities.

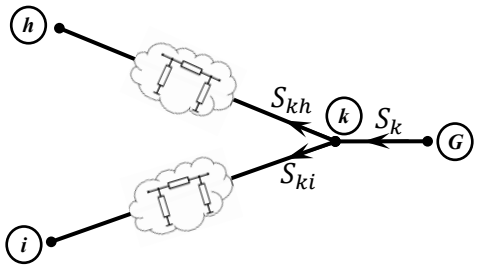

Figure 5.49 Sample network with two branches connected to a generator (power injector) along with the illustration of equivalent pi model

$\bar{S}_{kh} = (\bar{y}_{kh} + \bar{y}_{k0})^* \bar{V}_k \bar{V}_k^* - \bar{y}_{kh}{}^* \bar{V}_k \bar{V}_h^*$

$\bar{S}_{ki} = (\bar{y}_{ki} + \bar{y}_{k0})^* \bar{V}_k \bar{V}_k^* - \bar{y}_{ki}{}^* \bar{V}_k \bar{V}_i^*$

In node k, the injected power, G is equal to the total power fluxes:

$\bar{S}_k = \bar{S}_{kh} + \bar{S}_{ki}$

$$\bar{S}_k = (\bar{y}_{kh} + \bar{y}_{k0})^* \bar{V}_k \bar{V}_k^* - \bar{y}_{kh}{}^* \bar{V}_k \bar{V}_h^* + (\bar{y}_{ki} + \bar{y}_{k0})^* \bar{V}_k \bar{V}_k^* - \bar{y}_{ki}{}^* \bar{V}_k \bar{V}_i^*$$

$$\bar{S}_k = (\bar{y}_{kh} + \bar{y}_{ki} + 2\bar{y}_{k0})^* |\bar{V}_k|^2 - (\bar{y}_{kh} \bar{V}_h + \bar{y}_{ki} \bar{V}_i)^* \bar{V}_k$$

The elements of node admittance can be written as:

$$\bar{y}_{kh} = g_{kh} + jb_{kh}$$

Note that $\bar{y}_{kh}$ is equal to $\bar{y}_{hk}$ and accordingly $g_{kh} = g_{hk}$ and $b_{kh} = b_{hk}$.

Consequently the complex node power injection can be expressed as:

$$P_k + jQ_k =$$
$$= (g_{kh} + jb_{kh} + g_{ki} + jb_{ki} + 2g_{k0} + j2b_{k0})^* |\bar{V}_k|^2 - (g_{kh} \bar{V}_h + jb_{kh} \bar{V}_h + g_{ki} \bar{V}_i + jb_{ki} \bar{V}_i)^* \bar{V}_k$$

$$P_k + jQ_k =$$
$$= (g_{kh} - jb_{kh} + g_{ki} - jb_{ki} + 2g_{k0} - j2b_{k0}) |\bar{V}_k|^2 - g_{kh} \bar{V}_k \bar{V}_h{}^* + jb_{kh} \bar{V}_k \bar{V}_h{}^* -$$
$$- g_{ki} \bar{V}_k \bar{V}_i{}^* + jb_{ki} \bar{V}_k \bar{V}_i{}^*$$

And using polar form of voltage it will be:

$$P_k + jQ_k =$$
$$= (g_{kh} - jb_{kh} + g_{ki} - jb_{ki} + 2g_{k0} - j2b_{k0}) |\bar{V}_k|^2 - g_{kh} |\bar{V}_k||\bar{V}_h| e^{j\theta_{kh}} + jb_{kh} |\bar{V}_k||\bar{V}_h| e^{j\theta_{kh}} -$$
$$- g_{ki} |\bar{V}_k||\bar{V}_i| e^{j\theta_{ki}} + jb_{ki} |\bar{V}_k||\bar{V}_i| e^{j\theta_{ki}}$$

Using Euler rule: $e^{j\theta} = \cos\theta + j \sin\theta$ we will have:

$$P_k + jQ_k =$$
$$= (g_{kh} + g_{ki} + 2g_{k0} - j(b_{kh} + b_{ki} + 2b_{k0})) |\bar{V}_k|^2 -$$
$$- g_{kh} |\bar{V}_k||\bar{V}_h| (\cos\theta_{kh} + j \sin\theta_{kh}) + jb_{kh} |\bar{V}_k||\bar{V}_h| (\cos\theta_{kh} + j \sin\theta_{kh}) -$$
$$- g_{ki} |\bar{V}_k||\bar{V}_i| (\cos\theta_{ki} + j \sin\theta_{ki}) + jb_{ki} |\bar{V}_k||\bar{V}_i| (\cos\theta_{ki} + j \sin\theta_{ki})$$

$$P_k + jQ_k =$$
$$= (g_{kh} + g_{ki} + 2g_{k0}) |\bar{V}_k|^2 - j(b_{kh} + b_{ki} + 2b_{k0}) |\bar{V}_k|^2 - g_{kh} |\bar{V}_k||\bar{V}_h| \cos\theta_{kh} -$$
$$- jg_{kh} |\bar{V}_k||\bar{V}_h| \sin\theta_{kh} + jb_{kh} |\bar{V}_k||\bar{V}_h| \cos\theta_{kh} - b_{kh} |\bar{V}_k||\bar{V}_h| \sin\theta_{kh} -$$
$$- g_{ki} |\bar{V}_k||\bar{V}_i| \cos\theta_{ki} - jg_{ki} |\bar{V}_k||\bar{V}_i| \sin\theta_{ki} + jb_{ki} |\bar{V}_k||\bar{V}_i| \cos\theta_{ki} - b_{ki} |\bar{V}_k||\bar{V}_i| \sin\theta_{ki}$$

$$P_k + jQ_k =$$
$$= (g_{kh} + g_{ki} + 2g_{k0})|\bar{V}_k|^2 - g_{kh}|\bar{V}_k||\bar{V}_h|\cos\theta_{kh} - b_{kh}|\bar{V}_k||\bar{V}_h|\sin\theta_{kh} -$$
$$- g_{ki}|\bar{V}_k||\bar{V}_i|\cos\theta_{ki} - b_{ki}|\bar{V}_k||\bar{V}_i|\sin\theta_{ki} \quad + \mathrm{j}[-(b_{kh} + b_{ki} + 2b_{k0})|\bar{V}_k|^2 -$$
$$- g_{kh}|\bar{V}_k||\bar{V}_h|\sin\theta_{kh} + b_{kh}|\bar{V}_k||\bar{V}_h|\cos\theta_{kh} - g_{ki}|\bar{V}_k||\bar{V}_i|\sin\theta_{ki} +$$
$$+ b_{ki}|\bar{V}_k||\bar{V}_i|\cos\theta_{ki}]$$

Splitting above equation into real and imaginary parts gives the active and reactive node power injection at node k in polar form.

$$P_k =$$
$$= (g_{kh} + g_{ki} + 2g_{k0})|\bar{V}_k|^2 - g_{kh}|\bar{V}_k||\bar{V}_h|\cos\theta_{kh} - b_{kh}|\bar{V}_k||\bar{V}_h|\sin\theta_{kh} -$$
$$- g_{ki}|\bar{V}_k||\bar{V}_i|\cos\theta_{ki} - b_{ki}|\bar{V}_k||\bar{V}_i|\sin\theta_{ki}$$

$$Q_k =$$
$$= -(b_{kh} + b_{ki} + 2b_{k0})|\bar{V}_k|^2 - g_{kh}|\bar{V}_k||\bar{V}_h|\sin\theta_{kh} + b_{kh}|\bar{V}_k||\bar{V}_h|\cos\theta_{kh} -$$
$$- g_{ki}|\bar{V}_k||\bar{V}_i|\sin\theta_{ki} + b_{ki}|\bar{V}_k||\bar{V}_i|\cos\theta_{ki}$$

Above equations are the total power fluxes equations for the sample network (top figure). To conclude it for a general network, we simplify and then use a summation notation to include all nodes. Therefore firstly for active node power it can be written that:

$$P_k =$$
$$= (g_{kh} + g_{ki} + 2g_{k0})|\bar{V}_k|^2 - (g_{kh}\cos\theta_{kh} + b_{kh}\sin\theta_{kh})|\bar{V}_k||\bar{V}_h| - (g_{ki}\cos\theta_{ki} +$$
$$+ b_{ki}\sin\theta_{ki})|\bar{V}_k||\bar{V}_i|$$

$$P_k = G_{kk}|\bar{V}_k|^2 - \sum_{\substack{j=1 \\ j\neq k}}^{n} |\bar{V}_k|\big|\bar{V}_j\big|\big(g_{kj}\cos\theta_{kj} + b_{kj}\sin\theta_{kj}\big)$$

Where the index j is the node number from 1 to n. For reactive node power it can be written in a similar way that:

$$Q_k = -B_{kk}|\bar{V}_k|^2 - \sum_{\substack{j=1 \\ j\neq k}}^{n} |\bar{V}_k|\big|\bar{V}_j\big|\big(g_{kj}\sin\theta_{kj} - b_{kj}\cos\theta_{kj}\big)$$

Matlab Codes: Implementation of Newton-Raphson Load Flow

```
function [V,phi] = newton(Ybus_nr)

%% Newton-Raphson Load Flow
global nbus baseMVA busdatas

%% Getting busdata
type = busdatas(:,2);       % Type of Bus 1-Slack, 2-PV, 3-PQ
V = busdatas(:,3);          % Slach Voltage and Voltage mag intitials
Vsp = busdatas(:,3);          % Slach Voltage and Voltage mag intitials

phi = busdatas(:,4);        % Voltage Angle intitials
Pg = busdatas(:,5)/baseMVA;

Qg = busdatas(:,6)/baseMVA;

Pl = busdatas(:,7)/baseMVA;

Ql = busdatas(:,8)/baseMVA;

Qmin = busdatas(:,9)/baseMVA;       % Minimum Reactive Power Limit..
Qmax = busdatas(:,10)/baseMVA;      % Maximum Reactive Power Limit..

Psp = Pg - Pl;    % calculate powers in the busses: P Specified
Qsp = Qg - Ql;    % calculate powers in the busses: Q Specified

pq = find(type == 3);                % PQ Buses(there is no generation)
pv = find(type == 2 | type == 1);    % PV Buses
npq = length(pq);                    % No. of PQ buses
G_nr = real(Ybus_nr);

B_nr = imag(Ybus_nr);

Tol = 1;

itr = 1;

%% Iteration Starts:
while (Tol > 1e-9 && itr < 100)

P = zeros(nbus,1);

Q = zeros(nbus,1);

% Calculate P and Q
for i = 1:nbus
      for k = 1:nbus
            P(i) = P(i) + V(i)* V(k)*(G_nr(i,k)*cos(phi(i)-phi(k)) +
B_nr(i,k)*sin(phi(i)-phi(k)));  % pp. 77 Wang.  (eq 2.9)
            Q(i) = Q(i) + V(i)* V(k)*(G_nr(i,k)*sin(phi(i)-phi(k)) -
B_nr(i,k)*cos(phi(i)-phi(k)));  % ...
      end
end
```

```
% Checking Q-limit violations..
if itr <= 7 && itr > 2    % Only checked up to 7th iterations..
    for n = 2:nbus
        if type(n) == 2
            QG = Q(n)+Ql(n);

            if QG < Qmin(n)
                V(n) = V(n) + 0.01;

            elseif QG > Qmax(n)
                V(n) = V(n) - 0.01;

            end
        end
    end
end

dP = Psp-P;  % Calculate change from specified value pp.78 Wang. (eq
2.13)
dQ1 = Qsp-Q; % ...
    k = 1;
    dQ = zeros(npq,1);
    for i = 1:nbus
        if type(i) == 3
            dQ(k,1) = dQ1(i);
            k = k+1;
        end
    end

r = [dP(2:nbus); dQ];       % Mismatch Vector, not considering the
first value that is the slack bus P,Q

%% The Jacobian matrix
% J1 - Derivative of Real Power Injections with Angles
J1 = zeros(nbus-1,nbus-1);

for i = 1:(nbus-1)
      m = i+1;
      for k = 1:(nbus-1)
            n = k+1;
            if n == m
                  for n = 1:nbus
                        J1(i,k) = J1(i,k) - V(m)*
V(n)*(G_nr(m,n)*sin(phi(m)-phi(n)) - B_nr(m,n)*cos(phi(m)-phi(n))); %
pp. 84 Wang. eq(2.41)
                  end
                  J1(i,k) = J1(i,k) - V(m)^2*B_nr(m,m);

            else
                  J1(i,k) = V(m)* V(n)*(G_nr(m,n)*sin(phi(m)-phi(n)) -
B_nr(m,n)*cos(phi(m)-phi(n))); % pp. 84 Wang. eq(2.42)
            end
      end
end
% J2 - Derivative of Real Power Injections with V
J2 = zeros(nbus-1,npq);
```

```
for i = 1:(nbus-1)
      m = i+1;
      for k = 1:npq
            n = pq(k);
            if n == m
                  for n = 1:nbus
                        J2(i,k) = J2(i,k) + V(n)*(G_nr(m,n)*cos(phi(m)-
phi(n)) + B_nr(m,n)*sin(phi(m)-phi(n)));
                  end
                  J2(i,k) = J2(i,k) + V(m)*G_nr(m,m);

            else
                  J2(i,k) = V(m)*(G_nr(m,n)*cos(phi(m)-phi(n)) +
B_nr(m,n)*sin(phi(m)-phi(n)));
            end
      end
end
% J3 - Derivative of Reactive Power Injections with Angles
J3 = zeros(npq,nbus-1);

for i = 1:npq
      m = pq(i);
      for k = 1:(nbus-1)
            n = k+1;
            if n == m
                  for n = 1:nbus
                        J3(i,k) = J3(i,k) + V(m)*
V(n)*(G_nr(m,n)*cos(phi(m)-phi(n)) + B_nr(m,n)*sin(phi(m)-phi(n)));
                  end
                  J3(i,k) = J3(i,k) - V(m)^2*G_nr(m,m);

            else
                  J3(i,k) = V(m)* V(n)*(-G_nr(m,n)*cos(phi(m)-phi(n)) -
B_nr(m,n)*sin(phi(m)-phi(n)));  % pp. 84 Wang. eq(2.44) !!!!! MANFI
            end
      end
end
% J4 - Derivative of Reactive Power Injections with V
J4 = zeros(npq,npq);

for i = 1:npq
      m = pq(i);
      for k = 1:npq
            n = pq(k);
            if n == m
                  for n = 1:nbus
                        J4(i,k) = J4(i,k) + V(n)*(G_nr(m,n)*sin(phi(m)-
phi(n)) - B_nr(m,n)*cos(phi(m)-phi(n)));
                  end
                  J4(i,k) = J4(i,k) - V(m)*B_nr(m,m);

            else
                  J4(i,k) = V(m)*(G_nr(m,n)*sin(phi(m)-phi(n)) -
B_nr(m,n)*cos(phi(m)-phi(n)));  % pp. 85 Wang. eq(2.48) !!!!! MANFI
            end
      end
end
```

```
J = [J1 J2;

     J3 J4];     % Jacobian Matrix    % J = Jacob(busdatas,ybus,nbus);

X = J\r;  % inv(J)*r; <TIME SAVING> %          Correction Vector
dTh = X(1:nbus-1);      % Change in Voltage Angle
dV = X(nbus:end);       % Change in Voltage Magnitude

%% record the phita V and phita Angle
dV_sq(itr,:) = dV';
dTh_sq(itr,:) = dTh';

%% Updating State Vectors
phi(2:nbus) = dTh + phi(2:nbus);    % Angle update

k = 1;
for i = 1:nbus
      if type(i) == 3
            V(i) = dV(k) + V(i);        % Voltage Magnitude update
            k = k+1;
      else
            V(i) = Vsp(i);    % reset the slack and PV bus voltages to
the specified values
      end
end

itr = itr + 1;   % iteration counter
Tol = max(abs(r));

end  % end of Iterations
% fprintf('N-R Iterations = %4d', itr);fprintf('\n');

%% Figure of convergence
% figure
% plot([1:itr-1],diag(dV_sq*dV_sq'),[1:itr-
1],diag(dTh_sq*dTh_sq'),'g');
% title('Load Flow: phita-V and phita-Phi decrease according to
Iterations'); xlabel('iteration'); ylabel('phita V & Angle'); grid on %
figure for convergence
end
```

Matlab Codes: Implementation of WLS State Estimation

```
max_iters = 50;       % number of iterations
tol       = 1e-6;    % normally e-6

%% State Vector initialization:
V_SE = ones(nbus,1);            % Initialize the bus voltages: all ones
V_SE(v_meas_bus_nr,1) = v_meas_perturbed;      % put the slack bus
voltage and PV bus voltages
phi_SE = zeros(nbus,1);         % Initialize the bus angles: all zeroz
% if pmu_meas_bus_nr
%       phi_SE(pmu_meas_bus_nr(:,2),1) = - phi_meas_perturbed; % put
the phases az inits
% end

state = [phi_SE(2:end); V_SE];     % State Vector size: 27 = (2*n)-1
iters = 0;
converged = 0;

while (~converged && iters < max_iters)
iters = iters + 1;
%% Measurement Function: f
f1 = V_SE(v_meas_bus_nr,1);  %  Voltage Magnitude (Traditional + PMU)
f2 = zeros(n_pi_meas,1);
f3 = zeros(n_qi_meas,1);
f4 = zeros(n_pf_meas,1);
f5 = zeros(n_qf_meas,1);
if pmu_meas_bus_nr
f6 = phi_SE(pmu_meas_bus_nr(:,1),1) - phi_SE(pmu_meas_bus_nr(:,2),1); %
PMU Phases
else f6 = [];
end

% V_SE = V_nr;
% phi_SE = phi_nr;

%Real power injection calculation OK
for i = 1:n_pi_meas
      m = pi_meas_bus_nr(i);
      for k = 1:nbus
            f2(i) = f2(i) + V_SE(m)*V_SE(k)*(G(m,k)*cos(phi_SE(m)-
phi_SE(k)) + B(m,k)*sin(phi_SE(m)-phi_SE(k)));
      end
end

% Reactive power injection calculations OK
for i = 1:n_qi_meas
      m = qi_meas_bus_nr(i);
      for k = 1:nbus
            f3(i) = f3(i) + V_SE(m)*V_SE(k)*(G(m,k)*sin(phi_SE(m)-
phi_SE(k)) - B(m,k)*cos(phi_SE(m)-phi_SE(k)));
      end
end
```

```
% Real power flows calculation OK
for i = 1:n_pf_meas
      m = pf_meas_bus_nr(i,1);
      n = pf_meas_bus_nr(i,2);
      f4(i) = -V_SE(m)^2*(G(m,n)) +
V_SE(m)*V_SE(n)*(G(m,n)*cos(phi_SE(m)-phi_SE(n)) +
B(m,n)*sin(phi_SE(m)-phi_SE(n)));
end

% Reactive power flows calculation OK
for i = 1:n_qf_meas
      m = qf_meas_bus_nr(i,1);
      n = qf_meas_bus_nr(i,2);
      f5(i) = V_SE(m)^2*(B(m,n)- bbus(m,n)) +
V_SE(m)*V_SE(n)*(G(m,n)*sin(phi_SE(m)-phi_SE(n)) -
B(m,n)*cos(phi_SE(m)-phi_SE(n)));
end

f = [f1; f2; f3; f4; f5; f6];

%% Jacobians
% g11 - Derivative of V_SE with respect to angles: All Zeros

g11 = zeros(n_v_meas,nbus-1);

% g12 - Derivative of V_SE with respect to V_SE
g12 = zeros(n_v_meas,nbus);
for k = 1:n_v_meas
      for n = 1:nbus
            if n == k
                  g12(k,n) = 1;
            end
      end
end

% g21 - Derivative of Real Power Injections with Angles
g21 = zeros(n_pi_meas,nbus-1);
for i = 1:n_pi_meas
      m = pi_meas_bus_nr(i);
      for k = 1:(nbus-1)
            if k+1 == m
                  for n = 1:nbus
                        g21(i,k) = g21(i,k) + V_SE(m)* V_SE(n)*(-
G(m,n)*sin(phi_SE(m)-phi_SE(n)) + B(m,n)*cos(phi_SE(m)-phi_SE(n)));
                  end
                  g21(i,k) = g21(i,k) - V_SE(m)^2*B(m,m);
            else
                  g21(i,k) = V_SE(m)*
V_SE(k+1)*(G(m,k+1)*sin(phi_SE(m)-phi_SE(k+1)) -
B(m,k+1)*cos(phi_SE(m)-phi_SE(k+1))); % k+1
            end
      end
end

% g22 - Derivative of Real Power Injections with V_SE
g22 = zeros(n_pi_meas,nbus);
```

```
for i = 1:n_pi_meas
      m = pi_meas_bus_nr(i);
      for k = 1:(nbus)
            if k == m
                  for n = 1:nbus
                        g22(i,k) = g22(i,k) +
V_SE(n)*(G(m,n)*cos(phi_SE(m)-phi_SE(n)) + B(m,n)*sin(phi_SE(m)-
phi_SE(n)));
                  end
                  g22(i,k) = g22(i,k) + V_SE(m)*G(m,m);
            else
                  g22(i,k) = V_SE(m)*(G(m,k)*cos(phi_SE(m)-phi_SE(k)) +
B(m,k)*sin(phi_SE(m)-phi_SE(k)));
            end
      end
end

% g31 - Derivative of Reactive Power Injections with Angles
g31 = zeros(n_qi_meas,nbus-1);
for i = 1:n_qi_meas
      m = qi_meas_bus_nr(i);
      for k = 1:(nbus-1)
            if k+1 == m
                  for n = 1:nbus
                        g31(i,k) = g31(i,k) + V_SE(m)*
V_SE(n)*(G(m,n)*cos(phi_SE(m)-phi_SE(n)) + B(m,n)*sin(phi_SE(m)-
phi_SE(n)));
                  end
                  g31(i,k) = g31(i,k) - V_SE(m)^2*G(m,m);
            else
                  g31(i,k) = V_SE(m)* V_SE(k+1)*(-
G(m,k+1)*cos(phi_SE(m)-phi_SE(k+1)) - B(m,k+1)*sin(phi_SE(m)-
phi_SE(k+1))); % k+1
            end
      end
end

% g32 - Derivative of Reactive Power Injections with V_SE
g32 = zeros(n_qi_meas,nbus);
for i = 1:n_qi_meas
      m = qi_meas_bus_nr(i);
      for k = 1:(nbus)
            if k == m
                  for n = 1:nbus
                        g32(i,k) = g32(i,k) +
V_SE(n)*(G(m,n)*sin(phi_SE(m)-phi_SE(n)) - B(m,n)*cos(phi_SE(m)-
phi_SE(n)));
                  end
                  g32(i,k) = g32(i,k) - V_SE(m)*B(m,m);
            else
                  g32(i,k) = V_SE(m)*(G(m,k)*sin(phi_SE(m)-phi_SE(k)) -
B(m,k)*cos(phi_SE(m)-phi_SE(k)));
            end
      end
end

% g41 - Derivative of Real Power Flows with Angles
```

```
g41 = zeros(n_pf_meas,nbus-1);
for i = 1:n_pf_meas
      m = pf_meas_bus_nr(i,1);
      n = pf_meas_bus_nr(i,2);
      for k = 1:(nbus-1)
            if k+1 == m
                  g41(i,k) = -V_SE(m)* V_SE(n)*(G(m,n)*sin(phi_SE(m)-
phi_SE(n)) - B(m,n)*cos(phi_SE(m)-phi_SE(n)));
            else if k+1 == n
                        g41(i,k) = V_SE(m)*
V_SE(n)*(G(m,n)*sin(phi_SE(m)-phi_SE(n)) - B(m,n)*cos(phi_SE(m)-
phi_SE(n)));
                  else
                        g41(i,k) = 0;
                  end
            end
      end
end

% g42 - Derivative of Real Power Flows with V_SE
g42 = zeros(n_pf_meas,nbus);
for i = 1:n_pf_meas
      m = pf_meas_bus_nr(i,1);
      n = pf_meas_bus_nr(i,2);
      for k = 1:nbus
            if k == m
                  g42(i,k) = V_SE(n)*(G(m,n)*cos(phi_SE(m)-phi_SE(n)) +
B(m,n)*sin(phi_SE(m)-phi_SE(n))) - 2*G(m,n)*V_SE(m);
            else if k == n
                        g42(i,k) = V_SE(m)*(G(m,n)*cos(phi_SE(m)-
phi_SE(n)) + B(m,n)*sin(phi_SE(m)-phi_SE(n)));
                  else
                        g42(i,k) = 0;
                  end
            end
      end
end

% g51 - Derivative of Reactive Power Flows with Angles
g51 = zeros(n_qf_meas,nbus-1);
for i = 1:n_qf_meas
      m = qf_meas_bus_nr(i,1);
      n = qf_meas_bus_nr(i,2);
      for k = 1:(nbus-1)
            if k+1 == m
                  g51(i,k) = V_SE(m)* V_SE(n)*(G(m,n)*cos(phi_SE(m)-
phi_SE(n)) + B(m,n)*sin(phi_SE(m)-phi_SE(n)));
            else if k+1 == n
                        g51(i,k) = - V_SE(m)*
V_SE(n)*(G(m,n)*cos(phi_SE(m)-phi_SE(n)) + B(m,n)*sin(phi_SE(m)-
phi_SE(n)));
                  else
                        g51(i,k) = 0;
                  end
            end
      end
end
```

```
% g52 - Derivative of Reactive Power Flows with V_SE
g52 = zeros(n_qf_meas,nbus);
for i = 1:n_qf_meas
      m = qf_meas_bus_nr(i,1);
      n = qf_meas_bus_nr(i,2);
      for k = 1:nbus
            if k == m
                  g52(i,k) = V_SE(n)*(G(m,n)*sin(phi_SE(m)-phi_SE(n)) -
B(m,n)*cos(phi_SE(m)-phi_SE(n)))...
                        + 2*V_SE(m)*(B(m,n) - bbus(m,n));
            else if k == n
                        g52(i,k) = V_SE(m)*(G(m,n)*sin(phi_SE(m)-
phi_SE(n)) - B(m,n)*cos(phi_SE(m)-phi_SE(n)));
                  else
                        g52(i,k) = 0;
                  end
            end
      end
end

% g61 - Derivative of PMU Phases with respect to angles
g61 = zeros(n_phi_meas,nbus-1);
for i = 1:n_phi_meas
      m = pmu_meas_bus_nr(i,1); % from
      n = pmu_meas_bus_nr(i,2); % to
      for k = 1:(nbus-1)
            if k+1 == m
                  g61(i,k) = 1;
            end
            if k+1 == n
                  g61(i,k) = -1;
            end
      end
end

% g62 - Derivative of PMU Phases with respect to V_SE
g62 = zeros(n_phi_meas,nbus);

%% Measurement Jacobian,     g = df / dx
g = [g11 g12;
     g21 g22;
     g31 g32;
     g41 g42;
     g51 g52;
     g61 g62];
% test if g is full rank
[mmm, nnn]  = size(g);
rk      = rank(g);
if rk < min(mmm, nnn)
     error('System is not observable');
end

%% Hessian Matrix or Gain Matrix(double derivative), H
H = g' * (sigma_square\g); % g'*inv(sigma_square)*g;  % <FOR TIME
SAVING CALCULATION>
```

```
%% Objective Function, J
% J = sum(sigma_square\res.^2);    % sum(inv(sigma_square)*res.^2);  %
<FOR TIME SAVING CALCULATION>

%% Residue
res = y_perturbed - f;
%% State Vector:
delta_x = H\(g'*(sigma_square\res)); %
inv(H)*(g'*inv(sigma_square)*res) % <FOR TIME SAVING CALCULATION>
state = state + delta_x;
phi_SE(2:end) = state(1:nbus-1);
V_SE = state(nbus:end);


%% check for convergence
normF = max(abs(delta_x));      %normF =
norm((g'*inv(sigma_square)*res), inf);
if normF < tol
        converged = 1;
end
% fprintf('WLS iteration # %4d: norm of mismatch: %5.20f\n', iters,
normF);

end %%%%%%%%%%%%%%%%%%% end of iterations

%% THEORY: Variance Covariance matrix of estimates sigma_x
sigma_x = diag(inv(g'*(sigma_square\g)));
sigma_x_v   = sqrt(sigma_x(nbus:end));
sigma_x_phi = [0; sqrt(sigma_x(1:nbus-1))*180/pi];
```

Matlab Codes: Building the bus admittance matrix

```
%% Formulation of Ybus by singular transformation method (With
Transformer Tap settings and Shunt Admittances)

function [Ybus A] = ybus_incidence(r,x,b)

global fb tb nbranch nbus linedatas baseMVA busdatas
tap = linedatas(:,6);     % Tap setting values (one for the other buses)
GS = busdatas(:,11);      % shunt conductance (MW at V = 1.0 p.u.)
BS = busdatas(:,12);      % shunt susceptance (MW at V = 1.0 p.u.)
Ysh = ( GS + 1j * BS) / baseMVA; % vector of shunt admittances
Z= r + 1i*x;                    % z matrix...
Y = 1./Z;

%% Formation of Bus Incidence matrix A              (signs: comes in is
-1, goes out is +1)
A=zeros(nbranch+nbus,nbus);
for i=1:nbus                    % building top I submatrix:
      for j=1:nbus
            if(i==j)
                  A(i,i)=1;
            end
      end
end
for i = nbus+1 : nbus+nbranch     % building Buttom A_branch submatrix:
      A( i , fb(i-nbus)) = 1;
      A( i , tb(i-nbus)) = -1;
end

%% Calculation of primitive matrix
Yprimitive = zeros(nbranch+nbus,1);
% For buses:
for i=1:nbranch
    Yprimitive(fb(i))   = Yprimitive(fb(i)) + 1i*b(i)/2 + (1-tap(i)) *
Y(i) / tap(i)^2;
    Yprimitive(tb(i))   = Yprimitive(tb(i)) + 1i*b(i)/2 + (tap(i)-1) *
Y(i) / tap(i);
end
Yprimitive(1:nbus) = Yprimitive(1:nbus) + Ysh;  % adding shunt
admittances

% Branches:
for i=1:nbranch
    Yprimitive(i+nbus) = Y(i) / tap(i);
end

%% Bus Admittance matrix:
Ybus = A' * diag(Yprimitive) * A;        %% shunt admittance
```

Matlab Codes: Calculation of Power injections and power flows measurements

```
%% Calculation of Power Injections (p.u)
% V - Voltage Magnitude pu
% phi - Voltage Angle in radians

function [Pi, Qi] = power_inj(V,phi,Ybus)
% function Si = power_inj(V,phi,Ybus)

global nbus

G = real(Ybus); % Bus Admittance matrix split:

B = imag(Ybus);



%% power injection calculations From WLS
Pi = zeros(nbus,1);

Qi = zeros(nbus,1);


for i = 1:nbus
      for j = 1:nbus
            Pi(i) = Pi(i) + V(i)*V(j)*(G(i,j)*cos(phi(i)-phi(j)) +
B(i,j)*sin(phi(i)-phi(j)));
            Qi(i) = Qi(i) + V(i)*V(j)*(G(i,j)*sin(phi(i)-phi(j)) -
B(i,j)*cos(phi(i)-phi(j)));
      end
end
```

```
%% Calculation of Line Power flows (p.u)
% V - Voltage Magnitude pu
% phi - Voltage Angle in radians

function [Pij, Qij, Pji, Qji] = power_flow(V,phi,Ybus)

global fb tb nbus nbranch b_perturbed

G = real(Ybus);

B = imag(Ybus);



%% Polar coordination:

% Shunt Admittance Matrix Formation:    % Off-diagonals are the mutual
admittances between the respective nodes
bbus_perturbed = zeros(nbus,nbus);
for k=1:nbranch
      bbus_perturbed(fb(k),tb(k)) = b_perturbed(k) ./ 2;
      bbus_perturbed(tb(k),fb(k)) = bbus_perturbed(fb(k),tb(k));
end

%  power flows calculation
for i = 1:nbranch
      m = fb(i);
      n = tb(i);
      Pij(i) = -V(m)^2*(G(m,n)) + V(m)*V(n)*(G(m,n)*cos(phi(m)-phi(n))
+ B(m,n)*sin(phi(m)-phi(n)));
      Qij(i) = V(m)^2*(B(m,n)- bbus_perturbed(m,n)) +
V(m)*V(n)*(G(m,n)*sin(phi(m)-phi(n)) - B(m,n)*cos(phi(m)-phi(n)));
      Pji(i) = -V(n)^2*(G(n,m)) + V(n)*V(m)*(G(n,m)*cos(phi(n)-phi(m))
+ B(n,m)*sin(phi(n)-phi(m)));
      Qji(i) = V(n)^2*(B(n,m)- bbus_perturbed(n,m)) +
V(n)*V(m)*(G(n,m)*sin(phi(n)-phi(m)) - B(n,m)*cos(phi(n)-phi(m)));
end
```

Matlab Codes: Measurement data calculation

```
%% Determining the Number of measurements:
n_v_meas      = length(v_meas_bus_nr);    % Number of Voltage
measurements
n_pi_meas     = length(pi_meas_bus_nr);   % Number of Real Power
Injection measurements
n_qi_meas     = length(qi_meas_bus_nr);   % Number of Reactive Power
Injection measurements
n_pf_meas     = length(pf_meas_bus_nr);   % Number of Real Power Flow
measurements
n_qf_meas     = length(qf_meas_bus_nr);   % Number of Reactive Power
Flow measurements
n_phi_meas    = length(pmu_meas_bus_nr); % Number of Voltage
measurements

%% Variance Covariance Matrix(weighting Matrix) construction:
sigma_vector = [
    sigma_v  * ones(n_v_meas,1)
    sigma_pi * ones(n_pi_meas, 1)
    sigma_qi * ones(n_qi_meas, 1)
    sigma_pf * ones(n_pf_meas, 1)
    sigma_qf * ones(n_qf_meas, 1)
    sigma_phi* ones(n_phi_meas,1)
    ];
sigma_square = diag(sigma_vector).^2; % Measurement Variance Covariance
matrix

%% Voltage Measurements:
v_meas = V_nr(v_meas_bus_nr); % set the NR voltages to the measured
voltage data.

%% PMU Measurements:
if pmu_meas_bus_nr
      phi_meas = phi_nr(pmu_meas_bus_nr(:,1),1) -
phi_nr(pmu_meas_bus_nr(:,2),1); % set the NR phases to the measured pmu
data.
else
      phi_meas = [];
end
%% Power Injection Measurements:
[Pi_nr Qi_nr] = power_inj(V_nr , phi_nr, Ybus_perturbed); % Bus Power
injections calculations
pi_meas = Pi_nr(pi_meas_bus_nr);  % set the NR active Power Injections
to the measured data.
qi_meas = Qi_nr(qi_meas_bus_nr);  % set the NR reactive Power
Injections to the measured data.

%% Power Flow Measuremets:
[Pij, Qij, Pji, Qji] = power_flow(V_nr , phi_nr, Ybus_perturbed); % Bus
Power flows calculations
% Active power flow:
pf_meas = [];
for i = 1:length(pf_meas_bus_nr)
        m = pf_meas_bus_nr(i,1);
```

```
        n = pf_meas_bus_nr(i,2);
        for p = 1:nbranch
                if m == fb(p) && n == tb(p)
                        pf_meas(i,1) = Pij(p);
                elseif m == tb(p) && n == fb(p)
                        pf_meas(i,1) = Pji(p);
                end
        end
end
% ReActive power flow:
qf_meas = [];
for i = 1:length(qf_meas_bus_nr)
        m = qf_meas_bus_nr(i,1);
        n = qf_meas_bus_nr(i,2);
        for p = 1:nbranch
                if m == fb(p) && n == tb(p)
                        qf_meas(i,1) = Qij(p);
                elseif m == tb(p) && n == fb(p)
                        qf_meas(i,1) = Qji(p);
                end
        end
end

%% Measurement Perturbation:
v_meas_perturbed   = normrnd(v_meas  , sigma_v  * v_meas);
pi_meas_perturbed  = normrnd(pi_meas , sigma_pi * abs(pi_meas));
qi_meas_perturbed  = normrnd(qi_meas , sigma_qi * abs(qi_meas));
pf_meas_perturbed  = normrnd(pf_meas , sigma_pf * abs(pf_meas));
qf_meas_perturbed  = normrnd(qf_meas , sigma_qf * abs(qf_meas));
phi_meas_perturbed = normrnd(phi_meas, sigma_phi* abs(phi_meas));

%% Perturbed Measurement Vector composition:
y_perturbed = [v_meas_perturbed
               pi_meas_perturbed
               qi_meas_perturbed
               pf_meas_perturbed
               qf_meas_perturbed
               phi_meas_perturbed];
```

Matlab Codes: Line Data File Structure (linedata.m)

```
function linedatas = linedata()
global test_case
switch test_case
%%
case 4
%          |  From |  To   |   R      |   X      |   B      |  X'mer    |
%          |  Bus  | Bus   |  pu      |  pu      |   pu     | TAP (a)   |
linedatas = [1       2       0.02       0.06       0.20         1
             1       3       0.02       0.06       0.25         1
             2       3       0.05       0.10       0.0          1
             2       4       0.0        0.08       0.0        0.98
             ];
%%
case 6
%          |  From |  To   |   R      |   X      |   B      |  X'mer    |
%          |  Bus  | Bus   |  pu      |  pu      |   pu     | TAP (a)   |
linedatas = [1       2       0.1        0.2        0.04         1
             1       4       0.05       0.2        0.04         1
             1       5       0.08       0.3        0.06         1
             2       3       0.05       0.25       0.06         1
             2       4       0.05       0.1        0.02         1
             2       5       0.1        0.3        0.04         1
             2       6       0.07       0.2        0.05         1
             3       5       0.12       0.26       0.05         1
             3       6       0.02       0.1        0.02         1
             4       5       0.2        0.4        0.08         1
             5       6       0.1        0.3        0.06         1
             ];
%%
case 14
%          |  From |  To   |   R      |   X      |   B      |  X'mer    |
%          |  Bus  | Bus   |  pu      |  pu      |   pu     | TAP (a)   |
linedatas = [1       2       0.01938    0.05917    0.0528       1
             1       5       0.05403    0.22304    0.0492       1
             2       3       0.04699    0.19797    0.0438       1
             2       4       0.05811    0.17632    0.0374       1
             2       5       0.05695    0.17388    0.0340       1
             3       4       0.06701    0.17103    0.0346       1
             4       5       0.01335    0.04211    0.0128       1
             4       7       0.0        0.20912    0.0        0.978
             4       9       0.0        0.55618    0.0        0.969
             5       6       0.0        0.25202    0.0        0.932
             6      11       0.09498    0.19890    0.0          1
             6      12       0.12291    0.25581    0.0          1
             6      13       0.06615    0.13027    0.0          1
             7       8       0.0        0.17615    0.0          1
             7       9       0.0        0.11001    0.0          1
             9      10       0.03181    0.08450    0.0          1
             9      14       0.12711    0.27038    0.0          1
            10      11       0.08205    0.19207    0.0          1
            12      13       0.22092    0.19988    0.0          1
            13      14       0.17093    0.34802    0.0          1 ];
And so on for other cases...
```

Matlab Codes: Bus Data File Structure (busdata.m)

```
% Returns Bus data
function busdatas = busdata()
global test_case baseMVA V_true Phi_true
switch test_case

% Bus Types:
% 1: Slack Bus: V and thera are known (P and Q must be solved)
% 2: PV Bus: P and V_mag are known <generator busses are PV>(Q and theta must solved)
% 3: PQ Bus: P and Q are known(V and theta must solved)

%% Example of 2.1 in Abur Book:
case 4
%          |Bus  | Type  | Vsp*|theta  | PGi  | QGi  | PLi  | QLi  |  Qmin  |
Qmax     | Gs    |  Bs  |
busdatas =[1     1    1.0      0   1.9963 .44939 0      0       0       0       0       0;
           2     3    1.0      0      0     0   .49944 .30229   0       0       0       0;
           3     3    1.0      0      0     0   1.2006 .79897   0       0       0       0.5;
           4     3    1.0      0      0     0   .25057 .09907   0       0       0       0;
            ];
baseMVA = 1;  % Base MVA
V_true = [1 0.9629 0.9597 0.9742]';
Phi_true = [0 -2.76 -3.58 -3.96]';

%%   6 bus example from pp. 104, 112, 119, 123-124, 549 of "Power Generation, Operation,
and Control, 2nd Edition",
%   by Allen. J. Wood and Bruce F. Wollenberg, John Wiley & Sons, NY, Jan 1996.
case 6
%          |Bus  | Type  | Vsp*|theta  | PGi  | QGi  | PLi  | QLi  |  Qmin  |
Qmax     | Gs    |  Bs  |
busdatas =[1     1      1.05   0    107.9  16     0      0      0       0       0      0;
           2     2      1.05   0     50    74.4   0      0      0       0       0      0;
           3     2      1.07   0     60    89.6   0      0      0       0       0      0;
           4     3      1.0    0      0     0     70     70     0       0       0      0;
           5     3      1.0    0      0     0     70     70     0       0       0      0;
           6     3      1.0    0      0     0     70     70     0       0       0      0;
            ];
baseMVA = 100;  % Base MVA
V_true = [241.5 241.5 246.1 227.6 226.7 231]'./230;   % baseKV is 230 and baseMVA is 100
Phi_true = [0 -3.7 -4.3 -4.2 -5.3 -5.9]';

%% IEEE 14 bus system
case 14
busdatas  =[1     1    1.060   0    232.4 -16.9    0     0       0       0       0       0;
            2     2    1.045   0      40   42.4   21.7   12.7    -40     50      0       0;
            3     2    1.010   0       0   23.4   94.2   19.0     0      40      0       0;
            4     3    1.0     0       0     0    47.8   -3.9     0       0      0       0;
            5     3    1.0     0       0     0     7.6    1.6     0       0      0       0;
            6     2    1.070   0       0   12.2   11.2    7.5    -6      24      0       0;
            7     3    1.0     0       0     0     0.0    0.0     0       0      0       0;
            8     2    1.090   0       0   17.4    0.0    0.0    -6      24      0       0;
            9     3    1.0     0       0     0    29.5   16.6     0       0      0       19;
            10    3    1.0     0       0     0     9.0    5.8     0       0      0       0;
            11    3    1.0     0       0     0     3.5    1.8     0       0      0       0;
            12    3    1.0     0       0     0     6.1    1.6     0       0      0       0;
            13    3    1.0     0       0     0    13.5    5.8     0       0      0       0;
            14    3    1.0     0       0     0    14.9    5.0     0       0      0       0];
baseMVA = 100;  % Base MVA
V_true = [1.060    1.045    1.010    1.019    1.020    1.070    1.062
1.090    1.056    1.051    1.057    1.055    1.050    1.036]';
Phi_true = [0   -4.98  -12.72  -10.33   -8.78  -14.22  -13.37  -13.36
-14.94  -15.10  -14.79  -15.07  -15.16  -16.04]';
And so on for other cases...
```

Matlab Codes: Measurement Data File Structure (measurement14.m)

```
%% Measurement Data Preparation:
%states = 27
%measurements = 1.5 * states = 41

%% The bus numbers that traditional voltage mag. measurement happens:
v_meas_bus_nr  = [1 2 3 6 8]';
%% The bus numbers that PMU measurement happens:
pmu_meas_bus_nr  = [
1 6
1 9
];

v_meas_bus_nr = unique([pmu_meas_bus_nr(:);v_meas_bus_nr]);
%% The bus numbers that active power injection measurement happens:
pi_meas_bus_nr = [1 2 6 8 9 10 11 12 14]';

%% The bus numbers that active and reactive power injection measurement
happens:
qi_meas_bus_nr = pi_meas_bus_nr;

%% The bus numbers that active power flow measurement happens: (Power
is flowing from the first number to the second)
pf_meas_bus_nr = [
1 2
1 5
2 3
2 4
3 4
4 5
4 7
5 6
6 13
];

%% The bus numbers that reactive power flow measurement happens:
qf_meas_bus_nr = pf_meas_bus_nr;
```

Matlab Codes: Implementation of Proposed Algorithm

```
%% Power System State Estimation Considering Parameters Uncertainty
tic
global fb tb nbranch nbus linedatas busdatas V_nr phi_nr test_case
r_perturbed x_perturbed b_perturbed r_nominal x_nominal b_nominal
baseMVA Phi_true V_true

%%  Initials:
test_case = 14;      % Run which case data? IEEE 14 or 30 or 57 or 118
bus test system?
measurement14;       % Measurement Data
MC_tests  = 1000;     % MC test numbers
% Power Network Parameters(r, x, b) noise:
sigma_params_all = [0 0.05 0.10 0.15 0.20 0.25];
showplots = 1;  % set it 1 if you want to see the figures
display_SE_results = 1;
%% Variance of Voltage magnitude, Active and reactive Power Injections
and flows:
sigma_v      = 0.001; % 1e-20; %
sigma_phi    = 0.0001; % 1e-20; %
sigma_pi     = 0.01; % 1e-20; %
sigma_qi     = 0.01; % 1e-20; %
sigma_pf     = 0.01; % 1e-20; %
sigma_qf     = 0.01; % 1e-20; %
rho          = 0.0;  % correlation factor
%% Reading Nominal Line Parameters and Ybus arrangement:
linedatas = linedata();  % Calling "linedata.m" for Line Data
fb = linedatas(:,1);     % From bus number
tb = linedatas(:,2);     % To bus number
nbranch = length(fb);    % number of branches
nbus = test_case;      % number of buses
negatives = 0;
r_nominal = linedatas(:,3);      % Resistance, R
x_nominal = linedatas(:,4);      % Reactance, X
b_nominal = linedatas(:,5);      % Shunt Admittance
busdatas = busdata();   % reading bus data
[Ybus_nominal A_incidence Yprimitive_nominal] =
ybus_modified(r_nominal,x_nominal,b_nominal);
G = real(Ybus_nominal); % Bus Admittance matrix split:
B = imag(Ybus_nominal);

%% sigma_params loop
for sigma_params_idx = 1:length(sigma_params_all)
sigma_params = sigma_params_all(sigma_params_idx);
V_error_seq   = [];
phi_error_seq = [];
V_SE_seq      = [];
phi_SE_seq    = [];
V_nr_seq      = [];
phi_nr_seq    = [];
sigma_x_v_seq   = [];
sigma_x_phi_seq = [];
```

```
%% MC iterations:
for MC_test = 1:MC_tests

%% Parameters Perturbation:
r_perturbed = normrnd(r_nominal, sigma_params .* r_nominal);
x_perturbed = normrnd(x_nominal, sigma_params .* x_nominal);
b_perturbed = normrnd(b_nominal, sigma_params .* b_nominal);
while find(r_perturbed < 0)
      negatives = negatives + length(find(r_perturbed<0));
      fprintf('\nRecalculating r again...'); pause(1);
      r_perturbed = normrnd(r_nominal, sigma_params .* r_nominal); %
Generate and add again random numbers
end
while find(x_perturbed < 0)
      negatives = negatives + length(find(x_perturbed<0));
      fprintf('\nRecalculating x again...'); pause(1);
      x_perturbed = normrnd(x_nominal, sigma_params .* x_nominal); %
Generate and add again random numbers
end
while find(b_perturbed < 0)
      negatives = negatives + length(find(b_perturbed<0));
      fprintf('\nRecalculating b again...'); pause(1);
      b_perturbed = normrnd(b_nominal, sigma_params .* b_nominal); %
Generate and add again random numbers
end

%% Correlating the Resistance parameters:
if rho > 0 && sigma_params > 0
r_nominal_nonzeros = nonzeros(r_nominal);
sigma_r_corr = zeros(length(r_nominal_nonzeros),1);
for i=1:length(r_nominal_nonzeros)        % diagonal elements:
      sigma_r_corr(i,i) = ( sigma_params * r_nominal_nonzeros(i) ) ^ 2;
end
for i=1:length(r_nominal_nonzeros)        % non-diagonal elements:
      for j=1:length(r_nominal_nonzeros)
            if i ~= j
                  sigma_r_corr(i,j) = rho *
sqrt(sigma_r_corr(i,i)*sigma_r_corr(j,j));
            end
      end
end

L_sigma_r_corr = chol(sigma_r_corr,'lower'); % Cholesky factorization:
produces an upper triangular matrix
r_perturbation = normrnd(0,1,length(r_nominal_nonzeros),1);   %
normrnd(0,sigma_params .* r_nominal,nbranch,1);
r_perturbed_nonzeros = L_sigma_r_corr * r_perturbation +
r_nominal_nonzeros;
r_perturbed = zeros(nbranch,1);
r_perturbed(find(r_nominal~=0)) = r_perturbed_nonzeros;

      % Recalculation in Negative case
      while find(r_perturbed<0)
            fprintf('Warning: The number of negative values for r while
correlating it in this MC trial: '); fprintf('%2g',
```

```
length(find(r_perturbed<0)); fprintf('\nRecalculating correlated r
again...'); pause(1);
            %       r_perturbed(find(r_perturbed<0)) = 0; % Changing
negative values to zero.
            negatives = negatives + length(find(r_perturbed<0));
            r_perturbation = normrnd(0,1,length(r_nominal_nonzeros),1);
% normrnd(0,sigma_params .* r_nominal,nbranch,1);
            r_perturbed_nonzeros = L_sigma_r_corr * r_perturbation +
r_nominal_nonzeros;
            r_perturbed = zeros(nbranch,1);
            r_perturbed(find(r_nominal~=0)) = r_perturbed_nonzeros;
      end
end
%% Bus Admittance Formation
[Ybus_perturbed A_incidence Yprimitive] =
ybus_modified(r_perturbed,x_perturbed,b_perturbed);

%% Newton Raphson calculations:
[V_nr,phi_nr] = newton(Ybus_perturbed);
phi_nr_dg = 180/pi*phi_nr;   % Angles in Degree

%% WLS State Estimation

% Shunt Admittance Matrix Formation:    % Off-diagonals are the mutual
admittances between the respective nodes
        bbus = zeros(nbus,nbus);
        for k=1:nbranch
            bbus(fb(k),tb(k)) = b_nominal(k) ./ 2;
            bbus(tb(k),fb(k)) = bbus(fb(k),tb(k));
        end

meas_calc;        % Calculates the measured values according to the
perturbed NR states.
wls;              % WLS State Estimation:
phi_SE_dg = 180/pi*phi_SE; % rad to degree

%% Collecting V and Phi errors in each iterarion
V_error = V_nr - V_SE;
phi_error = phi_nr_dg - phi_SE_dg;

phi_errors = sqrt(mean(phi_error_seq.^2))';


if abs(V_error) < 10    % to exclude incorrect answers
##############
        if abs(phi_error) < 20
                V_error_seq(end+1, :) = V_error; % each row is a new
iteration and columns are buses
                phi_error_seq(end+1, :) = phi_error;
                V_SE_seq(end+1, :) = V_SE;
                phi_SE_seq(end+1, :) = phi_SE_dg;
                sigma_x_v_seq(end+1, :) = sigma_x_v;
                sigma_x_phi_seq(end+1, :) = sigma_x_phi;
%               V_nr_seq(end+1, :) = V_nr;  % collecting
%               phi_nr_seq(end+1, :) = phi_nr_dg; % collecting
```

```
        end
end


%% Display the WLS results

if test_case >= 57 || mod(MC_test,20) == 0
    clc
    if display_SE_results
        disp('__________________State Estimation_________________');
        disp('Bus    V_SE    V_NR     V_Er                  Ph_SE     Ph_NR
Ph_Er');
        for m = 1:nbus
            fprintf('%3g', m); fprintf('%8.3f', V_SE(m));
fprintf('%7.3f', V_nr(m)); fprintf('%21.16f', V_nr(m)-V_SE(m));
fprintf('  %8.3f', phi_SE_dg(m)); fprintf(' %8.3f', phi_nr_dg(m));
fprintf('%21.16f', phi_nr_dg(m)-phi_SE_dg(m));fprintf('\n');
        end
        disp('_____________________________________________________');
    end % of display_SE_results
    fprintf('MC Trial Number: '); fprintf('%g',MC_test); fprintf('\n');
    fprintf('Sigma of Parameters: '); fprintf('%g',sigma_params);
fprintf('\n');
    if iters > 1
        fprintf('WLS Iterations = %4d', iters);fprintf('\n');
    end
end  % of display each 10 trial

end   % of MC


% For SE
mean_V_SE_all(:,sigma_params_idx) = mean(V_SE_seq)';
mean_V_phi_all(:,sigma_params_idx) = mean(phi_SE_seq)';
std_V_SE_all(:,sigma_params_idx) = std(V_SE_seq)';
std_V_phi_all(:,sigma_params_idx) = std(phi_SE_seq)';
% For SE Errors
mean_V_errors_all(:,sigma_params_idx) = mean(V_error_seq)';
mean_phi_errors_all(:,sigma_params_idx) = mean(phi_error_seq)';
std_V_errors_all(:,sigma_params_idx) = std(V_error_seq)';
std_phi_errors_all(:,sigma_params_idx) = std(phi_error_seq)';

% WLS theoritical STD
mean_sigma_x_v_all(:,sigma_params_idx) = mean(sigma_x_v_seq)';
mean_sigma_x_phi_all(:,sigma_params_idx) = mean(sigma_x_phi_seq)';


%% Correlation of SE errors
% corr_coefs = corrcoef(V_error_seq);    % returns a matrix R of
correlation coefficients, input matrix rows are observations and whose
columns are variables.
corr_coefs_upper = nonzeros(triu(corrcoef(V_error_seq),1));
mean_corr_coefs_V_all(sigma_params_idx) = mean(corr_coefs_upper);
std_corr_coefs_V_all(sigma_params_idx) = std(corr_coefs_upper);
% phi
corr_coefs_upper = [];
```

```
corr_coefs_upper = nonzeros(triu(corrcoef(phi_error_seq(:,2:end)),1));
mean_corr_coefs_phi_all(sigma_params_idx) = mean(corr_coefs_upper);
std_corr_coefs_phi_all(sigma_params_idx) = std(corr_coefs_upper);

end   % of parameters loop
```

Network Data for IEEE test cases

The network data for the test cases are shown here. In the process of programming, it is important to have a reliable reference data to confirm the results that are generated by the test program. For the author it was not easy to find the consistent data for some cases, for example line Susceptance (B) for IEEE 14-Bus case. In [Christie 1999] some of the provided data seems not to be consistent and regardless of sending email and asking for the modifications of their database, they have not yet made the corrections. This is why the network data are brought here.

IEEE 14-Bus Test Case

Network parameters and Bus data for this test case is shown in Table 5.4and Table 5.5 respectively.

Table 5.4 Branch data for IEEE 14-Bus test case

From Bus	To Bus	Resistance R	Reactance X	Susceptance B	Transformer Turns Ratio
1	2	0.01938	0.05917	0.0528	0
1	5	0.05403	0.22304	0.0492	0
2	3	0.04699	0.19797	0.0438	0
2	4	0.05811	0.17632	0.0374	0
2	5	0.05695	0.17388	0.034	0
3	4	0.06701	0.17103	0.0346	0
4	5	0.01335	0.04211	0.0128	0
4	7	0	0.20912	0	0.978
4	9	0	0.55618	0	0.969
5	6	0	0.25202	0	0.932
6	11	0.09498	0.1989	0	0
6	12	0.12291	0.25581	0	0
6	13	0.06615	0.13027	0	0
7	8	0	0.17615	0	0
7	9	0	0.11001	0	0
9	10	0.03181	0.0845	0	0
9	14	0.12711	0.27038	0	0
10	11	0.08205	0.19207	0	0
12	13	0.22092	0.19988	0	0
13	14	0.17093	0.34802	0	0

Table 5.5 Bus data for IEEE 14-Bus test case

Bus #	Bus Type	PV Bus Voltage	P_Gen MW	Q_Gen MVR	P_Load MW	Q_Load MVR	Gs: Shunt Conductance	Bs: Shunt Susceptance
1	1	1.06	232.4	-16.9	0	0	0	0
2	2	1.045	40	42.4	21.7	12.7	0	0
3	2	1.01	0	23.4	94.2	19	0	0
4	3	1	0	0	47.8	-3.9	0	0
5	3	1	0	0	7.6	1.6	0	0
6	2	1.07	0	12.2	11.2	7.5	0	0
7	3	1	0	0	0	0	0	0
8	2	1.09	0	17.4	0	0	0	0
9	3	1	0	0	29.5	16.6	0	19
10	3	1	0	0	9	5.8	0	0

11	3	1	0	0	3.5	1.8	0	0
12	3	1	0	0	6.1	1.6	0	0
13	3	1	0	0	13.5	5.8	0	0
14	3	1	0	0	14.9	5	0	0

```
Bus Types: 1 is Slack Bus, 2 is PV Bus and 3 is PQ Bus.
```

The bus admittance matrix for this test case is shown here. It can be used as a reference because in this bus admittance matrix, all the transformers and shunt elements are correctly considered.

The bus admittance matrix is a symmetric matrix and the nonzero elements of this matrix for IEEE 14-Bus case are shown in Table 5.6.

Table 5.6 Ybus nonzero elements for IEEE 14-Bus test case

(1,1)	6.02502905576822 - 19.4470702055144i
(2,1)	-4.99913160079803 + 15.2630865231796i
(5,1)	-1.02589745497019 + 4.23498368233483i
(1,2)	-4.99913160079803 + 15.2630865231796i
(2,2)	9.52132361081478 - 30.2707153987791i
(3,2)	-1.1350191923074 + 4.78186315175772i
(4,2)	-1.68603315061494 + 5.11583832587208i
(5,2)	-1.7011396670944 + 5.19392739796971i
(2,3)	-1.1350191923074 + 4.78186315175772i
(3,3)	3.12099490223296 - 9.81148012935164i
(4,3)	-1.98597570992556 + 5.06881697759392i
(2,4)	-1.68603315061494 + 5.11583832587208i
(3,4)	-1.98597570992556 + 5.06881697759392i
(4,4)	10.5129895220362 - 38.6351712076078i
(5,4)	-6.84098066149567 + 21.5785539816916i
(7,4)	0 + 4.88951266031734i
(9,4)	0 + 1.8554995578159i
(1,5)	-1.02589745497019 + 4.23498368233483i
(2,5)	-1.7011396670944 + 5.19392739796971i
(4,5)	-6.84098066149567 + 21.5785539816916i
(5,5)	9.56801778356026 - 35.5275394560448i
(6,5)	0 + 4.25744533525338i
(5,6)	0 + 4.25744533525338i
(6,6)	6.57992340746622 - 17.3407328099191i
(11,6)	-1.95502856317726 + 4.09407434424044i
(12,6)	-1.52596744045097 + 3.1759639650294i
(13,6)	-3.09892740383799 + 6.10275544819312i
(4,7)	0 + 4.88951266031734i
(7,7)	0 - 19.5490059482647i
(8,7)	0 + 5.67697984672154i
(9,7)	0 + 9.09008271975275i
(7,8)	0 + 5.67697984672154i
(8,8)	0 - 5.67697984672154i
(4,9)	0 + 1.8554995578159i
(7,9)	0 + 9.09008271975275i
(9,9)	5.32605503946736 - 24.0925063752679i
(10,9)	-3.90204955244743 + 10.3653941270609i
(14,9)	-1.42400548701993 + 3.0290504569306i
(9,10)	-3.90204955244743 + 10.3653941270609i
(10,10)	5.78293430614783 - 14.7683378765214i
(11,10)	-1.8808847537004 + 4.40294374946052i
(6,11)	-1.95502856317726 + 4.09407434424044i
(10,11)	-1.8808847537004 + 4.40294374946052i
(11,11)	3.83591331687766 - 8.49701809370096i
(6,12)	-1.52596744045097 + 3.1759639650294i

(12,12)	4.01499202727289 -	5.42793859120161i
(13,12)	-2.48902458682192 +	2.25197462617221i
(6,13)	-3.09892740383799 +	6.10275544819312i
(12,13)	-2.48902458682192 +	2.25197462617221i
(13,13)	6.72494614846623 -	10.6696935494707i
(14,13)	-1.13699415780633 +	2.31496347510535i
(9,14)	-1.42400548701993 +	3.0290504569306i
(13,14)	-1.13699415780633 +	2.31496347510535i
(14,14)	2.56099964482626 -	5.34401393203596i

IEEE 30-Bus Test Case

Network parameters and Bus data for this test case is shown in Table 5.7 and Table 5.8 respectively.

Table 5.7 Branch data for IEEE 30-Bus test case

From Bus	To Bus	Resistance R	Reactance X	Susceptance B	Transformer Turns Ratio
1	2	0.0192	0.0575	0.0528	0
1	3	0.0452	0.1652	0.0408	0
2	4	0.057	0.1737	0.0368	0
3	4	0.0132	0.0379	0.0084	0
2	5	0.0472	0.1983	0.0418	0
2	6	0.0581	0.1763	0.0374	0
4	6	0.0119	0.0414	0.009	0
5	7	0.046	0.116	0.0204	0
6	7	0.0267	0.082	0.017	0
6	8	0.012	0.042	0.009	0
6	9	0	0.208	0	0.978
6	10	0	0.556	0	0.969
9	11	0	0.208	0	0
9	10	0	0.11	0	0
4	12	0	0.256	0	0.932
12	13	0	0.14	0	0
12	14	0.1231	0.2559	0	0
12	15	0.0662	0.1304	0	0
12	16	0.0945	0.1987	0	0
14	15	0.221	0.1997	0	0
16	17	0.0524	0.1923	0	0
15	18	0.1073	0.2185	0	0
18	19	0.0639	0.1292	0	0
19	20	0.034	0.068	0	0
10	20	0.0936	0.209	0	0
10	17	0.0324	0.0845	0	0
10	21	0.0348	0.0749	0	0
10	22	0.0727	0.1499	0	0
21	23	0.0116	0.0236	0	0
15	23	0.1	0.202	0	0
22	24	0.115	0.179	0	0
23	24	0.132	0.27	0	0
24	25	0.1885	0.3292	0	0
25	26	0.2544	0.38	0	0
25	27	0.1093	0.2087	0	0
28	27	0	0.396	0	0.968
27	29	0.2198	0.4153	0	0
27	30	0.3202	0.6027	0	0
29	30	0.2399	0.4533	0	0
8	28	0.0636	0.2	0.0428	0
6	28	0.0169	0.0599	0.013	0

Table 5.8 Bus data for IEEE 30-Bus test case

Bus #	Bus Type	PV Bus Voltage	P_Gen MW	Q_Gen MVR	P_Load MW	Q_Load MVR	Gs: Shunt Conductance	Bs: Shunt Susceptance
1	1	1.06	232.4	-16.9	0	0	0	0
1	1		260.2	-16.1	0	0	0	0
2	2	1.043	40	50	21.7	12.7	0	0
3	3	1	0	0	2.4	1.2	0	0
4	3	1.06	0	0	7.6	1.6	0	0
5	2	1.01	0	37	94.2	19	0	19
6	3	1	0	0	0	0	0	0
7	3	1	0	0	22.8	10.9	0	0
8	2	1.01	0	37.3	30	30	0	0
9	3	1	0	0	0	0	0	0
10	3	1	0	0	5.8	2	0	0
11	2	1.082	0	16.2	0	0	0	0
12	3	1	0	0	11.2	7.5	0	0
13	2	1.071	0	10.6	0	0	0	0
14	3	1	0	0	6.2	1.6	0	0
15	3	1	0	0	8.2	2.5	0	0
16	3	1	0	0	3.5	1.8	0	0
17	3	1	0	0	9	5.8	0	0
18	3	1	0	0	3.2	0.9	0	0
19	3	1	0	0	9.5	3.4	0	0
20	3	1	0	0	2.2	0.7	0	0
21	3	1	0	0	17.5	11.2	0	0
22	3	1	0	0	0	0	0	0
23	3	1	0	0	3.2	1.6	0	0
24	3	1	0	0	8.7	6.7	0	4.3
25	3	1	0	0	0	0	0	0
26	3	1	0	0	3.5	2.3	0	0
27	3	1	0	0	0	0	0	0
28	3	1	0	0	0	0	0	0
29	3	1	0	0	2.4	0.9	0	0
30	3	1	0	0	10.6	1.9	0	0

Bus Types: 1 is Slack Bus, 2 is PV Bus and 3 is PQ Bus.

IEEE 57-Bus Test Case

Network parameters and Bus data for this test case is shown in Table 5.9 and Table 5.10 respectively.

Table 5.9 Branch data for IEEE 57-Bus test case

From Bus	To Bus	Resistance R	Reactance X	Susceptance B	Transformer Turns Ratio
1	2	0.0083	0.028	0.129	0
1	15	0.0178	0.091	0.0988	0
1	16	0.0454	0.206	0.0546	0
1	17	0.0238	0.108	0.0286	0
2	3	0.0298	0.085	0.0818	0
3	4	0.0112	0.0366	0.038	0
3	15	0.0162	0.053	0.0544	0
4	5	0.0625	0.132	0.0258	0
4	6	0.043	0.148	0.0348	0
4	18	0	0.43	0	0.978
4	18	0	0.555	0	0.97
5	6	0.0302	0.0641	0.0124	0
6	7	0.02	0.102	0.0276	0
6	8	0.0339	0.173	0.047	0
7	8	0.0139	0.0712	0.0194	0
7	29	0	0.0648	0	0.967
8	9	0.0099	0.0505	0.0548	0
9	10	0.0369	0.1679	0.044	0

9	11	0.0258	0.0848	0.0218	0
9	12	0.0648	0.295	0.0772	0
9	13	0.0481	0.158	0.0406	0
9	55	0	0.1205	0	0.94
10	12	0.0277	0.1262	0.0328	0
10	51	0	0.0712	0	0.93
11	13	0.0223	0.0732	0.0188	0
11	41	0	0.749	0	0.955
11	43	0	0.153	0	0.958
12	13	0.0178	0.058	0.0604	0
12	16	0.018	0.0813	0.0216	0
12	17	0.0397	0.179	0.0476	0
13	14	0.0132	0.0434	0.011	0
13	15	0.0269	0.0869	0.023	0
13	49	0	0.191	0	0.895
14	15	0.0171	0.0547	0.0148	0
14	46	0	0.0735	0	0.9
15	45	0	0.1042	0	0.955
18	19	0.461	0.685	0	0
19	20	0.283	0.434	0	0
21	20	0	0.7767	0	1.043
21	22	0.0736	0.117	0	0
22	23	0.0099	0.0152	0	0
22	38	0.0192	0.0295	0	0
23	24	0.166	0.256	0.0084	0
24	25	0	1.182	0	0
24	25	0	1.23	0	0
24	26	0	0.0473	0	1.043
25	30	0.135	0.202	0	0
26	27	0.165	0.254	0	0
27	28	0.0618	0.0954	0	0
28	29	0.0418	0.0587	0	0
29	52	0.1442	0.187	0	0
30	31	0.326	0.497	0	0
31	32	0.507	0.755	0	0
32	33	0.0392	0.036	0	0
34	32	0	0.953	0	0.975
34	35	0.052	0.078	0.0032	0
35	36	0.043	0.0537	0.0016	0
36	37	0.029	0.0366	0	0
36	40	0.03	0.0466	0	0
37	38	0.0651	0.1009	0.002	0
37	39	0.0239	0.0379	0	0
38	44	0.0289	0.0585	0.002	0
38	48	0.0312	0.0482	0	0
38	49	0.115	0.177	0.003	0
39	57	0	1.355	0	0.98
40	56	0	1.195	0	0.958
41	42	0.207	0.352	0	0
41	43	0	0.412	0	0
44	45	0.0624	0.1242	0.004	0
46	47	0.023	0.068	0.0032	0
47	48	0.0182	0.0233	0	0
48	49	0.0834	0.129	0.0048	0
49	50	0.0801	0.128	0	0
50	51	0.1386	0.22	0	0
52	53	0.0762	0.0984	0	0
53	54	0.1878	0.232	0	0
54	55	0.1732	0.2265	0	0
56	41	0.553	0.549	0	0
56	42	0.2125	0.354	0	0
57	56	0.174	0.26	0	0

Table 5.10 Bus data for IEEE 57-Bus test case

Bus #	Bus Type	PV Bus Voltage	P_Gen MW	Q_Gen MVR	P_Load MW	Q_Load MVR	Gs: Shunt Conductance	Bs: Shunt Susceptance
1	1	1.04	128.9	-16.1	55	17	0	0
2	2	1.01	0	-0.8	3	88	0	0
3	2	0.985	40	-1	41	21	0	0
4	3	1	0	0	0	0	0	0
5	3	1	0	0	13	4	0	0

6	2	0.98	0	0.8	75	2	0	0
7	3	1	0	0	0	0	0	0
8	2	1.005	450	62.1	150	22	0	0
9	2	0.98	0	2.2	121	26	0	0
10	3	1	0	0	5	2	0	0
11	3	1	0	0	0	0	0	0
12	2	1.015	310	128.5	377	24	0	0
13	3	1	0	0	18	2.3	0	0
14	3	1	0	0	10.5	5.3	0	0
15	3	1	0	0	22	5	0	0
16	3	1	0	0	43	3	0	0
17	3	1	0	0	42	8	0	0
18	3	1	0	0	27.2	9.8	0	10
19	3	1	0	0	3.3	0.6	0	0
20	3	1	0	0	2.3	1	0	0
21	3	1	0	0	0	0	0	0
22	3	1	0	0	0	0	0	0
23	3	1	0	0	6.3	2.1	0	0
24	3	1	0	0	0	0	0	0
25	3	1	0	0	6.3	3.2	0	5.9
26	3	1	0	0	0	0	0	0
27	3	1	0	0	9.3	0.5	0	0
28	3	1	0	0	4.6	2.3	0	0
29	3	1	0	0	17	2.6	0	0
30	3	1	0	0	3.6	1.8	0	0
31	3	1	0	0	5.8	2.9	0	0
32	3	1	0	0	1.6	0.8	0	0
33	3	1	0	0	3.8	1.9	0	0
34	3	1	0	0	0	0	0	0
35	3	1	0	0	6	3	0	0
36	3	1	0	0	0	0	0	0
37	3	1	0	0	0	0	0	0
38	3	1	0	0	14	7	0	0
39	3	1	0	0	0	0	0	0
40	3	1	0	0	0	0	0	0
41	3	1	0	0	6.3	3	0	0
42	3	1	0	0	7.1	4.4	0	0
43	3	1	0	0	2	1	0	0
44	3	1	0	0	12	1.8	0	0
45	3	1	0	0	0	0	0	0
46	3	1	0	0	0	0	0	0
47	3	1	0	0	29.7	11.6	0	0
48	3	1	0	0	0	0	0	0
49	3	1	0	0	18	8.5	0	0
50	3	1	0	0	21	10.5	0	0
51	3	1	0	0	18	5.3	0	0
52	3	1	0	0	4.9	2.2	0	0
53	3	1	0	0	20	10	0	6.3
54	3	1	0	0	4.1	1.4	0	0
55	3	1	0	0	6.8	3.4	0	0
56	3	1	0	0	7.6	2.2	0	0
57	3	1	0	0	6.7	2	0	0

Bus Types: 1 is Slack Bus, 2 is PV Bus and 3 is PQ Bus.

List of Figures

List of Tables

Index